Performance assessment of expansive slag concrete under different curing conditions

（異なる養生条件下における
スラグ膨張コンクリートの性能評価）

September 2020

HIROSHIMA UNIVERSITY

Nguyen Viet Hoang

Performance assessment of expansive slag concrete under different curing conditions

（異なる養生条件下における スラグ膨張コンクリートの性能評価）

Nguyen Viet Hoang

A THESIS SUBMITTED

FOR THE DEGREE OF DOCTOR OF ENGINEERING

DEPARTMENT OF CIVIL AND ENVIRONMENTAL ENGINEERING

HIROSHIMA UNIVERSITY

September 2020

ABSTRACT

Portland cement concrete usually manifests autogenous or drying shrinkage resulting in serious cracks and severe deterioration of concrete structures. To enhance the volumetric stability of concrete, one of the main measurements is to apply expansive concrete. There are two kinds of expansive concrete involving shrinkage compensating concrete (with low expansion energy) and chemical-prestressing concrete (with high expansion energy). The chemical-prestressing concrete not only compensates shrinkage but also introduces prestress inside concrete with restraining objects such as reinforced bar or the formwork.

The evaluation of expansion performance of expansive concrete is required for its quality control and applications. The conventional evaluation method stipulated in ASTM C806, ASTM C878/C878M or JIS A 6202 was used as a common estimation method for expansion. This technique was considered to be complicated and costly to implement. Then, a new evaluation method using a cylindrical mold has been proposed as the substitute for the conventional method, called as a simplified method. After proposing the new performance valuation technique of expansive concrete, it is worthwhile to verify its applicability on the reality. There have been few studies on the validation of the simplified method at normal condition. They indicated that the simplified method and conventional method well correlated at 20 °C condition. Besides, the steam curing was considered suitable for enhancing performances of concretes, particularly on mixes incorporating mineral admixtures, and it is widely applied to precast concrete. Further, there have not been any investigations on the expansion evaluation of expansive concrete in steam curing so far. In order to widen the application of the simplified method to evaluating the performance of expansive concrete in material design and construction, the verification of the applicability of the simplified method with steam curing is necessary.

Blast furnace slag (referred to as *slag* in this paper) is a byproduct of the iron and steel manufacturing process that has been increasingly used as a cementitious ingredient in cement and concrete composites. Generally, the inclusion of slag is regarded to be beneficial to the performance of mortar and concrete. However, many studies have observed larger autogenous shrinkage and more early-age cracking in slag concretes than in concretes without slag. While, expansive concrete is used as a countermeasure for shrinkage and cracking, the incorporation of slag in expansive concrete and the effects of such integration offer a promising target for investigation. Although the impacts of slag on the properties of normal concrete have been clarified in literature, the study on performance of expansive concrete incorporating slag is scarce, particularly in the term of durability.

The objectives of this study were therefore, firstly, to validate the applicability of the simplified method for expansion evaluation under steam curing; and secondly, to investigate the influence of slag type and curing condition on the engineering properties of expansive concrete with the validated simplified method.

This thesis includes five chapters, and detailed organization of the thesis is described as follows:

Chapter 1 shows the background, purposes, and methodology of this study.

Chapter 2 provides a brief literature review relating to the research contents.

Chapter 3 presents an experimental program to investigate the applicability of the simplified method under steam curing. Specimens were cured with steam or at 20 °C from their first casting up to 1 day. They were then sealed or water-cured at 20 °C for 7 days to investigate the effect of later curing. Two estimation methods for measuring the expansive strains under constraint were compared based on the expansive energies. The range of applicability of the simplified method was analyzed. A new concept for the simplified method of estimating the expansion by using the axial strain was then proposed. The experimental results showed that

two measurement methods exhibited a high correlation, which validates the use of the simplified method under steam curing.

Chapter 4 describes an investigation on the impact of slag type and curing method on the engineering properties of expansive concrete such as the strength, volumetric change and transport characteristics. The two different slag compositions evaluated were combined with ordinary Portland cement at 50% replacement by mass. Cylindrical specimens were cast and initially cured by one-day steam or seven-day sealed 20 ºC curing to investigate the effects of slag type and initial curing on the expansive concrete properties. The specimens were then exposed to the ambient environment with 60% relative humidity at 20 ºC until 91 days as the second stage of curing. The results indicate that pure slag impaired concrete performance, whereas outstanding improvement in performance was observed when using slag with gypsum. The results of this investigation can be used to provide improved concrete mix and curing design when using blast furnace slag in expansive concrete.

Chapter 5 states the conclusions of this research and recommendations for future works as well.

ACKNOWLEDGEMENT

The research presented in this thesis was carried out in the Graduate School of Engineering at the Hiroshima University, Japan.

I wish to express my deep appreciation and gratitude to my supervisor, Prof. Dr. Kenichiro Nakarai for his patient supervision, valuable guidance, critical suggestions, and continuous support throughout this research. I would also like to thank my co-supervisor, Assoc. Prof. Dr. Pham Hoang Kien, and Asst. Prof. Yuko Ogawa for their kind supports and many discussions during my research program.

I would like to gratefully acknowledge the All Japan Box-Culvert Association for their kindly supports in my research program.

I am particularly grateful to Mr. Akeru Okazaki, Ms. Saeko Kajita, Mr. Nguyen Huu May and the other students at the Structural Engineering Laboratory of Hiroshima University for assisting with the experimental campaign. I must also thank the Japan Students Service Organization (JASSO) for the funding support in my PhD's course. Besides, I would like to express my gratitude to University of Transport and Communications (Viet Nam) for giving me the opportunity of this course.

Last but not least, with great appreciation, I sincerely acknowledge the support from my wife, Phan Nhu Quynh, my parents, my parents in law, all of my family members, friends, and colleagues for their love, support and encouragement.

Hiroshima, September 2020

Nguyen Viet Hoang

CONTENTS

LIST OF FIGURES

LIST OF TABLES

Chapter 1. Introduction

1.1. General background

Concrete has inherent properties such as autogenous or drying shrinkages and low tensile strength [1, 2]. Therefore, concrete structures may contract injurious cracks deleteriously affecting the serviceability and durability of the structures, it is important to control the cracks [3, 4]. Given this background, expansive concrete has been developed and used as a countermeasure for cracking [5 - 7]. There are two kinds of expansive concrete involving shrinkage compensating concrete (with low expansion energy) and chemical-prestressing concrete (with high expansion energy). The chemical-prestressing concrete not only compensates shrinkage but also introduces prestress inside concrete with restraining objects such as reinforced bar or the formwork. At present, the most commonly used expansive agent is a sulphoaluminate expansive agent [8 – 10]. It's main compositions are Ye'elimite ($4CaO \cdot 3Al_2O_3 \cdot SO_3$), abbreviated as $C_4A_3\overline{S}$, anhydrite ($CaSO_4$) and lime (CaO), which forms ettringite during hydration, as Eq. (1.1). The gypsum and calcium hydroxide in Eq. (1.1) come from the hydration of anhydrite and lime in the expansive agent. The minerals of C_3A and C_4AF in Portland cement can react with gypsum and calcium hydroxide to form ettringite also, as Eqs. (1.2) and (1.3) [9].

$$C_4A_3\overline{S} + 8C\overline{S}H_2 + 6CH + 74H \rightarrow 3(C_3A \cdot 3C\overline{S} \cdot 32H) \quad (1.1)$$

$$C_3A + 3C\overline{S}H_2 + 26H \rightarrow C_3A \cdot 3C\overline{S} \cdot 32H \quad (1.2)$$

$$C_4AF + 6C\overline{S}H_2 + 2CH + 50H \rightarrow 2(C_3(A_{0.5}, F_{0.5}) \cdot 3C\overline{S} \cdot 32H) \quad (1.3)$$

The expansion performance of expansive concrete needs to be evaluated for quality control and

application. Conventional evaluation methods for expansive concrete are based on uniaxial constraints, e.g., ASTM C806 [11] for cement mortar, ASTM C878/C878M [12] for shrinkage-compensating concrete, and JIS A 6202 [13] for expansive concrete. However, these techniques are considered complicated and costly to implement [14, 15]. On the other hand, new simplified methods of evaluating expansive concrete by using a cylindrical mold have been proposed as a substitute for the conventional methods [15 - 17].

The proposed evaluation technique for expansive concrete should be verified for its applicability in reality. Some studies have validated the simplified method under normal conditions [16, 18]. They indicated that the simplified and conventional methods show a strong correlation at 20 °C. Besides, the steam curing was considered suitable for enhancing performances of concretes, particularly on mixes incorporating mineral admixtures, and it is widely applied to precast concrete [19, 20]. Further, there have not been any investigations on the expansion evaluation of expansive concrete in steam curing so far. In order to widen the application of the simplified method to evaluating the performance of expansive concrete in material design and construction, the verification of the applicability of the simplified method with steam curing is essential.

From the viewpoints of the sustainable development, the use of slag, a byproduct from the iron and steel manufacturing process, as a cementitious ingredient in either cement or concrete composites has been increasing [21 - 23]. Generally, the inclusion of slag is regarded to be beneficial to the performance of mortar and concrete [24]. The main factors influencing the reactivity of slag are its chemical composition, glass content, and particle size distribution. The hydration of pure slag is often relatively slow, thus an additional activator (e.g., alkali [25], lime [26], or sulfate source [27]) is typically required to achieve sufficient reactivity. In particular, once slag combined with PC, the calcium hydroxide (CH) from the hydrating cement serves as an activating component promoting the slag dissolution and the formation of

calcium silicate hydrate ($C-S-H$) [28]. In the case of the calcium sulfate source added in the slag cement system, the dissolved aluminum, calcium and silicon ions from the slag react with the calcium sulfate ($C\overline{S}$) forming ettringite ($C_6A\overline{S_3}H_{32}$) and $C-S-H$ phases, as demonstrated in this simplified Eq. (1.4) [29].

$$C_5S_3A + 3C\overline{S} + CH + 34H \rightarrow C_6A\overline{S_3}H_{32} + 3CSH \qquad (1.4)$$

Furthermore, many studies [30 – 32] have observed larger autogenous shrinkage and more early-age cracking in slag concretes than in concretes without slag. The addition of slag to a concrete mix also leads to an increase in drying shrinkage and a decrease in cracking resistance [33, 34].

Based on the aforementioned characteristics of slag and expansive concrete, the incorporation of such materials offers a promising target for investigation. Although the impacts of slag on the properties of conventional concrete have been clarified in literature [21 - 24, 30 - 34], the study on performance of expansive concrete incorporating slag is scarce.

In the practical, evaluation of concrete quality up to the depth of concrete cover is substantial for proper maintenance of reinforced concrete structures [35, 36]. One of the employed methods to analyze the existing concrete performance is the compressive strength. However, compressive strength alone cannot be an indicator for mass transfer resistance of concrete [37]. Besides, carbon dioxide, chloride ion and water ingress are the primary cause of detrimental effects in concrete. Their penetration into concrete is governed by the pore structure. Thus, a number of previous researches [35, 37 - 39] considered transport characteristics, namely air permeability and capillary water absorption, to be substantial indicators for the magnitude of durability of concrete.

1.2. Objectives of the research

Based on all above-mentioned issues, this research project investigates several properties of expansive slag concrete subjected to different curing conditions.

The specific objectives of the present study are as follows:

- To validate the applicability of the simplified method to expansion evaluation of expansive concrete.
- To investigate the impact of slag types on the strength, volumetric change and durability properties of expansive concrete under different curing conditions with the validated simplified method.

1.3. Methodology of the research

First, to verify the applicability of the simplified estimation method to expansive concrete, two estimation methods for measuring the expansive strains under constraint were compared based on the expansive energies. Specimens were cured with steam or at 20 °C from their first casting up to 1 day. They were then sealed or water-cured at 20 °C for 7 days to investigate the effect of later curing. The specimens for the simplified method were measured their expansive strains in the circumferential and axial directions, whereas the strain of samples for the conventional method were obtained in a uniaxial direction.

Then, to quantify the effects of the different incorporated slags on the engineering properties of expansive concrete, the two different slag compositions evaluated were combined with ordinary Portland cement at 50% replacement by mass. A sulfoaluminate-type expansive agent was used in a constant amount of 50 kg/m^3 in all specimens. Cylindrical specimens were cast and initially cured by one-day steam or seven-day sealed 20 ºC curing to investigate the effects

of slag type and initial curing on the expansive concrete properties. The specimens were then exposed to the ambient environment with 60% relative humidity at 20 ºC until 91 days as the second stage of curing. The compressive strength tests of the ϕ100 × 200 mm cylindrical specimens were performed to examine strength development. The simplified method for measuring the restrained expansion of concrete validated in the foregoing experiment was applied with a cylindrical tinplate mold (ϕ100 × 200 mm, 0.28-mm thick) to estimate the volumetric change. The air permeability and water absorption tests were employed to assess the durability of the concrete.

1.4. Thesis outline

This thesis is divided into of five chapters, and detailed organization of the thesis is described as follows (see **Fig. 1.1**).

Chapter 1 presents the background, purposes, and methodology of this study.

Chapter 2 provides a review of the existing literature on the application of expansive concrete and its estimation methods, the utilization of slag and its effects on concrete properties.

Chapter 3 validates the applicability of simplified method to expansion evaluation of expansive concrete.

Chapter 4 investigates the effect of slag type and curing condition on the performance of expansive concrete, such as compressive strength, expansion/shrinkage behaviors and transport characteristics. The validated method in the previous chapter is used to evaluate the expansive behaviors.

Chapter 5 states a brief summary of the research and conclusions drawn from this study and suggestions for further research.

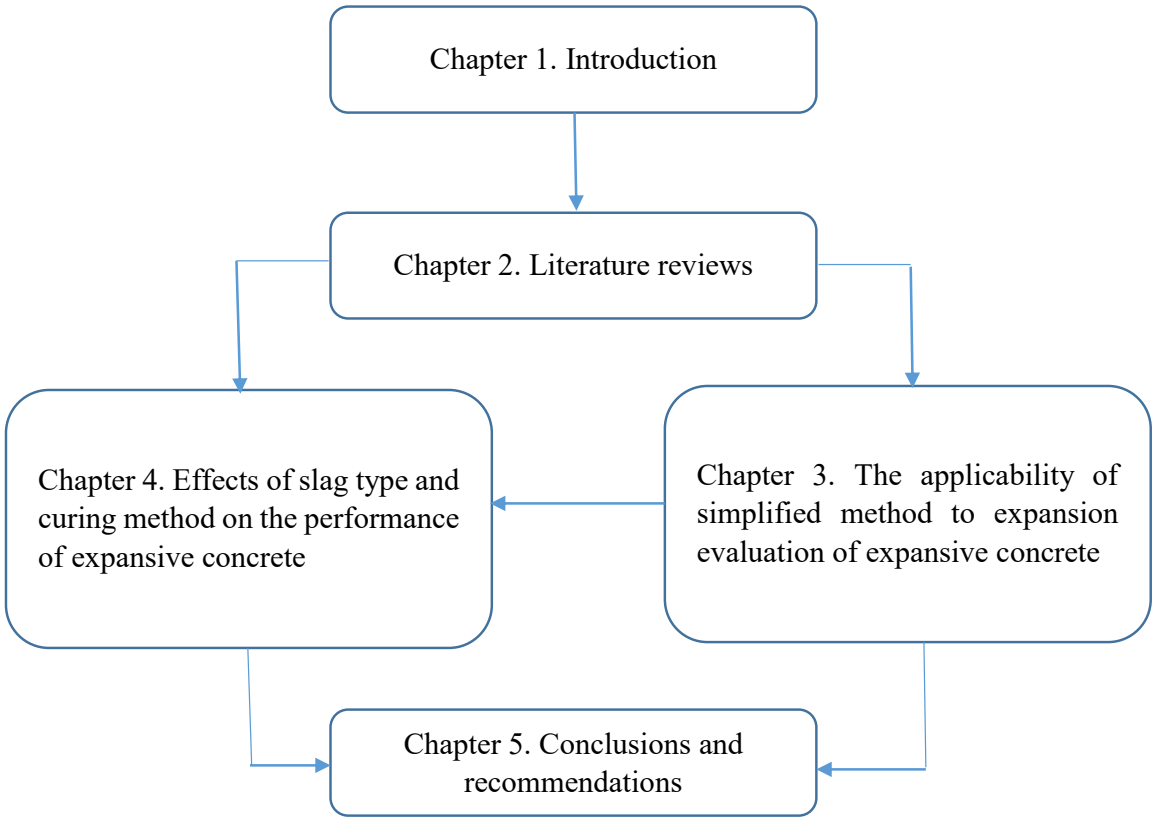

Fig. 1.1. Structure of the thesis

References in chapter 1

[1] C. Hua, P. Acker, A. Ehrlacher, Analyses and models of the autogenous shrinkage of hardened cement paste: I. Modelling at macroscopic scale, Cement Concr. Res. 25 (1995) 1457–1468.

[2] W. Hansen, Drying shrinkage mechanisms in Portland cement paste. J. Am. Cer. Soc. 70 (1970) 323–328.

[3] AIJ (Architectural Institute of Japan), Recommendations for practice of crack control in reinforced concrete buildings (design and construction), 2006.

[4] JCI (Japan Concrete Institute), Research committee report on shrinkage of concrete, 2010.

[5] S. Nagataki, H. Gomi, Expansive agents (mainly ettringite), Cement Concr. Compos. 20 (2-3) (1998) 163-170.

[6] M. S. Meddah, M. Suzuki, R. Sato, Influence of a combination of expansive and shrinkage-reducing admixture on autogenous deformation and self-stress of silica fume high-performance concrete, Constr. Build. Mater. 25 (2011) 239–250.

[7] HG. Choi, M. Tsujino, T. Noguchi, R. Kitagaki, Expansion/contraction behavior and cracking control effect of expansive concrete in building structure. Proc. Jpn. Concr. Inst. 34 (1) (2012) 424–429.

[8] Q. Cao, Y. Cheng, M. Cao, Q. Gao, Workability, strength and shrinkage of fiber reinforced expansive self-consolidating concrete, Constr. Build. Mater. 131 (2017) 178–185.

[9] J. Han, D. Jia, P. Yan, Understanding the shrinkage compensating ability of type K expansive agent in concrete, Constr. Build. Mater. 116 (2016) 36–44.

[10] W. Nocun´-Wczelik, Z. Konik, A. Stok, Blended systems with calcium aluminate and calcium sulphate expansive additives, Constr. Build. Mater. 25 (2011) 939–943.

[11] ASTM C 806, Test Method for Restrained Expansion of Expansive Cement Mortar, ASTM International, West Conshohocken, 2018.

[12] ASTM C878 / C878M, Standard Test Method for Restrained Expansion of Shrinkage-Compensating Concrete, West Conshohocken, 2014.

[13] JIS A 6202:2017, Expansive additive for concrete, Japanese Industrial Standards Committee, Tokyo, 2017.

[14] US3779085 A (1973), E. Rice, Means and method of testing expansive concrete, 73/803.

[15] US5487307 A (1997), Method and apparatus for testing concrete expansion.

[16] A. Hosoda, M. Morioka, M. Tanimura, T. Kanda, E. Sakai, T. Kishi, Technical Committee on Performance Evaluation of High Performance Expansive Concrete and System for Crack Control, Technical Committee Reports 2011, Japan Concrete Institute (JCI), Tokyo, Japan, 2011, pp. 65–92.

[17] M. Tsujino, H. Hashida, R. Yuasa, T. Kikuchi, Quality control of expansive concrete using a thin cylindrical steel mold, Proc. JCI 34 (1) (2012) 520–525 (in Japanese).

[18] K. Nakarai, Y. Kurihara, H. Hashida, M. Tsujino, Analysis of applicability of simplified estimation method of expansive cement concrete using cylindrical light-weight steel mold based on mechanical work, Cem. Sci. Concr. Technol. 65 (1) (2011) 209–216 (in Japanese).

[19] A.M. Ramezanianpour, Kh. Esmaeili, S.A. Ghahari, A.A. Ramezanianpour, Influence of initial steam curing and different types of mineral additives on mechanical and durability properties of self-compacting concrete, Constr. Build. Mater. 73 (2014) 187–194.

[20] A.A. Ramezanianpour, M.H.Khazali, P. Vosoughi, Effect of steam curing cycles on strength and durability of SCC: a case study in precast concrete, Constr. Build. Mater. 49 (2013) 807–813.

[21] K.G. Babu, V.S.R. Kumar, Efficiency of GGBS in concrete, Cem. Concr. Res. 30 (2000) 1031–1036.

[22] D. Suresh, K. Nagaraju, Ground granulated blast slag (GGBS) in concrete – A review, J. Mechan. Civ. Engin. 12 (2015) 76–82.

[23] E. Aprianti, A huge number of artificial waste material can be supplementary cementitious material (SCM) for concrete production—A review Part II, J. Cl. Prod. 142 (2017) 4178–4194.
[24] E. Özbaya, M. Erdemirb, H.İ. Durmuş, Utilization and efficiency of ground granulated blast furnace slag on concrete properties—A review, Constr. Build. Mater. (2016) 423–434.
[25] F. Sajedi, H.A. Razak, The effect of chemical activators on early strength of ordinary Portland cement-slag mortars, Constr. Build. Mater. 24 (2010) 1944–1951.
[26] L. Courard, F. Michel, Limestone fillers cement based composites: Effects of blast furnace slags on fresh and hardened properties, Constr. Build. Mater. 51 (2014) 439–445.
[27] M. Singh, M. Garg, Calcium sulfate hemihydrate activated low heat sulfate resistant cement, Constr. Build. Mater. 16 (2002) 181–186.
[28] H. Taylor, Cement Chemistry, Thomas Telford Publishing, London, 2004.
[29] C.A. da Luz, R.D. Hooton, Influence of curing temperature on the process of hydration of supersulfated cements at early age, Cem. Concr. Res. 77 (2015) 69–75.
[30] I. Pane, W. Hansen, Investigation on key properties controlling early-age stress development of blended cement concrete, Cem. Concr. Res. 38 (2008) 1325–1335.
[31] K. Tang, S. Millard, G. Beattie, Technical and economic aspects of using GGBFS for crack control mitigation in long span reinforced concrete structures, Constr. Build. Mater. 39 (2013) 65–70.
[32] J.C. Chern, Y.W. Chan, Deformations of concretes made with blast-furnace slag cement and ordinary Portland cement, ACI Mater. J. 86 (1989) 372–382.
[33] T. Kanda, H. Momose, K. Imamoto, Shrinkage cracking resistance of blast furnace slag blended cement concrete-Influencing factors and enhancing measures, J. Adv. Concr. Technol. 13 (2015) 1–14.
[34] M. Saric-Coric and P.C. Aïtcin, Influence of curing conditions on shrinkage of blended cements containing various amounts of slag, ACI Mater. J. 100 (2003) 477–484.

[35] D.W.S. Ho, G.J. Chirgwint, A performance specification for durable concrete, Constr. Build. Mater. 10 (1996) 375–319.

[36] M. H. Nguyen, K. Nakarai, S. Nishio, Durability index for quality classification of cover concrete based on water intentional spraying tests, Cem. Concr. Compos. 104 (2019) 103355.

[37] A. Abbas, M. Carcassès, J.P. Ollivier, The importance of gas permeability in addition to the compressive strength of concrete, Mag. Concr. Res. 52 (1) (2000) 1–6.

[38] D.N. Katpady, H. Hazehara, M. Soeda, T. Kubota, S. Murakami, Durability assessment of blended concrete by air permeability, Intern. J. Concr. Struct. Mater. 12 (2018) 30.

[39] N.S. Martys, C.F. Ferraris, Capillary transport in mortars and concrete, Cem. Concr. Res. 27 (5) (1997) 747 – 760.

Chapter 2. Literature reviews

2.1. Introduction

This chapter reviews previous works within the scope of this topic that have been carried out by various researchers. Concrete experiences volume changes independent from external loads, usually shrinkage. In fact, there are many types of shrinkage but the more relevant ones are autogenous shrinkage and drying shrinkage. Considering certain structural uses, concrete shrinkage may cause cracking that must be avoided so the development of expansive concretes is a good alternative to increase the durability parameters of many construction applications, both for new construction and refurbishment. The expansion performance of expansive concrete needs to be evaluated for its quality control and application. Thus, estimation methods for quality control of expansive concrete are reviewed in section 2.2. The traditional and new methods for evaluation of expansion of concrete are listed. The common curing method applied to precast-concrete production are also presented.

For the concrete engineering, blast furnace slag as a cementitious material has been applied popularly because of beneficial properties such as reducing cement amount, improving mechanical and durability characteristics. However, the larger autogenous shrinkage and more early-age cracking commonly occur in slag concretes. The section 2.3 overviews all relevant information about blast furnace slag – from production and processing to the effect that slag additions have on the concrete performance such as strength, volumetric change and durability characteristics. Based on results of literature, needs for the present study is discussed.

2.2. Methods for quality control of expansive concrete

2.2.1. Expansive concrete

Expansive concrete is the general term for concrete consisting of an expansive agent mixed together with cement, water, fine and coarse aggregates, and other admixtures. This concrete, in contrast to conventional concretes based on Ordinary Portland Cement (OPC), expands during the first hydration steps. Two basic classes for expansive concrete are shrinkage compensating concrete and chemical-prestressing concrete. The main difference between them is the magnitude of the eventual expansion, larger in the latter. When reinforced concretes using expansive concretes are classified from the standpoint of function, they may be broadly divided into shrinkage compensated concrete and chemically prestressed concrete. By restraining expansion of expansive concrete with objects such as reinforcing bars, chemical prestress of compressive stress will be induced in the concrete, while in the objects such as reinforcing bars, chemical prestrain of initial tensile strain will be induced. Shrinkage compensated concrete is reinforced concrete imparted with a small chemical prestress of a degree to offset or reduce tensile stress occurring due to drying shrinkage or other causes. As for chemically prestressed concrete, it is a reinforced concrete having chemical prestress imparted with a large chemical prestress by addition of a large amount of expansive agent compared with shrinkage compensated concrete so that chemical prestress will remain even when drying shrinkage has been offset [1].

In most cases where expansive concretes are applied, such as pavements without expansion or contraction joints, roofs made of monolithic concrete without roofing or taxiways without joints, shrinkage compensating-concrete is used. However, there are certain cases where a larger amount of expansion is required, thus the use of chemical-prestressing concretes is mandatory [2- 5]. The mostly common method for reducing shrinkage and producing expansive concrete is to form expansive ettringite [6], other expansive agents such as the free lime-based

and MgO-type are also used [7 – 9]. Among different ettringite-triggered expansive agents, the sulphoaluminate based is the most commonly used [10, 11]. Its main compositions are Ye'elimite ($4CaO \cdot 3Al_2O_3 \cdot SO_3$), abbreviated as $C_4A_3\overline{S}$, anhydrite ($CaSO_4$) and lime (CaO), which forms ettringite during hydration, as Eq. (2.1). The gypsum and calcium hydroxide in Eq. (2.1) come from the hydration of anhydrite and lime in the expansive agent. The minerals of C_3A and C_4AF in Portland cement can react with gypsum and calcium hydroxide to form ettringite also, as Eqs. (2.2) and (2.3) [10].

$$C_4A_3\overline{S} + 8C\overline{S}H_2 + 6CH + 74H \rightarrow 3(C_3A \cdot 3C\overline{S} \cdot 32H) \quad (2.1)$$

$$C_3A + 3C\overline{S}H_2 + 26H \rightarrow C_3A \cdot 3C\overline{S} \cdot 32H \quad (2.2)$$

$$C_4AF + 6C\overline{S}H_2 + 2CH + 50H \rightarrow 2(C_3(A_{0.5}, F_{0.5}) \cdot 3C\overline{S} \cdot 32H) \quad (2.3)$$

Fresh concrete of expansive concrete shows about the same nature with ordinary concrete in which expansive agents are absent [1]. It is known that the expansion rate, when restraint and other conditions are constant, will have a roughly proportional relationship with the unit expansive agent content [12, 13]. Consequently, if the required expansion rate is set for a structure in which expansive concrete is to be used, it will be possible for an expansive agent content corresponding to this expansion rate to be determined. **Fig. 2.1** shows that the expansive rate becomes larger with the increase of unit expansive agent content. **Fig. 2.2** is an example showing relations among unit expansive agent content, compressive strength and expansion rate. It is shown that restraint expansion rate becomes larger with the increase of expansive agent content. However, the strength of expansive concrete having expansive agent content within 30 kg/m^3 and cured under non-restraint condition shows about the same value with ordinary concrete. The strength decreases when expansive rate further increases to some extent. **Table 2.1** exhibits the types of expansive admixtures and standard quantities per unit

volume of concrete for shrinkage-compensating and chemical prestressing concretes [14].

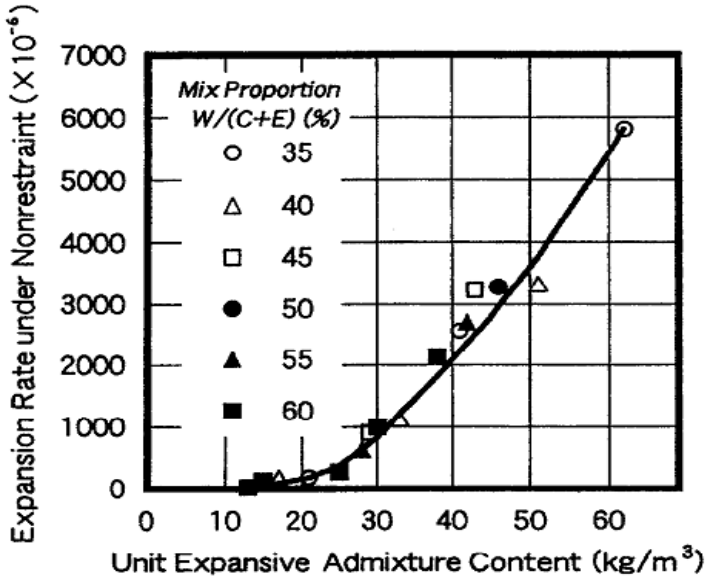

Fig. 2.1. Relationship between unit expansive admixture content and non-restrain expansion rate [12].

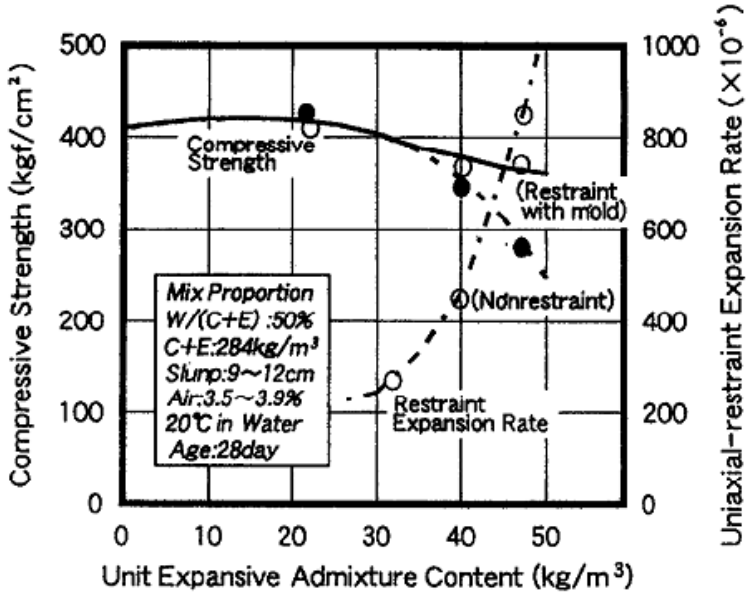

Fig. 2.2. Relations among unit expansive admixture content, compressive strength and restrain expansion rate [13].

Table 2.1 Types of expansive agents and standard quantities per unit volume of concrete [14]

Type of expansive concrete	Type of expansive agent		Standard quantity of expansive agent per unit volume of concrete (kg/m^3)
Shrinkage-compensating concrete	For ordinary concrete	Conventional type	30
		Low ratio of additives	20
	For mass concrete	Conventional type	30
		Low ratio of additives	20
Chemical prestressing concrete	For ordinary concrete		35 ÷ 50
	For concrete products		30 ÷ 60

2.2.2. Estimation methods for expansion of expansive concrete

The expansion performance of expansive concrete needs to be evaluated in order to assure that the shrinkage-compensated and chemical prestressed concretes have a desired expansion characteristic. Some conventional evaluation methods for expansive concrete are based on uniaxial constraints, e.g., ASTM C806 [15] for cement mortar, ASTM C878/C878M [16] for shrinkage-compensating concrete, and JIS A 6202 [17] for expansive concrete. These tests typically consist of a prismatic specimen with a restraining steel bar at the centroid of the specimen and a length comparator used for measuring the change in length. **Fig. 2.3** illustrates the schematic measurement setup of the conventional method [18]. However, these techniques are considered complicated and costly to implement [19, 20]. In particular, the test procedures in ASTM require the specimen to be demolded no less than 6 h after casting. In a field construction context, this means that the laboratory technician needs to work overtime or two shifts. There is also a remarkable delay from the time casting to the first significant expansion measurement being taken. Furthermore, demolding weak concrete bars and recording data

require proficient technicians so that the best accuracy can be achieved. Consequently, the measurement equipment specified in these methods are not available at many ready-mixed concrete plants, so the plants do not provide a suitable environment.

Besides, some studies have investigated the expansive properties of expansive concrete under multiaxial constraints using a concentric double pipe [21, 22]. The effects of eccentricity of the inner steel pipe against the outer steel pipe have also been considered [23]. However, these kinds of techniques do not seem to be popular and are complex. They necessitate delicacy and competence to be properly performed. In addition, expansive properties under an annular constraint can be assumed by multiaxially amplifying the notion concerning the amount of work under a uniaxial constraint [24]. Therefore, a measurement method that allows evaluation anywhere by anyone is a pressing need in order to meet the growing demand for expansive concrete.

Rice [19] presented a new method of testing expansive concrete wherein a concrete sample is permitted to expand while subjected to a predetermined restraint, and subsequently to contraction. The means of test comprises a split cylindrical mold which receives a concrete sample contained in a pair of plastic bags having low friction characteristics; a measuring device indicates the amount of expansion and contraction occurring in the cylindrical mold. In addition, Landgren et al. [20] invented a method with an improvement apparatus for measuring on-site expansive volumetric changes in hardened, shrinkage-compensated concrete samples. It comprises a container having an open top and a cylindrical sidewall for receiving the curable sample therein. A strain gauge is secured to the sidewall of the container to sense circumferential expansion of the container as the volume change of the sample. In an exemplary embodiment, the container herein is a 26 gauges steel cylindrical one gallon pail, having a welded seam. Furthermore, Tsujino et al. [25] proposed a radically simplified method of restrained expansion measurement using lightweight steel molds which is also used for

measuring compressive strength. This is a method in which a strain gauge is glued in the circumferential direction, at mid-depth of a lightweight steel mold to measure the strain of the mold under expansive pressure from the inside. The outline of measurement setup for the simplified method is displayed in **Fig. 2.4**. This method is regarded as having a number of advantages over the traditional ones. Specifically, it provides a testing process that can be conducted at a construction site by unskilled workers. The specimen does not need to be demolded for strain measurements. Indeed, data are recorded automatically and continuously right after casting. Moreover, the cylindrical specimen can be used to measure the compressive strength of expansive concrete. The newly proposed performance evaluation technique for expansive concrete should be verified for its applicability in reality. Some studies have validated the simplified method under normal conditions [26 - 28]. They indicated that the simplified and conventional methods show a strong correlation at 20 °C. In the study of Nakarai et al. [27], the applicability of the newly simplified estimation method of expansive cement concrete with cylindrical light-weight steel mold is analyzed based on the concept of the mechanical work. They reported that the uniaxial strain of standard specimen can be quantitatively predicted from the circumferential strain of the simplified method (see **Fig. 2.5**). Hosoda et al. [28] conducted a round-robin test at five testing institutions and found the linear relationship between two measurement methods as shown in **Fig. 2.6**, suggesting that the simplified method is capable of substituting the method of JIS A 6202.

In the reality, the use of precast concrete (PC) members in construction industry is on the rise to ensure uniformity of high-strength concrete structures and reduce durations [29, 30]. To eliminate factors leading to increase in construction costs, in situ production of PC members could be considered [31]. However, as in situ PC production requires not only work space availability, but also alignment of material supply with the frame work schedule, it is necessary to plan just-in-time production and installation [32]. In such cases, a significant number of PC

members need to be produced in a short period of time, and PC members must be strong enough to withstand the lifting load, which requires a rapid curing approach. Therefore, the steam curing is considered in the in-situ PC production since the curing ensures the development of PC member strength to 70% of standard design strength in a day, which allows for PC member installation by lifting [33 – 35]. Various methods have been used including steam curing at atmospheric pressure (temperature less than 100 ºC), steam curing at high pressure (autoclaving), electrical heating of reinforcement, imposing electrical current to concrete directly, and microwave heating. Among these, steam curing at low pressure is most common, especially for large precast units [36 – 40].

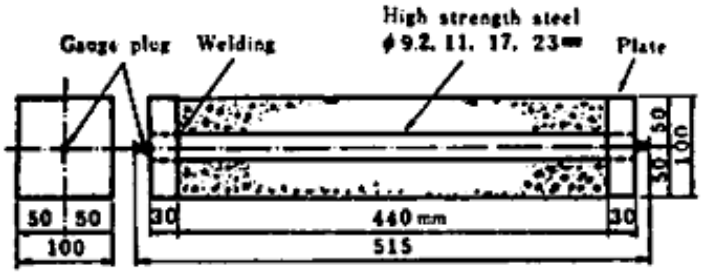

Fig. 2.3. The restrained test specimen for the conventional method [18].

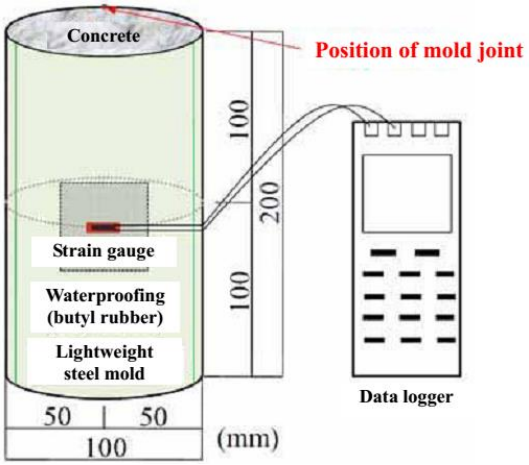

Fig. 2.4. Outline of test specimen for the simplified method [25].

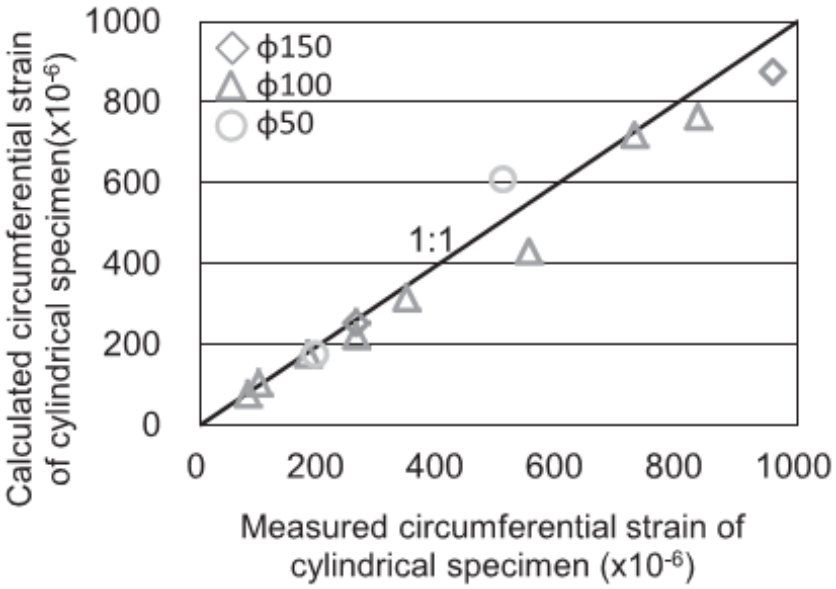

Fig. 2.5. Relation between the measured and calculated circumferential strain of cylindrical specimen (=50, 100, 150 mm, sealed curing, 7 days) [27].

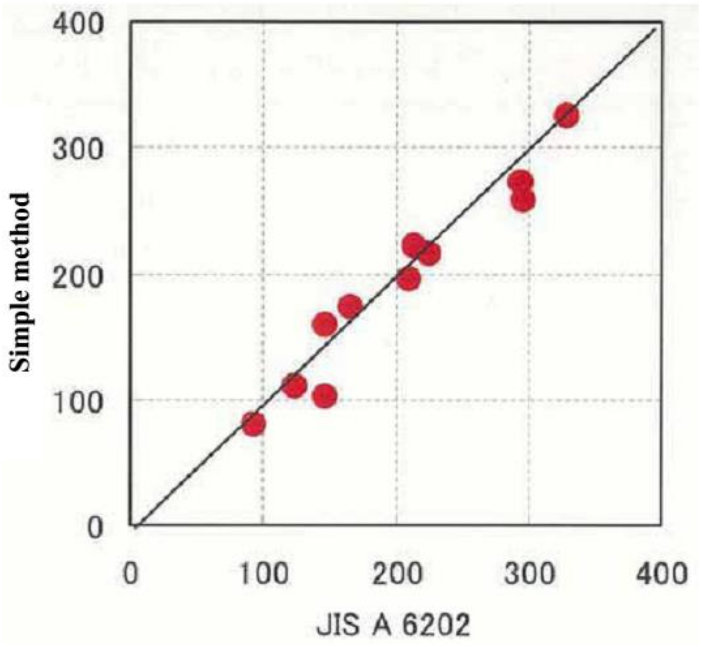

Fig. 2.6. Comparison between measurements by JIS A 6202 and the simplified method [28].

2.3. Utilization and effects of slag on concrete properties

2.3.1. History of blast furnace slag

The latent hydraulic reactivity of blast-furnace slag (slag) was discovered in 1862 by Emil Langen in Germany [41]. The first use of slags in cements dates back to 1865, when in Germany a slag-lime cement was commercially produced. By 1901 the manufacture of iron Portland cement containing maximum 30% of slag became accepted and in 1907, the first blast furnace cement with up to 85% slag content was produced [42]. Ever since, slag has been successfully used in cementitious applications.

2.3.2 Production of slag

Blast furnace slag is produced in a blast furnace concurrently with Fe. **Fig. 2.7** schematically represents obtaining the blast furnace slag from the iron ore. Iron oxides are reduced to igneous Fe in the furnace by adding a flux such as limestone or dolomite and a fuel and with a reducing agent such as coke [43]. The igneous slag indwells on the pig iron and its temperature is close to that of the igneous iron, which is between 1400 and 1600 ºC. The slag rises to the surface and is tapped off from be timely. If the igneous slag is cooled fast a glassy Ca–Al–Mg silicate forms. There are two common practices to fast cool of igneous slag. In the first practices high-pressure water (about 0.6 MPa) jets is used to granulate igneous slag directly at the furnace as it departs the nozzle. In this practice, 3 m^3 of water is used for a ton of slag and after treatment about 30% of water is exist in the obtained slag. As a second practices, palletization, which was developed in Canada in the 1970s, is used. The igneous slag is cooled firstly with water then flung into the air by a rotary drum (300 rpm). The water consumption is about 1 m^3/t of slag and the residual water content in the slag is only approximately 10% [44]. After the granulated blast furnace slag is obtained, it must be dehydrated, dried, and ground before using as a binder material. Magnets are often used before and after grinding to remove remaining

iron. For increased cementitious activity at early ages, the slag is normally ground finer than Portland cement. As is well known that reaction rate increases with improving the fineness of pozzolans like as Portland cement [45].

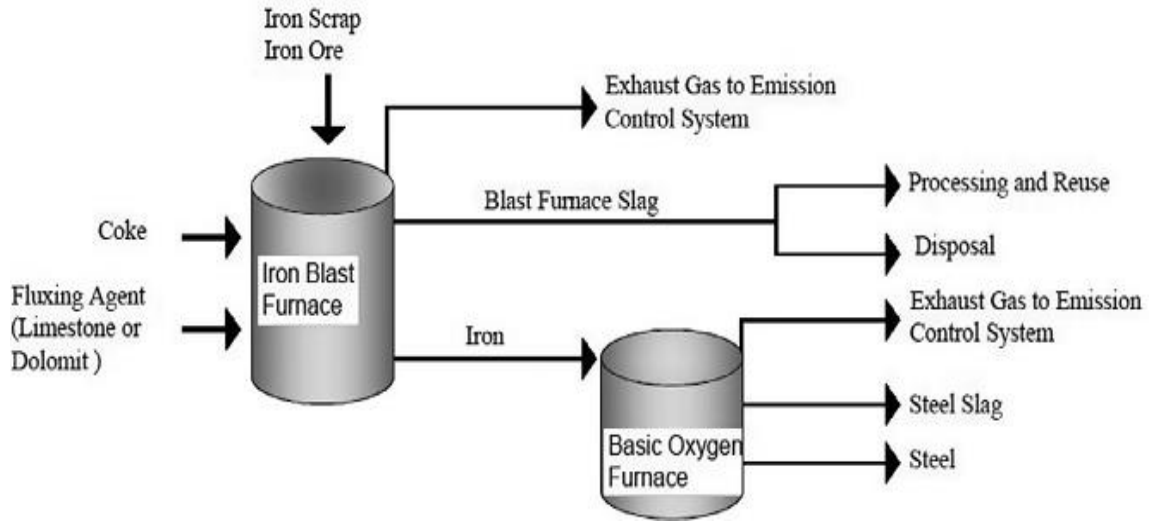

Fig. 2.7. Production progress of slag [43].

2.3.3. Chemical composition and hydration mechanism

The composition of blast-furnace slag is changed depend on the ores, fluxing stone and impurities in the coke feed into the blast furnace. Normally, silica, calcium, aluminum, magnesium, and oxygen are more than 95% in the composition of the blast-furnace slag. Typical chemical compositions of slag produced in different countries are tabulated in **Table 2.2** [46]. For the better hydraulic activity of slag, its chemical composition is very important. As chemically, slags can be classified into their basicity index. CaO/SiO_2 ratio given by Nkinamubanzi et al. [47] is the simplest basicity indices and it was mentioned that calcium over siliceous oxide ratio must be greater than 1. Hydraulic activity depends on the basicity of the slag, the more basic the slag, the greater its hydraulic activity in the presence of alkaline activators [48]. Keeping the basicity constant, increasing the Al_2O_3 content increases the

strength and a deficiency in CaO can be reimbursed by a greater amount of alumina (MgO). The effect of MgO as a replacement for CaO appears to be influenced both on the basicity and the MgO content of the slag. Deviations in the MgO content up to about 8–10% may have slight effect on strength development; however, more than 10% MgO may have a negative effect [48]. Moreover, it was mentioned that hydraulic activity increases with increasing calcium, aluminum and magnesium oxide contents and decreases with increasing SiO_2 content. According to TS EN 197-1 and British Standards, the ratio of the mass of CaO plus MgO to the mass of SiO_2 must exceed 1.0. This ratio assures about high alkalinity, without which the slag would be hydraulically inactive [48, 49]. The chemistry of slag and hydration phases developed in $CaO–SiO_2–Al_2O_3$ system is demonstrated in **Fig. 2.8** [50]. It is admitted by researcher that the principal hydration product of slag with Portland cement and water is Calcium–Silicate–Hydrate (C–S–H) as seen in **Fig. 2.8 (B)**. Regourd [45, 51–54] showed that a slight instantaneous reaction also happen when slag cement is mixed with water, favorably emancipating Ca and Al ions to solution. The reaction is limited, however, until supplementary alkali, $Ca(OH)_2$, or sulfates are presented for reaction. The hydration of slag cement in blend with Portland cement at normal temperature is a two-phase reaction. Primarily and through the early hydration, the major reaction is with alkali hydroxide, but consequent reaction is largely with $Ca(OH)_2$ [45].

It is widely recognized that slag alone shows few cementing properties when mixing with pure water unless they are activated with activating chemicals [55 – 57]. Alkaline solutions (such as sodium and potassium hydroxides) are often used to activate slag in order to produce a strong binding property. However, the use of these activators has not been commercially implemented in the construction industry because they are not safe for on-site workers due to their high pH toxicity. It is also too expensive to manufacture price-competitive cementless binders for Portland cement (OPC) [58]. Recently, lime (CaO) is investigated for use in activating slag

because it has a significantly lower cost and a lower alkalinity (pH = ~12.5 maximum) than alkaline solutions [59 - 61]. The major chemical reaction for creating strength in the CaO-activated slag system is similar to the pozzolanic reaction, i.e., the formation of calcium silicate hydrate (C-S-H). Although $Ca(OH)_2$ is chemically similar to CaO, because the dissolution of CaO in water produces $Ca(OH)_2$, the use of CaO exhibits a significantly better strength than $Ca(OH)_2$ for activating slag [60].

In fact, when using alkaline or lime activators, the corresponding increase in paste pH can lead to increased corrosion of any reactive metals present in the wastes. Therefore, it is desirable to increase the reactivity of slag without increasing pH. Collier et al. [62] investigated the effect of sulfate activation on the early age hydration of BFS:PC composite cement, and indicated that activation with gypsum produced the highest rate of slag reaction. Previous studies have explored the use of calcium sulfate sources for increasing the strength of binders for slag [63, 64] and as an additive to alkali-activated slag [65] or to Portland cement [66]. In these studies, the varying contents of gypsum affected the strength development. In particular, when the calcium sulfate sources activated the slag, ettringite [$Ca_6Al_2(SO_4)_3(OH)_{12}.26H_2O$] was predominantly produced as a major hydration product and it contributed to the early strength development. Matschei et al. [67] reported that when calcium sulfates (e.g., $CaOSO_4$, and $CaOSO_4.\ 2H_2O$) are incorporated into slag, the behavior of its self-activation could be significantly different from that of slag without any calcium sulfates because of the considerable promotion of hydration of slag with even small quantity of activators. In the case of the calcium sulfate source added in the slag cement system, the dissolved aluminum, calcium and silicon ions from the slag react with the calcium sulfate ($C\overline{S}$) forming ettringite ($C_6A\overline{S_3}H_{32}$) and calcium silicate hydrate ($C-S-H$) phases, as demonstrated in Eq. (2.4) [68].

$$C_5S_3A + 3C\overline{S} + CH + 34H \rightarrow C_6A\overline{S_3}H_{32} + 3CSH \qquad (2.4)$$

Table 2.2 Typical ranges of selected properties of granulated blast-furnace slags produced worldwide and in specific regions [46]

Parameter	Unit	Min	Max	North America	Central and Latin America	Western Europe	Eastern Europe	India, Japan, Australia, RSA
SiO_2	%	32	42	34.6 – 39.9	33.5 – 34.8	32.0 – 39.4	33.5 – 41.5	32.6 – 36.9
CaO	%	35	48	35.3 – 42.8	39.1 – 43.8	34.9 – 44.3	36.9 – 47.5	33.0 – 43.0
Al_2O_3	%	6	> 19	6.6 – 11.5	10.0 – 13.0	9.5 – 12.5	5.5 – 12.4	10.2 – 19.3
MgO	%	3	14	7.0 – 13.1	5.9 – 9.9	5.0 – 13.4	2.5 – 11.2	4.9 – 13.8
TiO_2	%	0.2	> 2	0.3 – 0.8	0.5 – 0.6	0.4 – 1.3	0.2 – 1.3	0.6 – 2.1
Na_2O	%	0.3	1.2	0.3 – 0.8	0.4 – 0.8	0.3 – 1.2	0.6 – 1.1	0.4 – 0.8
SO_3*	%	1	4	2.0 – 3.0	1.1 – 3.7	2.0 – 4.5	1.6 – 3.8	1.7 – 4.0
CaO/SiO_2	-	0.9	1.3	0.9 – 1.2	1.1 – 1.3	1.0 – 1.3	0.9 – 1.3	0.9 – 1.3
Glass content	%	66	100	Not analysed				
Bulk density	Kg/l	0.6	1.3	Not analysed				

* Although expressed as SO_3 in the chemical analysis, essentially all sulfur in slag is present in sulfide form due to the reducing conditions in the blast furnace (% SO_3 = 2.5×%S^-).

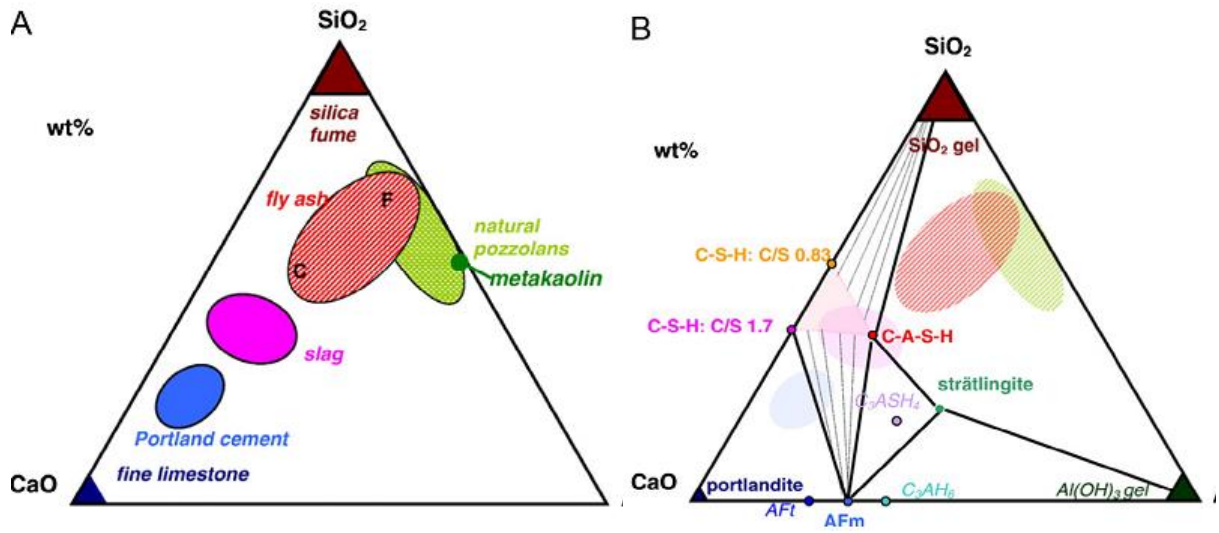

Fig. 2.8. (A) $CaO–Al_2O_3–SiO_2$ ternary diagram of cementitious materials, (B) hydrate phases in the $CaO–Al_2O_3–SiO_2$ system [50].

2.3.4. Impact of slag on volumetric change of concrete

Concrete structures performances are directly affected by the time-dependent properties of concrete such as drying and autogenous shrinkages. Incompatible results are presented related with effects of slag on the creep and drying shrinkage of the concretes in the literature. El-Cabib and Syed [69] investigated the free shrinkage of self-consolidating concrete produced with high volumes of slag. They concluded that replacing up to 70% of cement by slag lessens the free shrinkage of concrete greater than 45% when compared to concrete includes only PC. Darquennes et al. [70] reported that for a content of slag inferior or equal to 50%, the evolution rate and the amplitude at long term of the total shrinkage are lower than that of a PC concrete. Over 50% of mineral additions, the total shrinkage is similar. These different behaviors are principally due to the porous structure of cementitious materials. Brooks et al. [71] implied that concrete containing slag content between the 30% and 70% had similar shrinkage compared with concrete containing only PC. A review by Hooton et al. [72] found that with low-alumina slag, drying shrinkage of concretes over a range of replacement levels was similar to that of

OPC concrete. There did not appear to be a difference in relative drying shrinkage between concretes made with blended cement and those made with slag added separately at the time of mixing. Shariq et al. [73] investigated the creep and drying shrinkage of concrete containing slag with the cement replacement of 20%, 40% and 60%. The test results indicate that all the slag concrete mixes show higher shrinkage strain with higher cement replacement (see **Fig. 2.9**). In many studies [74–76], larger autogenous shrinkage and early age cracking was featured for the slag included concretes than that of concretes without slag. Lee et al. [77] reported that the inclusion of slag especially at higher contents increased the autogenous shrinkage when compared with plain concrete specimens. **Fig. 2.10** shows the increasing effect of 30% and 50% cement replacement with slag on the autogenous shrinkage with water to binder ratio of 0.27 and 0.32. The results were indicative of higher increase in the autogenous shrinkage as the water-to-binder ratio decreased. Obviously, the amount of slag has an influence on the results as well as the amount of calcium sulfate added [78].

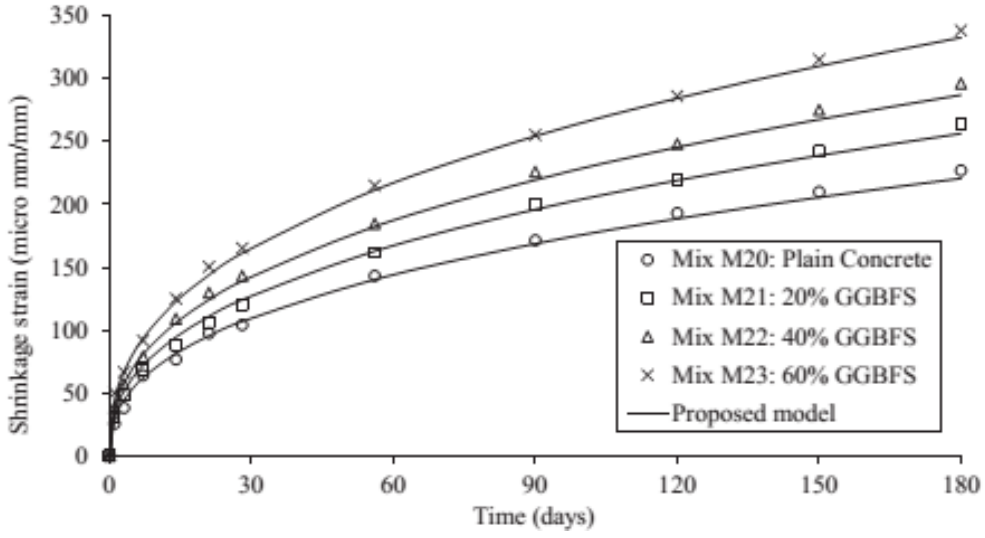

Fig. 2.9. Shrinkage strain of experimental data and proposed model for mix group M2 [73].

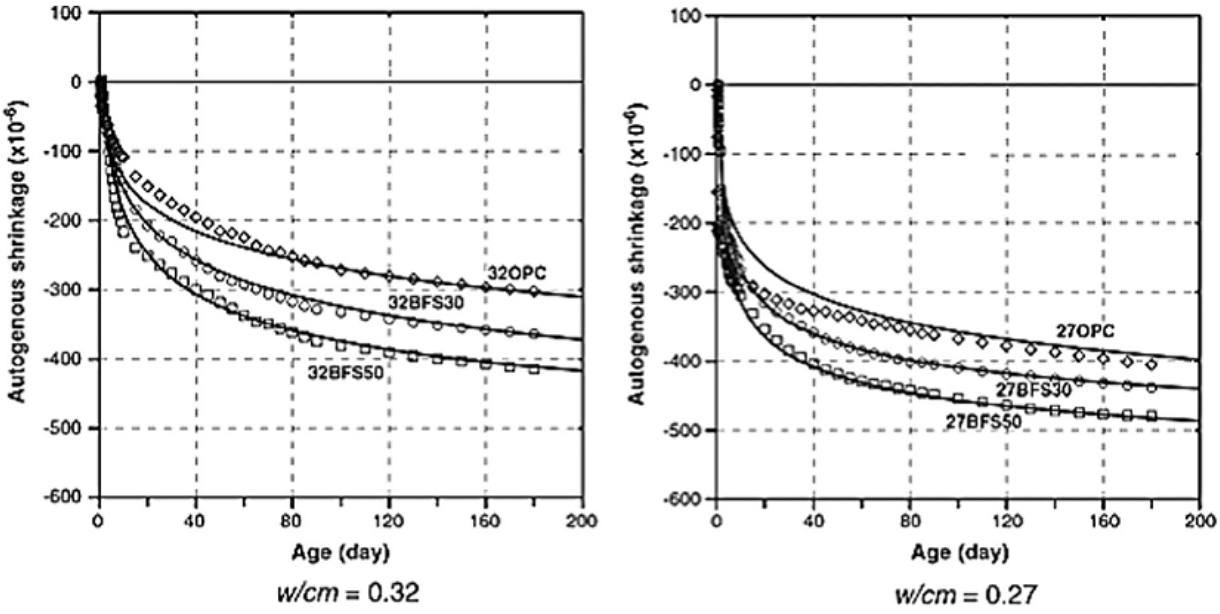

Fig. 2.10. Effect of slag content on autogenous shrinkage of concrete with low water to binder ratio [77].

2.3.5. Impact of slag on compressive strength

Strength development of slag included concretes can be fluctuate in a widespread range subjected to the slag substitution level, water to binder ratio, total cementitious materials content, curing type, testing age etc. There is a general consensus among the researcher that early-age strength gain of the slag included concretes is usually inversely correlated to the slag percent used in the mixture [79]. Normally, slag in concrete leads to lower early compressive strength gain but higher later strength [80 - 82] (see **Fig. 2.11**). The early age compressive strength development of mixtures containing slag is also highly depend on temperature. Results of [83] revealed that under normal curing environments, slag mortars and concretes attained compressive strength relatively slow than PC ones. However, at elevated temperatures, strength attaining is far quicker and the progress in primary strength is more noteworthy at higher levels of slag (see **Fig. 2.12**). Effects of slag replacement ratio from 50% to 80% and curing type (air and wet curing) on high performance concretes compressive strength are explored by Guneyisi

and Gesoglu [84]. They concluded that compressive strength decreased gradually with the augmentation of slag content. This is more pronounced for concretes subjected to air curing condition. However, at the 90 days, for the wet cured concrete, it was monitored that the existence of slag is greatly positive at 50% and 60% substitution with a compressive strength beyond the control concrete (see **Fig. 2.13**). A number of previous studies have been indicated that an optimum cement replacement level regarding fresh concrete properties and late strength development is about 50%, beyond that replacement ratio effect of slag was inconsequential [46, 85, 86].

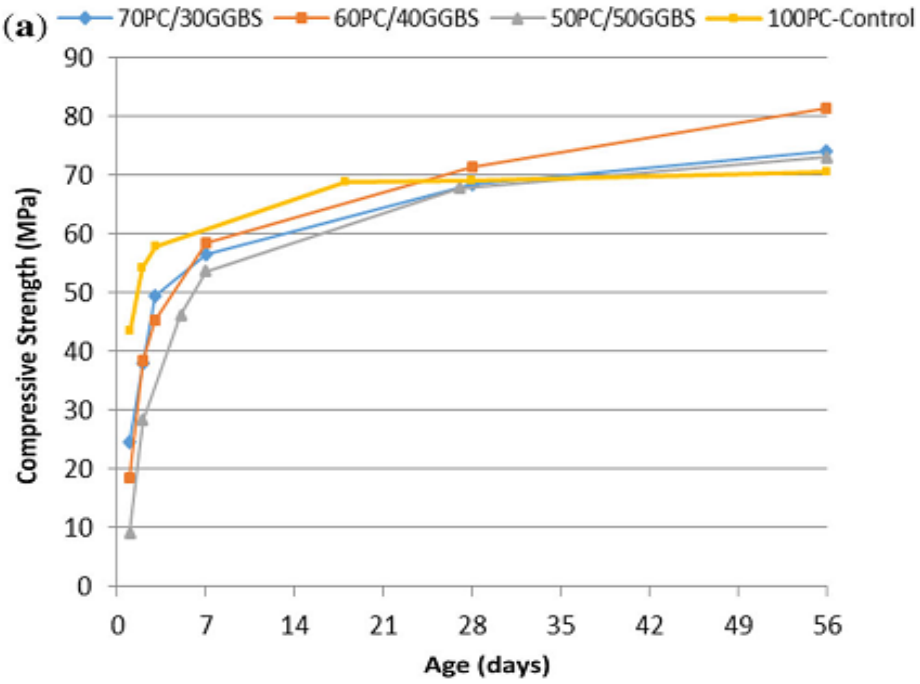

Fig. 2.11. Compressive strength development of GGBS (slag) concrete under normal curing at 20ºC [81].

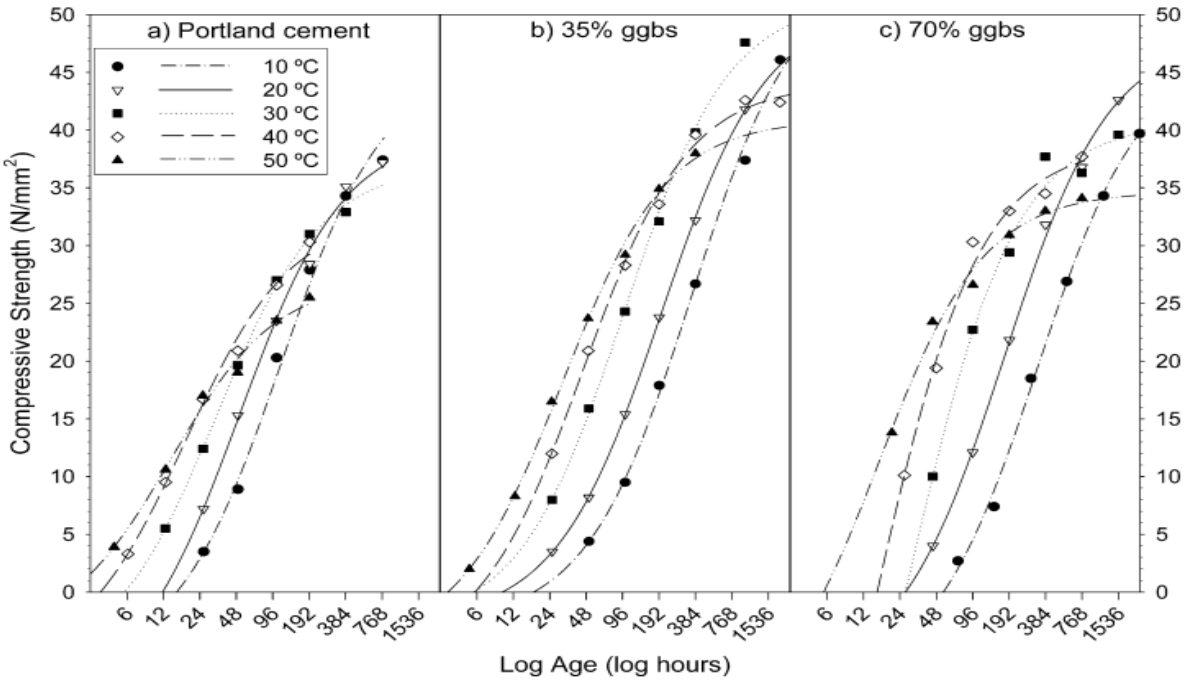

Fig. 2.12. Strength developments of mortars at different curing temperatures [83].

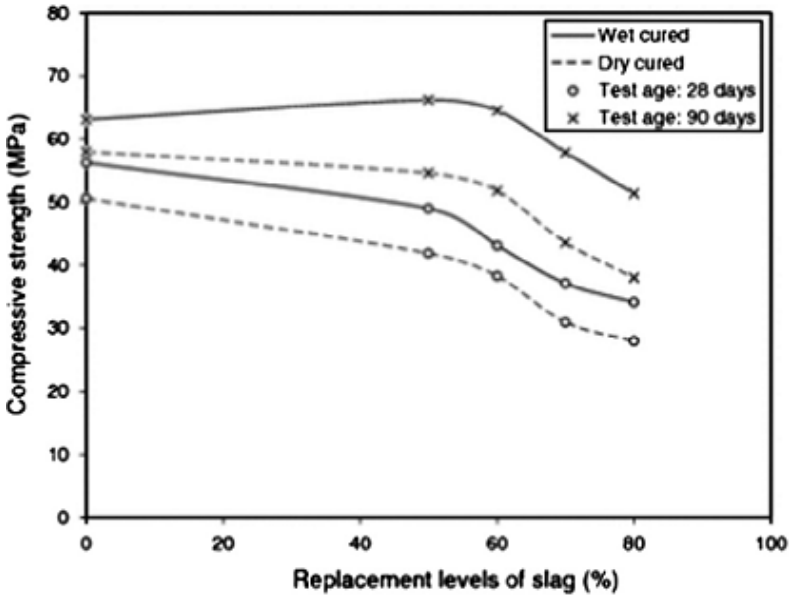

Fig. 2.13. Effects of slag replacement and curing conditions on compressive strength of slag included concretes [84].

2.3.6. Impact of slag on transport properties

The cover concrete plays a key role as the first protective layer for the durability of reinforced concrete structures [87 – 89]. Throughout the service life of a concrete structure, harmful substances in the ambient environment can penetrate or transport into this layer because of its porous microstructure and cause deterioration [90, 91].

The ingress of various ions, liquids and gases from the environment is responsible for the deterioration of concrete directly or indirectly. For instance, the ingress of chlorides or carbon dioxide would depassivate the steel in concrete, and in the presence of oxygen and water, steel may start corroding. Similarly, the ingress of chemicals, such as acids, alkalies and sulfates are responsible for the chemical deterioration of concrete [92]. Therefore, properly assessing the transport properties of cover concrete is a critical and meaningful task for ensuring the longevity and durability of the concrete structure [87, 89, 91]. Additionally, from a practical viewpoint, transport properties are increasingly acknowledged as durability index techniques for classifying cover concrete quality [93], and can be classified into absorption, permeability, and diffusion [89]. Among these, water absorption and air permeability are indicated as appropriate indexes that can provide useful information relating to the pore structure and permeation characteristic of the cover concrete for characterizing and classifying the durability of concrete structures [94 – 96].

It is well understood and documented that use of slag in concrete production modifies the pore sizes and reduces the permeability of concrete substantially due to reaction of slag with the calcium hydroxide and alkalis released during the Portland cement hydration [54, 97 - 99]. Bouikni et al. [100] showed on the basis of pore refinement, that a high OPC replacement of 50 and 65% by slag showed an enhanced performance regarding transport properties, even though total porosity of concrete increased with increasing slag replacement. The capability of slag to reduce concrete permeability is widely accepted however the extent of its impact varies

in literature. Berndt [101] performed permeability tests on concrete specimens with slag/binder ratios of 0%, 50% and 70%, which were wet cured for 84 days and found similar permeability coefficients for all mixes. Contrarily, Cheng et al. [102] obtained permeability coefficients at 91 days, which decreased with increasing slag content. Graf et al. [103] reported that slag concrete can have lower permeability than an equivalent OPC concrete with good curing, but a higher permeability when curing is poor. Effect of water-binder ratio (w/b) and testing age are also studied, and results are simulated in **Fig. 2.14** [104]. Changing the w/b did not significantly alter the effect of slag inclusion on the gas permeability of high performance concrete (HPC). Influence of testing age is obvious on the gas permeability of concretes irrespective of the w/b due to the higher pozzolanic reaction ability at later age and finer size of slag used. Research of G. Camarini [105] on the curing effects on air permeability of concrete reported that steam curing increased air permeability of concretes with slag, and it is higher for lower slag content (see **Fig. 2.15**).

Tasdemir [106] investigated the combined effects of mineral admixtures and curing conditions on the sorptivity of concrete, the sorptivity coefficient of concrete was very sensitive to the curing condition, and the effect of curing condition on the sorptivity coefficient of concrete seems to be higher in low-strength concretes. Liu et al. [107] studied the effect of curing conditions on the permeability of concrete with high volume mineral admixtures. They indicated that the water absorption, capillary water absorption, sorptivity coefficient decrease with the increasing of the curing time, humidity, temperature and slag content. The positive effect of slag on the sorptivity of mortars and concretes has been mentioned in the literature not only for low slag content [108] but especially for higher slag rates up to 50% [109]. An example for the variation in water absorption rate with concrete age and curing condition for the control and slag concretes are given in **Fig. 2.16** [84]. It is clear that rate of water absorption decreases systematically with an increase in curing period (from 28 to 90 days), and the

gradients of the water absorption tends to decrease with increase in the replacement level of slag. Generally, slag concrete performed better than the control concrete and marked improvements in terms of lower rate of water penetration through capillary suction were apparent, particularly under wet curing condition. Hadj-sadok et al. [98] investigated on durability of mortar and concretes containing slag with low hydraulic activity revealed that the coefficient of sorptivity decreases with age of curing and the w/b. Nevertheless, the presence of slag generates an increase in the sorptivity for concrete mixtures with the w/b of 0.65 at 28 and 90 days of curing. As the w/b decreases to 0.42, the sorptivity coefficient at the age of 28 days is similar for all concrete mixtures studied in the present work. At the age of 90 days, a slight reduction of sorptivity coefficient is noticed for concretes containing slag, particularly for concrete mixture B50 (50% slag replacement) (see **Fig. 2.17**)

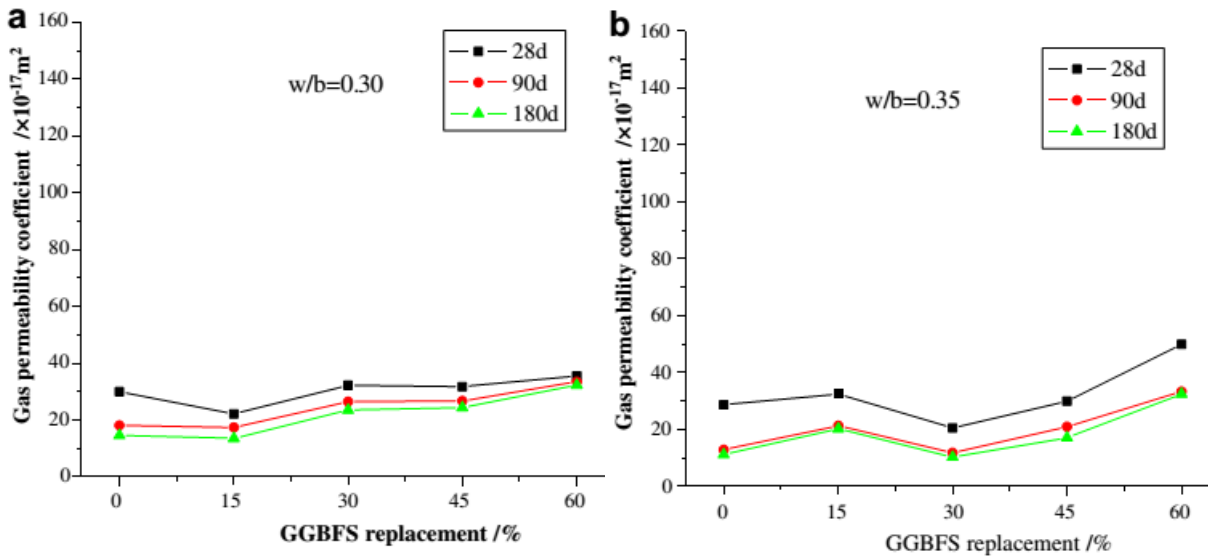

Fig. 2.14. Influence of slag on air permeability of HPC at various w/b ratios [104].

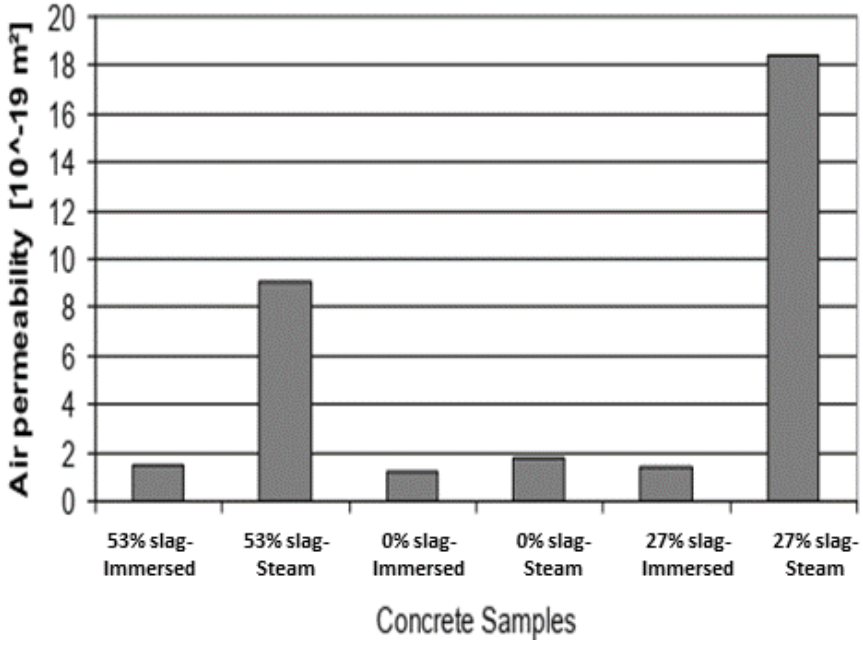

Fig. 2.15. Air permeability of concrete with different curing conditions [105].

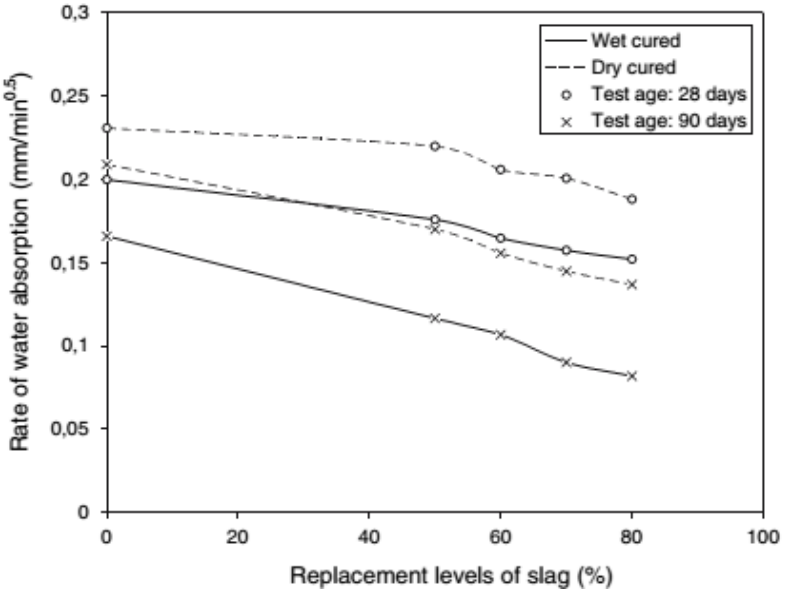

Fig. 2.16. Effects of slag replacement and curing conditions on 28 and 90 days water absorption rate of concretes [84].

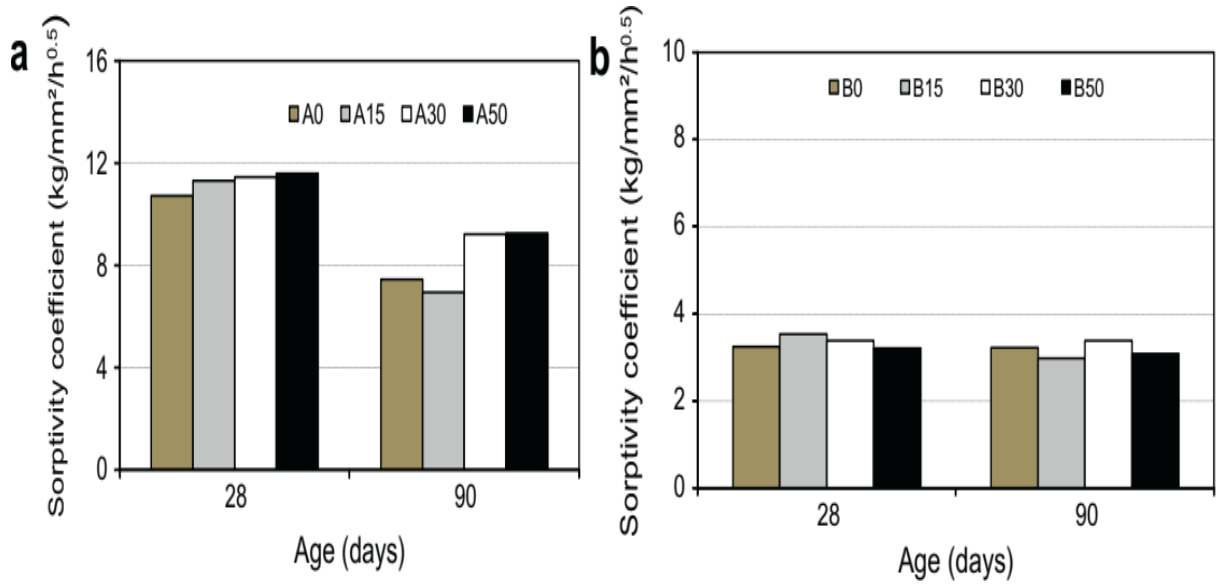

Fig. 2.17. Coefficient of absorption of concrete with: (a) w/b = 0.65 and (b) w/b = 0.42 [110].

2.4. Summary

A comprehensive literature review on the application of expansive concrete as well as estimation methods for its quality control, and the impact of slag on concrete performance has been performed. The expansive concrete is prevalently applied as a countermeasure for shrinkage and cracking in structures. In addition to estimation method for quality control expansive concrete, the newly simplified method for assessment of expansion behavior has been verified in normal condition at 20°C. In the practical, the steam curing is considered suitable for enhancing performances of concretes, particularly on mixes incorporating mineral admixtures, and it is widely applied to precast concrete. However, there have not been any investigations on the applicability of the simplified method to the expansion evaluation of expansive concrete in steam curing so far. In order to widen the application of the simplified method to evaluating the performance of expansive concrete in material design and construction, the verification of the applicability of the simplified method with steam curing is

essential. Thus, in this study, an experimental program was performed to investigate the applicability of the simplified method under steam curing.

Besides, the literature has pointed out the utilization and the efficiency of slag on the properties of mortar/concrete. The suitability of a particular type of slag for use in cementitious materials depends primarily on its reactivity. The main factors influencing the reactivity of slag are its chemical composition, glass content, and particle size distribution. The hydration of the ordinary slag is often relatively slow, it needs to be promoted by incorporating activators. Additionally, many researches indicated that the addition of slag to a concrete mix leads to an increase in drying and autogenous shrinkage, hence decrease in cracking resistance. One of the main countermeasures against such issues is to apply an expansive concrete to compensate for shrinkage and improve cracking resistance by enhancing volumetric stability. Hence, the incorporation of slag in expansive concrete and the effects of such integration offer a promising target for investigation. Although the impacts of slag on the properties of normal Portland cement concrete have been clarified in literature, the study on performance of expansive concrete incorporating slag is scarce. This study therefore investigated the impact of slag types on the engineering properties of expansive concrete. The compressive strength, volumetric change, and two major durability indexes, namely air permeability and water sorptivity, of concrete specimens initially cured under different conditions were examined to quantify the effects of the different incorporated slags.

The comprehensive information about mechanisms of interaction between concrete mix materials during the curing process and their effect on concrete properties could provide best practices for the improved design of concrete mixes, and a better utilization of slag in the field of novel concrete composite materials.

References in chapter 2

[1] Committee on Concrete of the Japan Society of Civil Engineers, Recommended Practice for Expansive Concrete, Concrete library of JSCE, No.23, 1994.

[2] A. Klein, T. Karby, M. Polivka, Properties of an expansive cement for chemical prestressing, ACI J. Proc. 58 (1961) 59–82.

[3] S. Nagataki, H. Gomi, Expansive agents (mainly ettringite), Cem. Concr. Compos. 20 (2-3) (1998) 163-170.

[4] ACI Committee 223. Guide for the use of shrinkage compensating concrete. ACI 223R, 2010.

[5] A. Samdariya, G. Sant, M. Dehadrai, J. Weiss, Concrete durability and service life planning – ConcreteLife'09. RILEM Publications SARL; 2009, pp. 457–465.

[6] D.P. Bentz, O.M. Jensen, Mitigation strategies for autogenous shrinkage cracking, Cement Concr. Compos. 26 (6) (2004) 677–685.

[7] T. Higuchi, M. Eguchi, M. Morioka, E. Sakai, Hydration and properties of expansive additive treated high temperature carbonation, Cem. Concr. Res. 64 (10) (2014) 11–16.

[8] W. Sun, H. Chen, X. Luo, H. Qian, The effect of hybrid fibers and expansive agent on the shrinkage and permeability of high-performance concrete, Cem. Concr. Res. 31 (4) (2001) 595–601.

[9] L. Mo, M. Deng, M. Tang, Effects of calcination condition on expansion property of MgO-type expansive agent used in cement-based materials, Cem. Concr. Res. 40 (3) (2010) 437–446.

[10] J. Han, D. Jia, P. Yan, Understanding the shrinkage compensating ability of type K expansive agent in concrete, Constr. Build. Mater. 116 (2016) 36–44.

[11] D.Y. Yoo, J.J. Park, S.W. Kim, Y.S. Yoon, Combined effect of expansive and shrinkage-reducing admixtures on the properties of ultra high performance fiber-

reinforced concrete, J. Compos. Mater. 48 (16) (2014) 1981–1991.

[12] T. Monji, I. Inoue, I. Yoshikawa, A study on mix design of concrete containing expansive admixture, CAF Review of the 25th General Meeting, 25 (1971) 200-203.

[13] K. Kokubu, Study in freezing and thawing resistance of expansive concrete, JSCE J., 6 (394) (1983) 145-154.

[14] Japan Society of Civil Engineers, Standard Specifications for Concrete Structures Materials and Constructions, JSCE, Tokyo, Japan, 2007, pp. 261–271.

[15] ASTM C 806, Test Method for Restrained Expansion of Expansive Cement Mortar, ASTM International, West Conshohocken, 2018.

[16] ASTM C878 / C878M, Standard Test Method for Restrained Expansion of Shrinkage-Compensating Concrete, West Conshohocken, 2014.

[17] JIS A 6202:2017, Expansive additive for concrete, Japanese Industrial Standards Committee, Tokyo, 2017.

[18] H. Okamura, Y. Tsuji, K. Maruyama, Application of expansive concrete in structural elements, J. Facul. Eng. Univ. Tokyo 34 (3) (1978) 481–507.

[19] US3779085 A (1973), E. K. Rice, Means and method of testing expansive concrete, 73/803.

[20] US5487307 A (1996), R. Landgren, W. F. Perenchio, Method and apparatus for testing concrete expansion.

[21] K. Takayuki, H. Hiroshi, T. Yukikazu, Y. Makoto, Inflation energy of expanded concrete subjected to triaxial restraint by double steel pipe and steel rod, Concr. Eng. Annu. Pap. 15 (1) (1993) 441–446 (in Japanese).

[22] T. Nishikori, Basic study on utilization of expanded concrete to lining iron pipe, Report of JSSE Papers, Report 262 (1977) 129–142 (in Japanese).

[23] K. Tongue, Y. Nyamdoji, Y. Okamura, K. Tsuji, Expansive properties of expansive concrete restrained by eccentric double steel pipe, Cem. Sci. Concr. Technol. 66 (1) (2012) 319–325 (in Japanese).

[24] Y. Tsuji, Estimation of expansive energy in concrete engineering, Concr. J. 26 (10) (1988) 5–13 (in Japanese).

[25] M. Tsujino, H. Hashida, T. Kikuchi, H. Tanaka, Investigation on low shrinkage concrete with expansive additive and limestone aggregate (No.2, quality control method of expansive concrete), AIJ conference proceedings (Hokouriku), A-1, 2010, pp.925-926 (in Japanese).

[26] M. Tsujino, H. Hashida, T. Yuasa, K. Takahashi, Testing method for simple restrained expansion of expansive concrete, JCI proceedings, 33 (1) (2011) 437-442 (in Japanese).

[27] K. Nakarai, Y. Kurihara, H. Hashida, M. Tsujino, Analysis of applicability of simplified estimation method of expansive cement concrete using cylindrical light-weight steel mold based on mechanical work, Cem. Sci. Concr. Technol. 65 (1) (2011) 209–216 (in Japanese).

[28] A. Hosoda, M. Morioka, M. Tanimura, T. Kanda, E. Sakai, T. Kishi, Technical Committee on Performance Evaluation of High Performance Expansive Concrete and System for Crack Control, Technical Committee Reports 2011, Japan Concrete Institute (JCI), Tokyo, Japan, 2011, pp. 65–92.

[29] W.K. Hong, S.Y. Jeong, S.C. Park, J.T. Kim, Experimental investigation of an energy-efficient hybrid composite beam during the construction phase, Energy and Buildings 46 (2012) 37–47.

[30] S. Lee, J. Joo, J.T. Kim, S. Kim, An analysis of the CO2 reduction effect of a column beam structure using composite precast concrete members, Indoor and Built Environment 21 (1) (2012) 150–162.

[31] H.T. Jung, M.S. Lee, A study on the site-production possibility of the prefabricated PC components, Conference of Architectural Institute of Korea 12 (2) (1992) 409–496.

[32] L.S. Pheng, C.J. Chuan, Just-in-time management of precast concrete components, Journal of Construction Engineering and Management 127 (6) (2001) 494–501.

[33] H.S. Kwon, S.J. Kim, M.H. Gong, M.S. Park, S.J. Jung, An experimental study on the strength development of high strength mortar by steam curing, Journal of Architectural Institute of Korea 24 (7) (2008) 85–92.

[34] M. Suzuki, T. Oka, K. Okada, The estimation of energy consumption and CO2 emission due to housing construction in Japan, Energy and Buildings 22 (1995) 165–169.

[35] S.Q. Chen, N.P. Li, J. Guan, Y.Q. Xie, F.M. Sun, J. Ni, A statistical method to investigate national energy consumption in the residential building sector of China, Energy and Buildings 40 (2008) 654–665.

[36] J. Hanson, Optimum steam curing procedure in precasting plants. ACI J Proc 1963.

[37] S.D. Hwang, R. Khatib, H.K. Lee, K. Khayat, Optimization of steam-curing regime for high-strength, self-consolidating concrete for precast, prestressed concrete applications, PCI J. 57 (2012) 48–61.

[38] Q.B. Yang, Q.R. Yang, P.R. Zhu, Scaling and corrosion resistance of steam-cured concrete, Cem. Concr. Res. 33 (7) (2003) 1057–1061.

[39] A.M. Ramezanianpour, Kh. Esmaeili, S.A. Ghahari, A.A. Ramezanianpour, Influence of initial steam curing and different types of mineral additives on mechanical and durability properties of self-compacting concrete, Constr. Build. Mater. 73 (2014) 187–194.

[40] A.A. Ramezanianpour, M.H.Khazali, P. Vosoughi, Effect of steam curing cycles on strength and durability of SCC: a case study in precast concrete, Constr. Build. Mater. 49 (2013) 807–813.

[41] F.M. Lea, The chemistry of cement and concrete, 3rd ed. Chemical Publishing Co. New York, 1971, pp. 454-489.

[42] M. Moranville-Regourd, Cements made from Blast furnace Slag. In: Hewlett PC (ed) Lea's Chemistry of Cement and Concrete, Edward Arnold (Publishers) Ltd., London, 1998, pp. 633-674.

[43] N.M. Piatak, M.B. Parsons, R.R. Seal, Characteristics and environmental aspects of slag: a review, Appl. Geochem. 57 (2015) 236–266.

[44] C. Shi, J. Qian, High performance cementing materials from industrial slags – a review, Resour. Conserv. Recycl. 29 (2000) 195–207.

[45] ACI 233 R03, Slag Cement in Concrete and Mortar, Detroit, Michigan, 2000.

[46] N. De Belie, M. Soutsos, E. Gruyaert, Properties of fresh and hardened concrete containing supplementary cementitious materials: state-of-the-art report of the RILEM technical committee 238-SCM Working Group 4, vol. 25. Springer International Publishing, Cham, 2018.

[47] P.C. Nkinamubanzi, M. Baalbaki, J. Bickley, P.C. Aitcin, The use of slag for making high performance concrete, in: Sixth NCB International Seminar on Cement and Building Materials, XIII, NCB, New Delhi, 1998, pp. 13–39.

[48] S.C. Pal, A. Mukherjee, S.R. Pathak, Investigation of hydraulic activity of ground granulated blast furnace slag in concrete, Cem. Concr. Res. 33 (2003) 1481–1486.

[49] A.M. Neville, Properties of Concrete, fourth ed., ELBS Publication, Addison–Wesley Longman Limited, Essex, UK, 1996.

[50] B. Lothenbach, K. Scrivener, R.D. Hooton, Supplementary cementitious materials, Cem. Concr. Res. 41 (2011) 1244–1256.

[51] M. Regourd, Characterization of thermal activation of slag cements, in: Proceedings of 7th International Congress on the Chemistry of Cements, Septima, Paris, vol. 2, III-3, 1980, pp. 105–111.

[52] M. Regourd, Microanalytical studies (X-ray photo electron spectrometry) of surface hydration reactions of cement compounds, Philos. Trans. R. Soc. London Ser. A 310 (1511) (1980) 85–91.

[53] M. Regourd, Structure and behavior of slag Portland cement hydrates, in: Proceedings of 7th International Congress on the Chemistry of Cements, Septima, Paris, vol. 1, III-2, 1980, pp. 10–18.

[54] H.F.W. Taylor, "Cement Chemistry," 2nd Edition, Thomas Telford, London, 1997.

[55] S. Song, H.M. Jennings, Pore solution chemistry of alkali-activated ground granulated blast-furnace slag, Cem. Concr. Res. 29 (1999) 159–170.

[56] F. Bellmann, J. Stark, Activation of blast furnace slag by a new method, Cem. Concr. Res. 39 (2009) 644–650.

[57] C.Q. Hua, A.T. Hamou, S. Sarkar, Strength and Microstructural Properties of Water Glass Activated Slag, MRS Proceedings, UK, 1991, pp. 49.

[58] H. Park, Y. Jeong, Y. Jun, J.H. Jeong, J.E. Oh, Strength enhancement and pore-size refinement in clinker-free CaO activated GGBFS systems through substitution with gypsum, Cem. Concr. Compos. 68 (2016) 57 – 65.

[59] K. Gu, F. Jin, A. Al-Tabbaa, B. Shi, Activation of ground granulated blast furnace slag by using calcined dolomite, Constr. Build. Mater. 68 (2014) 252 - 258.

[60] M.S. Kim, Y. Jun, C. Lee, J.E. Oh, Use of CaO as an activator for producing a price-competitive non-cement structural binder using ground granulated blast furnace slag, Cem. Concr. Res. 54 (2013) 208 - 214.

[61] K. Gu, F. Jin, A. Al-Tabbaa, B. Shi, J. Liu, Mechanical and hydration properties of ground granulated blast furnace slag pastes activated with MgO-CaO mixtures, Constr. Build. Mater. 69 (2014) 101 - 108.

[62] N.C. Collier, X.Li, Y. Bai, N.B. Milestone, The effect of sulfate activation on the early age hydration of BFS:PC composite cement, J. Nucle. Mater. 464 (2015) 128–134.

[63] A. Gruskovnjak, B. Lothenbach, F. Winnefeld, R. Figi, S.-C. Ko, M. Adler, et al., Hydration mechanisms of super sulphated slag cement, Cem. Concr. Res. 38 (7) (2008) 983-992.

[64] M. Singh, M. Garg, Calcium sulfate hemihydrate activated low heat sulfate resistant cement, Constr. Build. Mater. 16 (3) (2002) 181 - 186.

[65] J.J. Chang, W. Yeih, C.C. Hung, Effects of gypsum and phosphoric acid on the properties of sodium silicate-based alkali-activated slag pastes, Cem. Concr. Comp. 27 (1) (2005) 85 - 91.

[66] D. Bondar, E. Coakley, Use of gypsum and CKD to enhance early age strength of High Volume Fly Ash (HVFA) pastes, Constr. Build. Mater. 71 (0) (2014) 93 - 108.

[67] T. Matschei, F. Bellmann, J. Stark, Hydration behaviour of sulphate-activated slag cements, Adv. Cem. Res. 17 (4) (2005) 167 - 178.

[68] C.A. da Luz, R.D. Hooton, Influence of curing temperature on the process of hydration of supersulfated cements at early age, Cem. Concr. Res. 77 (2015) 69–75.

[69] H. El-Chabib, A. Syed, Properties of self-consolidating concrete made with high volumes of supplementary cementitious materials, J. Mater. Civ. Eng. 25 (2013) 1579–1586.

[70] A. Darquennes, E. Roziere, M.I.A. Khokhar, P. Turcry, A. Loukili, F. Grondin, Long-term deformations and cracking risk of concrete with high content of mineral additions, Mater. Struct. 45 (2012) 1705–1716.

[71] J.J. Brooks, P.J. Wainwright, M. Boukendakji, Influence of slag type and replacement level on strength, elasticity, shrinkage, and creep of concrete, in: Proceedings of the Fourth International Conference on Fly Ash, Silica Fume, Slag, and Natural Pozzolans in Concrete, SP-132, American Concrete Institute, Farmington Hills, Mich., vol. 2, 1992, pp. 1325–1341.

[72] R.D. Hooton, K. Stanish, J.P. Angel, J. Prusinski, The Effect of Ground Granulated Blast Furnace Slag (Slag Cement) on the Drying Shrinkage of Concrete - a Critical Review of the Literature SP 263, 2009, pp. 79 – 94.

[73] M. Shariqa, J. Prasad, H. Abbas, Creep and drying shrinkage of concrete containing GGBFS, Cem. Concr. Compos. 68 (2016) 35 – 45.

[74] I. Pane, W. Hansen, Investigation on key properties controlling early-age stress development of blended cement concrete, Cem. Concr. Res. 38 (2008) 1325–
1335.

[75] E. Tazawa, S. Miyazawa, Influence of cement and admixture on autogenous shrinkage of cement paste, Cem. Concr. Res. 25 (1995) 281–287.

[76] I. Maruyama, A. Teramoto, Impact of time-dependent thermal expansion coefficient on the early-age volume changes in cement pastes, Cem. Concr. Res. 41 (2011) 380–391.

[77] K.M. Lee, H.K. Lee, S.H. Lee, G.J. Kim, Autogenous shrinkage of concrete containing granulated blast-furnace slag, Cem. Concr. Res. 36(7) (2006) 1279 – 1285.

[78] ACI 233R-03, Slag Cement in Concrete and Mortar. American Concrete Institute, 2011.

[79] E. Özbaya, M. Erdemirb, H.İ. Durmuş, Utilization and efficiency of ground granulated blast furnace slag on concrete properties—A review, Constr. Build. Mater. (2016) 423–434.

[80] M. Ramalekshmi, R. Sheeja and R. Gopinath, “Experimental Behaviour of Reinforced Concrete with Partial Replacement of Cement with Ground Granulated
Blast Furnace Slag”, International Journal of Engineering Research & Technology (IJERT), Vol. 3, Issue 3, Mar. 2014, pp.525-534, ISSN: 2278-0181.

[81] S. Samad, A. Shah, M.C. Limbachiya, Strength development characteristics of concrete produced with blended cement using ground granulated blast furnace slag (GGBS) under various curing conditions, Sādhanā, 42 (2017) 1203–1213.

[82] R. Rughooputh, J. Rana, Partial Replacement of Cement by Ground Granulated Blast Furnace Slag in Concrete, Journal of Emerging Trends in Engineering and Applied Sciences (JETEAS), Vol. 5, Issue 5, 2014, pp. 340-343, ISSN: 2141-7016.

[83] S.J. Barnett, M.N. Soutsos, S.G. Millard, J.H. Bungey, Strength development of mortars containing ground granulated blast-furnace slag: Effect of curing temperature and determination of apparent activation energies, Cem. Concr. Res. 36 (2006) 434 – 440.

[84] E. Guneyisi, M. Gesoglu, A study on durability properties of high-performance concretes incorporating high replacement levels of slag, Mater. Struct. 41 (2008) 479–493.

[85] D. N. Richardson, Strength and durability of a 70% ground granulated blast furnace slag concrete mix, Organizational Research Report No. RI99-035/RI99-035B, Missouri Department of Transportation, USA, (2006).

[86] A. Oner, S. Akyuz, An experimental study on optimum usage of GGBS for the compressive strength of concrete, Cem. Concr. Compos. 29 (2007) 505–514.

[87] Z. Cui, A. Alipour, Cover concrete cracking and service life prediction of reinforced concrete structures in corrosive environments, Constr. Build. Mater. 147 (2017) 352–361.

[88] Ł. Sadowski, T.G. Mathia, Multi-scale metrology of concrete surface morphology: fundamentals and specificity, Constr. Build. Mater. 113 (2016) 613–621.

[89] A.E. Long, G.D. Henderson, F.R. Montgomery, Why assess the properties of near-surface concrete ?, Constr. Build. Mater. 15 (2001) 65–79.

[90] S.W.Tang, Y.Yao, C. Andrade, Z.J. Li, Recent durability studies on concrete structure, Cem. Concr. Compos. 78 (2015) 143–154.

[91] H. Beushausen, R.Torrent, M.G. Alexander, Performance-based approaches for concrete durability: State of the art and future research needs, Cem. Concr. Res. 119 (2019) 11-20.

[92] L. Basheer, J. Kropp, D. J. Cleland, Assessment of the durability of concrete from its permeation properties: a review, Constr. Build. Mater. 15 (2001) 93 – 103.

[93] F.T. Olorunsogo, N. Padayachee, Performance of recycled aggregate concrete monitored by durability indexes, Cem. Concr. Res. 32 (2002) 179–185.

[94] D.W.S. Ho, G.J. Chirgwint, A performance specification for durable concrete, Constr. Build. Mater. 10 (1996) 375–319.

[95] D.N. Katpady, H. Hazehara, M. Soeda, T. Kubota, S. Murakami, Durability assessment of blended concrete by air permeability, Intern. J. Concr. Struct. Mater. 12 (2018) 30.

[96] K. Nakarai, K. Shitama, S. Nishio, Y. Sakai, H. Ueda, T. Kishi, Long-term permeability measurements on site-cast concrete box culverts, Constr. Build. Mater. 198 (2019) 777-785.

[97] E. Gruyaert, Effect of blast-furnace slag as cement replacement on hydration, microstructure, strength and durability of concrete, Ghent, Ghent University, 2011.

[98] A. Hadj-Sadok, S. Kenai, L. Courard, A. Darimont, Microstructure and durability of mortars modified with medium active blast furnace slag, Const. Bldg. Matls. 25 (2011) 1018–1025.

[99] M.A.M. Johari, J.J. Brooks, S. Kabir, P. Rivard, Influence of supplementary cementitious materials on engineering properties of high strength concrete, Const. Bldg. Mater. 25 (2011) 2639 – 2648.

[100] A. Bouikni, R.N. Swamy, A. Bali, Durability properties of concrete containing 50% and 65% slag. Const. Bldg. Mater. 23 (2009) 2836–2845.

[101] M.L. Berndt, Properties of sustainable concrete containing fly ash, slag and recycled concrete aggregate, Const. Bldg. Mater. 23 (2009) 2606 - 2613.

[102] A. Cheng, R. Huang, J.K. Wu, C.H. Chen, Influence of GGBS on durability and corrosion behavior of reinforced concrete, Matls. Chem. Phys. 93 (2005) 404 - 411.

[103] H. Graf, H. Grube, The influence of curing on the gas permeability of concrete with different compositions. Proc. RILEM Seminar on Durability of Concrete Structures under Normal Outdoor Exposure, Hanover University, 1984, pp. 80 - 87.

[104] S. Hui-sheng, X. Bi-wan, Z. Xiao-chen, Influence of mineral admixtures on compressive strength, gas permeability and carbonation of high performance concrete, Constr. Build. Mater. 23 (2009) 1980–1985.

[105] G. Camarini, Curing effects on air permeability of concrete, Adv. Mater. Res. 214 (2011) 602 – 606.

[106] C. Tasdemir, Combined effects of mineral admixtures and curing conditions on the sorptivity coefficient of concrete, Cem. Concr. Res. 33 (2003) 1637–1642.

[107] B. Liu, G. Luo, Y. Xie, Effect of curing conditions on the permeability of concrete with high volume mineral admixtures, Constr. Build. Mater. 167 (2018) 359–371.

[108] E. Vejmelkova, M. Pavlikova, Z. Keršner, P. Rovnanikova, M. Ondracek, M. Sedlmajer, High performance concrete containing lower slag amount: a complex view of mechanical and durability properties, Constr. Build. Mater. 23(6) (2009) 2237–2245.

[109] M.G. Alexander, B.J. Magee, Durability performance of concrete containing condensed silica fume, Cem. Concr. Res. 29(6) (1999) 917–922.

Chapter 3. The applicability of simplified method to expansion evaluation of expansive concrete

3.1. Introduction

A simplified method has been proposed as a substitute for conventional methods to evaluate the behavior of expansive concrete. Some studies have validated the simplified method under normal conditions. They indicated that the simplified and conventional methods show a strong correlation at 20 °C. Besides, in the steam curing, as a typical curing method in precast concrete field, there have not been any investigations into the expansion evaluation so far. Thus, in this chapter, the applicability of the simplified method to expansive concrete that is steam-cured under constraint was experimentally investigated by comparison to the results with the conventional method based on the expansive energies. The specimens were cured with steam or at 20 °C from the initial casting for 1 day. They were then sealed or immersed in water at 20 °C for 7 days. The specimens for the simplified method were measured strains in the circumferential and axial directions, whereas the sample for the conventional method were obtained a strain in a uniaxial direction. The range of applicability of the simplified method was analyzed. A new concept for the simplified method of estimating the expansion by using the axial strain was then proposed. Based on the results of the experiment, the use of the simplified method under steam curing was verified.

3.2. Outline of experiments

3.2.1. Materials and mixture proportions

Table 3.1 presents the properties of the materials used in this experiment. The chemical compositions of the cement and expansive agent are given in **Table 3.2**. The mixture

proportions of the expansive concrete, which was adopted from the mix design usually used in some precast concrete factories as shown in **Table 3.3**. In general, the amount of cement substituted by the expansive agent is about around 30–60 kg/m^3 for chemically prestressed concrete [1]. To evaluate the performance of the chemically prestressed concrete, unit contents of 30, 50, and 60 kg/m^3 for the expansive agent were used in this experiment. For the material design, the slump of the concrete mixture was 8.0 ± 2.0 cm, and the air content was 4.5% ± 1.5%.

Table 3.1 Material properties

Materials	Type	Properties	Notion
Cement	Ordinary Portland cement conforming to JIS R 5210 (equivalent to CEM I cement type in BS EN 197-1)	Density: 3.16 g/cm3 Specific surface area: 3370 cm2/g (Strength class: similar to 42.5 N strength class in BS EN 197-1)	C
Expansive agent	Ettringite type (based on calcium sulfoaluminate)	Density: 2.95 g/cm^3 Specific surface area: 2900 cm^2/g	Ex
Fine aggregate	Crushed sandstone	Fineness modulus: 2.97 Surface-dry density: 2.58 g/cm^3 Water absorption: 1.63 %	S
Coarse aggregate	Crushed rhyolitic gravel	Grain sizes: 5–20 mm full grade Surface-dry density: 2.61 g/cm^3 Water absorption: 0.64 %	G
Chemical agents	Air entraining and water reducing agents	Denatured rosin acid-based and ligninsulfonic acid type	Ad

Table 3.2 Chemical compositions of the cement and expansive agent (%)

Components	SiO_2	Al_2O_3	Fe_2O_3	CaO	MgO	K_2O	Na_2O	SO_3	LOI
C	20.06	5.12	3.05	64.85	1.29	0.38	0.29	1.92	2.27
Ex	1.5	9.0	0.6	51.8	1.4	0.29	0.15	29	2.55

Note: LOI is loss of ignition.

Table 3.3 Mix proportions of expansive concrete

Specimen names	W/B (%)	s/a (%)	Unit mass (kg/m^3) W	C	Ex	S	G
Ex30	45	43	168	343	30	769	1030
Ex50			168	323	50	769	1030
Ex60			168	313	60	769	1030

Note: W/B is the water-to-binder (C + Ex) mass ratio. s/a is the sand-to-aggregate volume ratio.

3.2.2. Preparation of specimens and experimental methods

(a) Evaluating the expansive strain with a restraining bar (JIS method)

In this study, the conventional evaluation method for expansive concrete was carried out by using a prismatic specimen (100 mm × 100 mm × 360 mm) with a restraining bar at the centroid of the specimen as stipulated in the JIS A 6202 standard [2]. The expansive strains of each specimen were measured by attaching two self-temperature-compensated wire strain gauges to the upper and lower surfaces at the center portion of the restraining bar [3–5]. The strain gauges

were used instead of the dial gauge instrument to automatically and continuously record data. The temperature of each specimen was obtained continuously with a thermocouple near the strain gauge inside the concrete. **Fig. 3.1(a)** outlines the specimen test for the JIS method. The expansive strains of the specimen were measured from initial casting to 7 days. At least three duplicate specimens were prepared under each condition, and the average measured value of the three specimens was used for the discussion.

Strain gauges were bonded to the restraining bar before being treated by three cycles of thermal history with a maximum temperature of 70 °C. This treatment was conducted to calibrate the strain gauge by alleviating its residual strain to make the thermal change small before operation. An example of the preprocessing result is shown in **Fig. 1(a)** (Appendix A).

The strains due to the thermal output [6] of the restraining device were measured by recording changes in the strain of the dummy restraining device during the heat treatment process before the experiments (see appendix A). The thermal output was canceled by being subtracted from the measured strain of specimens.

(b) Evaluating the expansive strain with a cylindrical mold (simplified method)

The simplified method for measuring the constrained expansion of expansive concrete uses a cylindrical tinplate mold (ϕ100 mm × 200 mm, 0.28 mm thickness) with an open top, an uninterrupted upstanding sidewall, and a closed bottom as shown in **Fig. 3.1(b)**. For a cylindrical specimen, the expansive strain has been observed to be almost constant at the middle height, but it decreases at the edge because of closed bottom or open top [7]. Thus, the strains generated at the mid-height were used as the measurement target [8–10]. Two strain gauges were glued horizontally and vertically at mid-height on the outside surface of the mold. The expansive strains of samples were also measured until 7 days after casting. At least three duplicate specimens were made for each case. A thermocouple was used to monitor the temperature inside the specimens.

The strain gauges were used after the residual strain due to the thermal change was confirmed to be small. One example of the preprocessing result is shown in **Fig. 1(b)** (Appendix A). The thermal outputs of the restraining device were also eliminated before the data analysis.

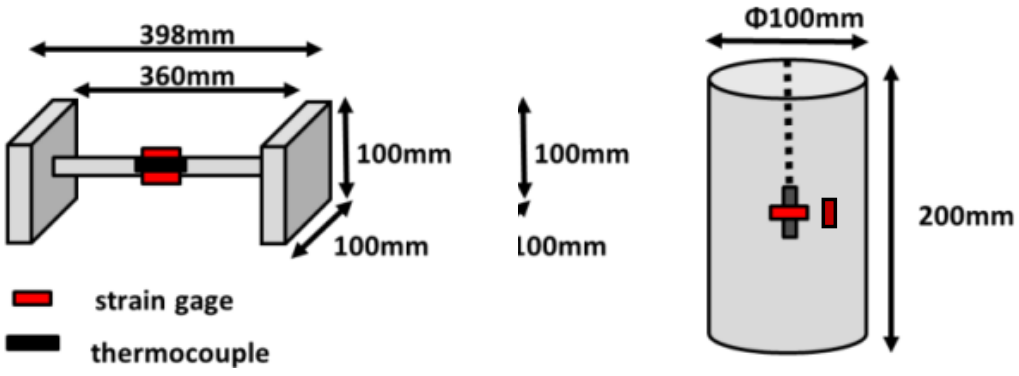

(a) (b)

Fig. 3.1. Specimens for the (a) JIS and (b) simplified methods.

(c) Mixing and casting procedures

First, fine materials including the cement, expansive agent, and sand were mixed together in a forced mechanical mixer for 30 s to achieve an initial homogeneity. Thereafter, a blend of water and chemical agents was steadily added to the drying mixture followed by 60 s of mixing. The wet mixture was mixed for 30 s more to achieve a higher homogeneity. Finally, coarse aggregates were poured in the mixture and incorporated by operating the mixer for 2 min. The fresh state of the fabricated concrete mixes was assessed by measuring the slump flow and air content according to ASTM C 143/C 143M [11] and ASTM C 231[12], respectively.

Immediately after the mixing process, all specimens were molded as stipulated for both evaluation methods of expansive concrete. This casting procedure conforms to ASTM C 192/C 192M [13].

3.2.3. Curing conditions

Several preceding studies applied a 24 h steam curing cycle with elevated temperature at atmospheric pressure, which was considered sufficient to effectively enhance the performance of precast concretes and the rate of concrete element production [14 - 18]. A typical steam curing cycle consists of a pre-curing treatment of up to 4 h and a heating and cooling rate of 10 – 45 ºC/h. The maximum temperature reached in steam curing is usually limited to 60±5 ºC and this temperature is kept constant at the maximum value for 6 - 18 h. However, the high temperature for longer hours (for instance during steam curing) can lead to detrimental changes in porosity and pore size distribution of concrete which can significantly reduce mechanical and durability properties, especially over the long term [18 - 20]. **Fig. 3.2** shows the target ambient temperature profile used in this experiment which is similar to a typical steam curing process in general precast concrete factories [21 - 23]. Steam from a pipeline was applied for 24 h to maintain an ambient relative humidity of 90% ± 10% and the temperature was elevated to a maximum of 65 °C (i.e., steam curing). In addition, the sealed specimens were cured in a room where the temperature was controlled at 20 °C as the reference (i.e., 20 °C curing). The specimens cured under steam or at 20 °C for 24 h were then sealed or cured in water at 20 °C for up to 7 days of aging to investigate the effect of the later curing conditions. In the case of the simplified method, all specimens were cured without demolding over 7 days. The JIS samples were demolded after being aged for 1 day. Sealed specimens were wrapped with two layers of adhesive aluminum foil to prevent moisture loss.

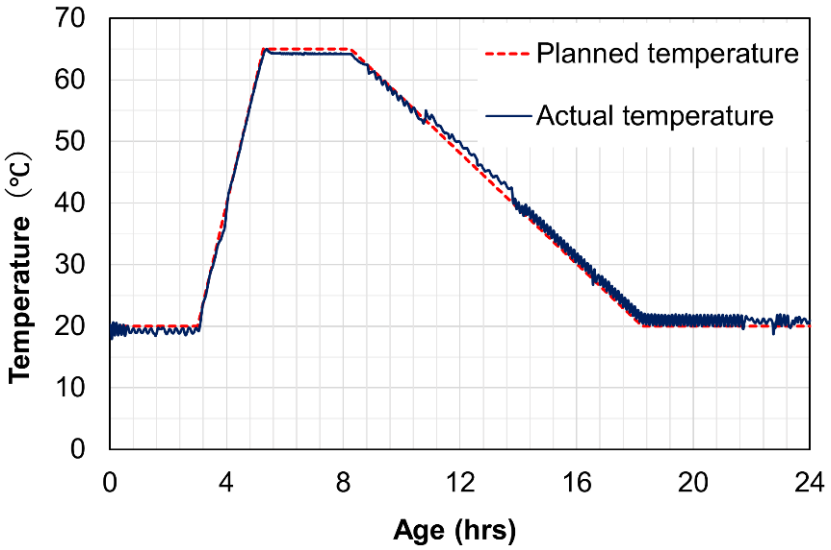

Fig. 3.2. Steam curing cycle.

3.3. Experimental results and discussion

3.3.1. Time histories of the expansive strains

Fig. 3.3 shows the time histories of the expansive strains at 20 °C curing that were measured with the two testing methods over 7 days. The expansive strains showed typical behavior by increasing quickly over the first 3 days with no or just slight increases afterwards. This can be ascribed to the developing strength of the concrete inhibiting its expansion [21, 24]. Regarding the curing conditions after 1 day, water curing increased the expansive strains because it stimulated the hydration degree of the expansive agent [25]. The JIS method showed a substantial increase in the measured strains.

Fig. 3.4 presents the time histories of the expansive strains with steam curing according to the two measurement methods. In this case, the growth in the expansive strain was sharply accelerated for the first day of aging. In detail, the expansive strain showed a slight decrease followed by an increase during this period. These trends can be attributed to the difference between the coefficients of thermal expansion of the concrete and restraining steel as the curing temperature changed [26, 27]. The expansive strains did not increase with further aging after 1

day. This indicates that the hydration of the expansive agent was almost complete after 1 day because of the high temperature during steam curing. The expansive strain slightly decreased later during the curing period; this may have been caused by autogenous shrinkage of the hardening concrete [28 - 30]. In the case of Ex60, the circumferential strain of the cylindrical samples jumped to an extreme value and greatly diverged from those with the other dosages. This may be because of the plastic deformation of the cylindrical steel mold when the expansive force induced stress that exceeded the offset yield strength of the mold [31]. This offset yield strength was determined according to ASTM D 638 – 02a [32] based on the empirical results from a previous study [9]. The strain of the steel mold corresponding to the offset yield strength was 810×10^{-6}, as shown in **Fig. 3.5**. The measured strains of over 810×10^{-6} with the simplified method means that the expansive behavior was overestimated, as discussed later.

The measured strains with steam curing were notably larger than those with 20 °C curing. This may be because when the concrete was cured at a high elevated temperature, the supply of activation energy [33] and formation of massive stick-like ettringite in the cement paste matrix [21] hastened expansion in the initial curing period. In contrast, the chemical reaction transpired stagnantly with 20 °C curing, and mostly crystalline ettringite grew in pores to contribute less to expansion [21].

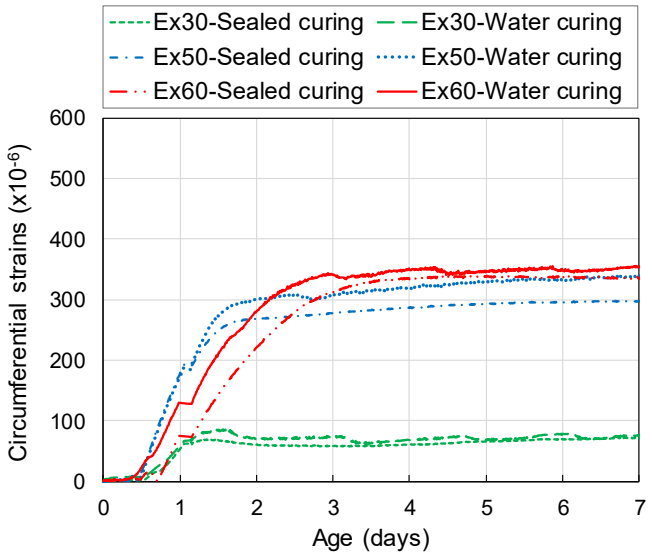

(a)

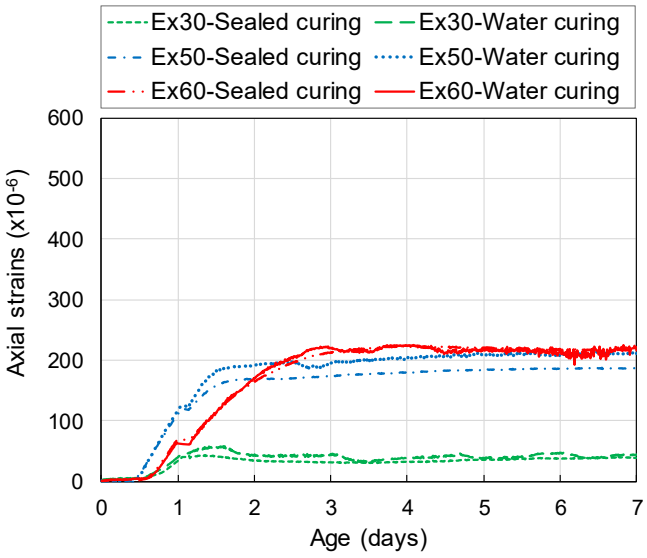

(b)

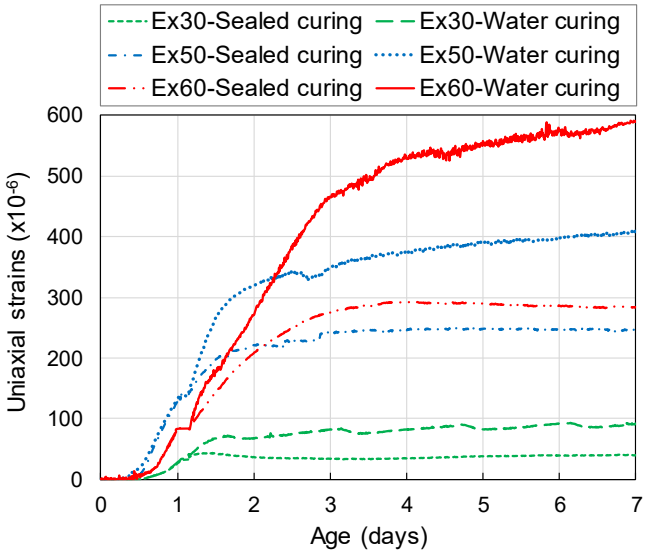

(c)

Fig. 3.3. Time histories of the expansive strains during curing at 20 °C: (a) circumferential strains of the cylindrical specimens, (b) axial strains of the cylindrical specimens, and (c) uniaxial strains of the JIS specimens.

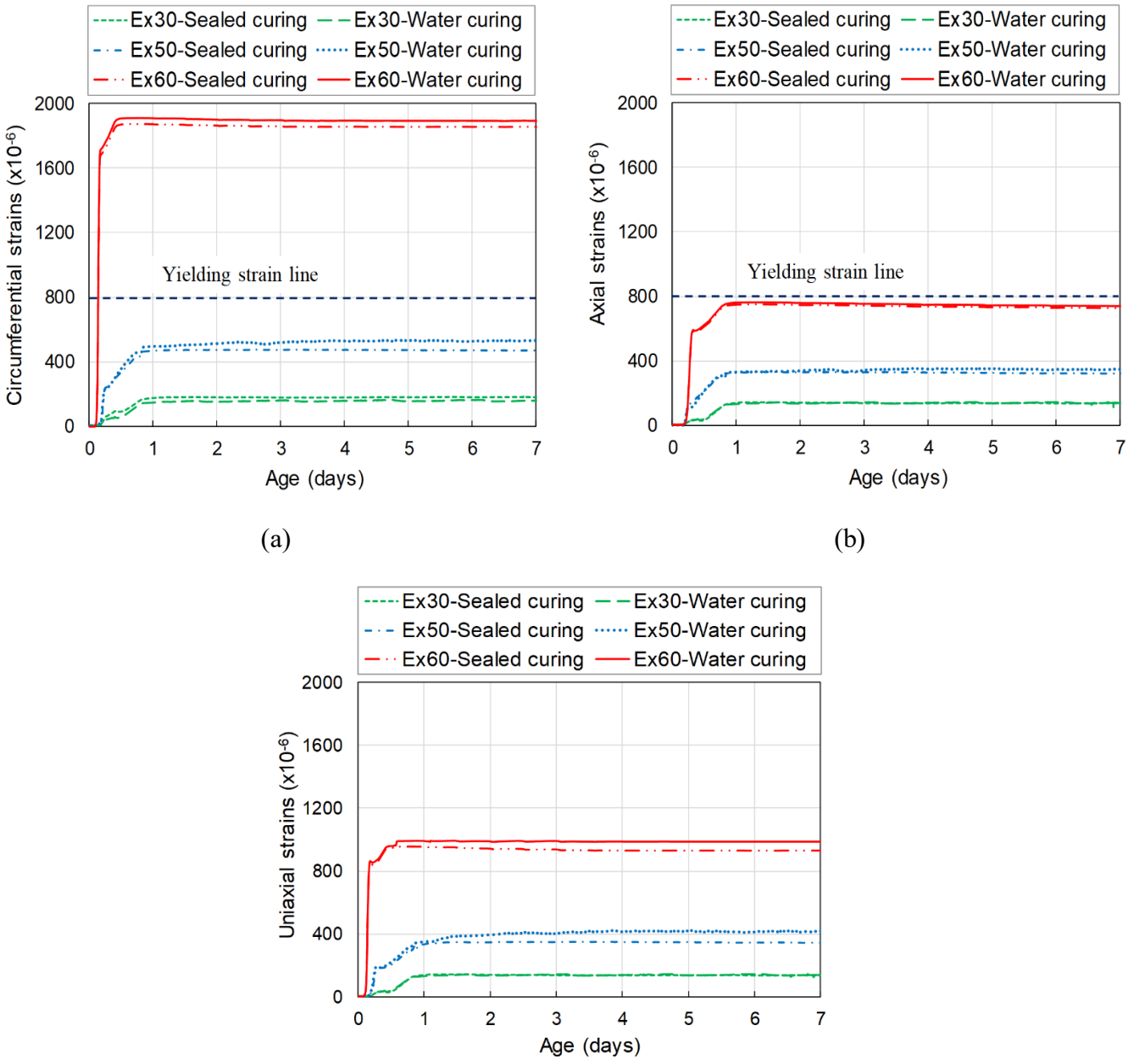

Fig. 3.4. Time histories of the expansive strains with steam curing: (a) circumferential strains of the cylindrical specimens, (b) axial strains of the cylindrical specimens, and (c) uniaxial strains of the JIS specimens.

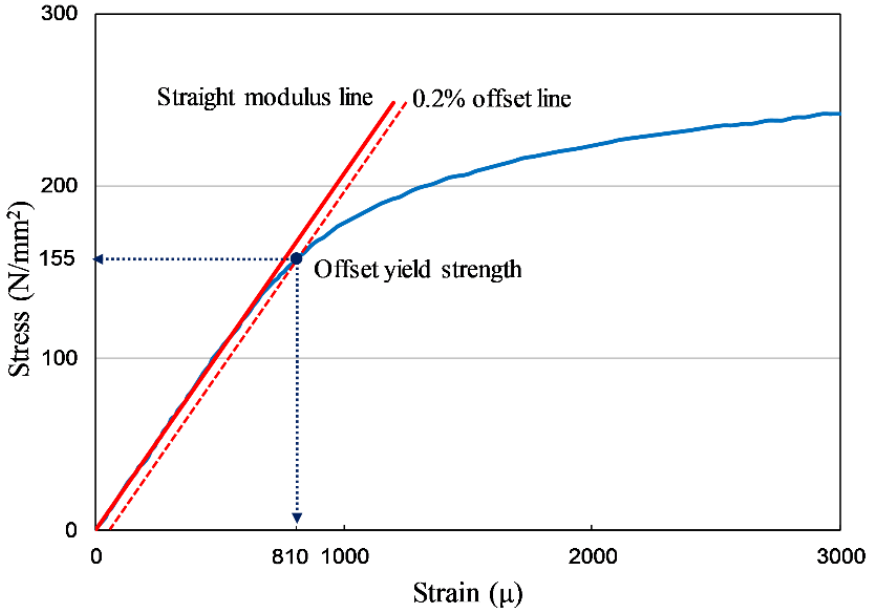

Fig. 3.5. Stress–strain curve for the steel mold with the simplified method [9].

3.3.2. Effect of curing and constraint conditions on expansion

3.3.2.1. Method of consideration

To investigate the relationships between the expansive strains measured with the two estimation methods under various conditions, the expansive energy was determined [33 - 35]. The expansive energy of concrete used for the JIS uniaxial constraint method can be calculated as follows [34 - 36]:

$$U_{JIS} = \frac{1}{2} \cdot \rho \cdot E_s \cdot \varepsilon_{JIS}^2 \qquad (3.1)$$

where U_{JIS} is the calculated expansive energy of concrete per unit volume (N/mm^2) with the JIS method, ε_{JIS} is the measured expansion strain of the JIS samples, ρ is the restraining steel ratio of the uniaxially restraining steel bar (= 0.0096), and E_s is the Young's modulus of the bar (= 2.1 × 10^5 N/mm^2).

The simplified method with the thin cylindrical steel mold having an open top has been verified in preceding studies [9, 10, 37]. Accordingly, the internal expansive pressure was determined from the strain generated in the cylindrical steel mold by using the thin-wall hollow cylinder model with circumferential and axial components. Normally, the circumferential strain is used as the expansive strain of concrete with the simplified method because of the greater measured value as ascertained in previous studies [9, 10]. The expansive energies in the circumferential and axial directions of the cylindrical specimens can be obtained with Eqs. (3.2) and (3.3), respectively [10, 34]:

$$U_\theta = \frac{t}{r} \cdot \frac{E_S}{1-\nu^2} \cdot (\varepsilon_\theta + \nu \cdot \varepsilon_z) \cdot \varepsilon_\theta \quad (3.2)$$

$$U_z = \frac{t}{r} \cdot \frac{E_S}{1-\nu^2} \cdot (\varepsilon_z + \nu \cdot \varepsilon_\theta) \cdot \varepsilon_z \quad (3.3)$$

where U_θ is the calculated expansive energy of concrete per unit volume (N/mm^2) in the circumferential direction, U_z is the calculated expansive energy of concrete per unit volume (N/mm^2) in the axial direction, ε_θ is the measured circumferential strain of the cylindrical specimens, ε_z is the measured axial strain of the cylindrical specimens, t is the thickness of steel mold (= 0.28 mm), r is the mold radius (= 50 mm), and ν is Poisson's ratio of the steel mold (= 0.3).

The relations among the expansive energies obtained with the two measurement methods are described in Eqs. (3.4) and (3.5), which were derived from the experimental results of previous studies [10]. The relationships of the expansive strains can be deduced from the expansive energy obtained from Eqs. (3.1) – (3.5) and are expressed in Eqs. (3.6) and (3.7).

$$U_\theta = 2 \cdot U_{JIS\_seal} \quad (3.4)$$

$$U_z = U_{JIS\_seal} \tag{3.5}$$

$$\varepsilon_\theta = \left(\frac{r}{t}\cdot(1-\nu^2)\cdot\rho\cdot\left(1+\frac{-\nu+\sqrt{\nu^2+8}}{4}\cdot\nu\right)^{-1}\right)^{\frac{1}{2}}\cdot\varepsilon_{JIS\_seal} = 1.14\cdot\varepsilon_{JIS\_seal} \tag{3.6}$$

$$\varepsilon_z = \left(\frac{1}{2}\cdot\frac{r}{t}\cdot\rho\cdot(1-\nu^2)\cdot\frac{-\nu+\sqrt{\nu^2+8}}{3\cdot\nu+\sqrt{\nu^2+8}}\right)^{\frac{1}{2}}\cdot\varepsilon_{JIS\_seal} = 0.73\cdot\varepsilon_{JIS\_seal} \tag{3.7}$$

Here, U_{JIS_seal} and ε_{JIS_seal} are the calculated expansive energy per unit volume (N/mm^2) and measured uniaxial strain of the JIS samples when sealed after aging for 1 day, respectively.

3.3.2.2. Effect of constraints on expansion

The influences of the constraints by the cylindrical steel mold and JIS uniaxial restraining bar on the expansion of the expansive concrete were considered under the same curing conditions. The specimens were cured with steam or at 20 °C for 1 day. They were then sealed at 20 °C for 7 days. The results as the specimens were aged for the 7 days were then compared.

Figs. 3.6 and **3.7** show the correlation between the uniaxial energies of the JIS samples and energies of the cylindrical specimens under the sealed condition. Most of the cylindrical specimens had circumferential energies that were about twice as large as the uniaxial energies of the JIS samples. The axial energies of the cylindrical specimens were close to the uniaxial energies. These relations agree with the existing empirical Eqs. (3.4) and (3.5) that were obtained from the previous study at 20 °C curing.

With regard to the Ex60 specimens cured in steam, the results showed a divergent tendency when the expansive energy measured with the JIS method approached ~500 N/mm^2 (see **Figs. 3.6(a)** and **3.7(a))**. As discussed in Section 3.3.1, this divergence may be explained by the increased circumferential strain of the cylindrical specimens due to the yielding of the lightweight steel mold (see **Fig. 3.4(a)**). Accordingly, the applicability of the simplified method

to evaluating expansive concrete with a large degree of expansion without modification to consider the yielding effect is questionable.

Fig. 3.8 shows the correlations among the strains obtained with the two testing methods under the sealed condition. For the circumferential strain of the simplified method, the relations almost conformed to the calculated Eq. (3.6) except for Ex60 with steam curing (see **Fig. 3.8(a)**). Specifically, the circumferential strains of the cylindrical specimens in this case became abnormally excessive because of the yielding effect, which resulted in the great divergence. On the other hand, the relations between the axial strains of the cylindrical specimens and uniaxial strains of the JIS specimens demonstrated a high correlation and good agreement with Eq. (3.7) regardless of whether the thin steel mold yielded (see **Fig. 3.8(b)**). Therefore, using the simplified method with the axial strain appears to be a valid approach to obtaining the expansive strain of concrete. Using the axial strain of the cylindrical specimen provides the simplified method with universal applicability to expansive concrete, even if the large expansion ratio causes yielding in the circumferential direction. In detail, **Fig. 3.8(b)** shows that the simplified method using axial strain can be used for concrete with an expansion ratio of up to ~1000×10^{-6} according to the JIS method. This implies that using the simplified method with the axial strain can overcome the limitations when the circumferential strain is used.

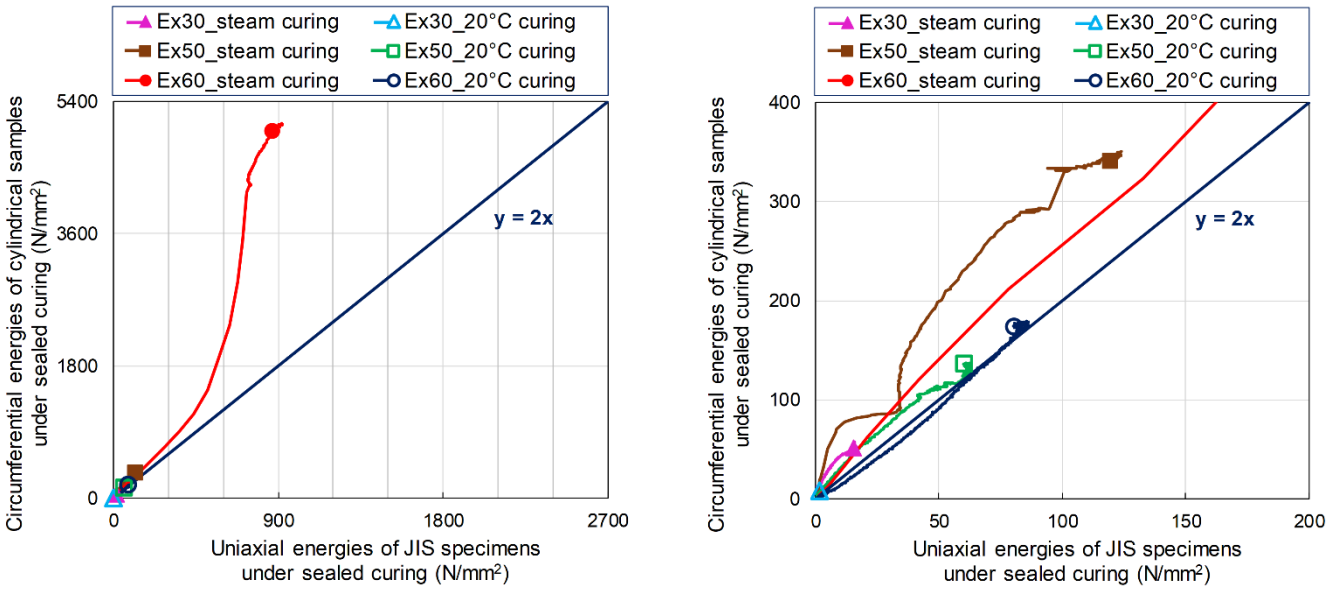

Fig. 3.6. Correlation between the circumferential energies of the cylindrical specimens and uniaxial energies of the JIS specimens under the sealed condition: (a) overview and (b) close-up view.

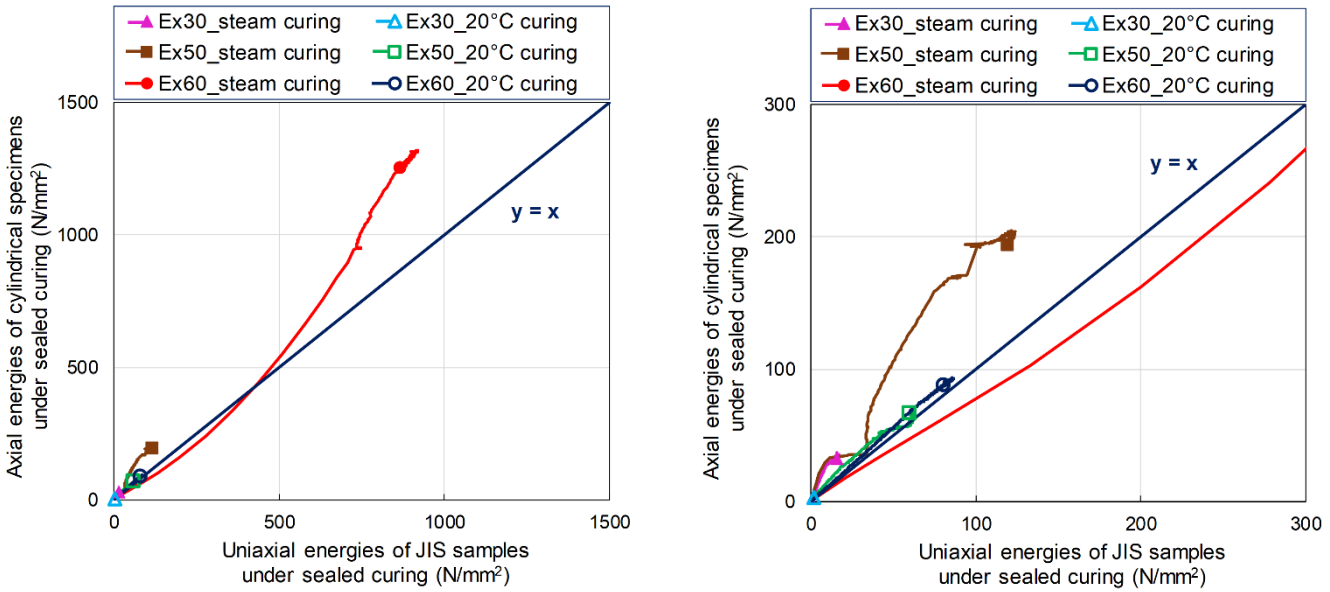

Fig. 3.7. Correlation between the axial energies of the cylindrical specimens and uniaxial energies of the JIS specimens under the sealed condition: (a) overview and (b) close-up view.

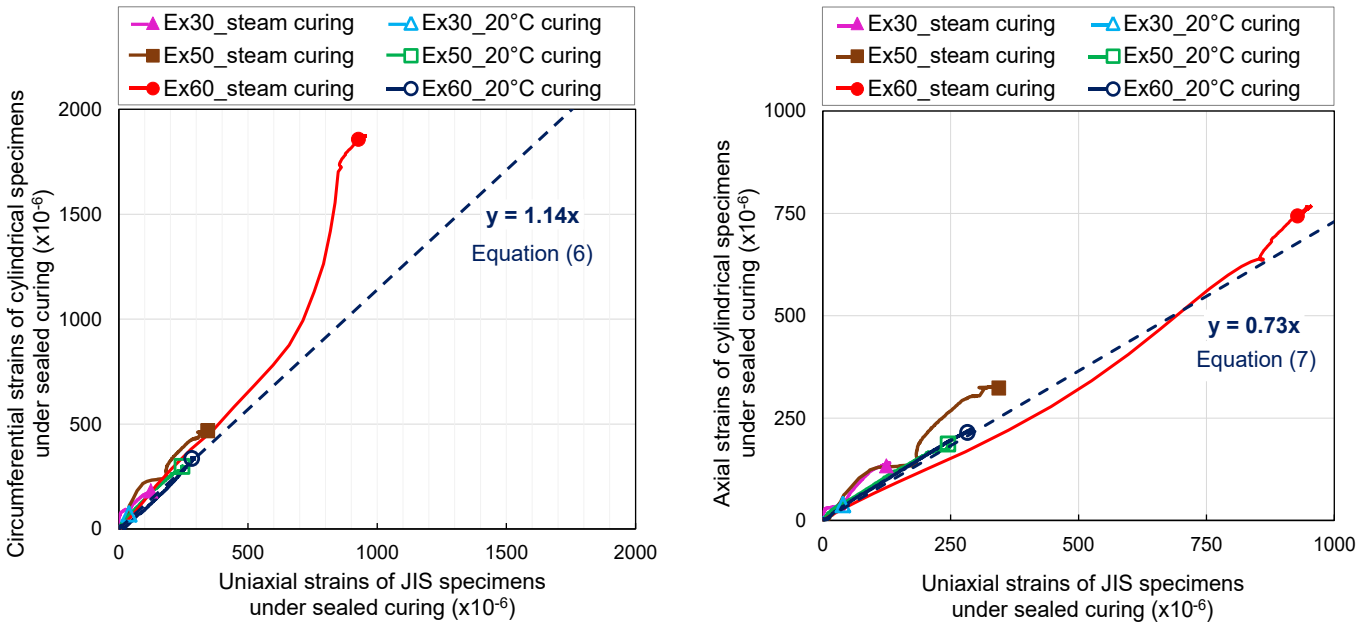

Fig. 3.8. Relationships among expansive strains obtained with both testing methods under the sealed condition: (a) circumferential strain–uniaxial strain and (b) axial strain–uniaxial strain.

3.3.2.3. Effect of the curing conditions on expansion

The expansion performance of concrete has been reported to be enhanced with water curing than when sealed [10, 38]. **Fig. 3.9** shows the effect of water curing on the expansive energy. Steam and 20 °C curing were employed for the first day of aging. Subsequently, samples were separately cured in water and sealed at the same temperature of 20 °C for 7 days. The measured expansive energies of the specimens over 7 days were compared. The JIS specimens were in contact with the water on all sides, whereas the specimens for the simplified method had only the top surface in contact with the water.

With the simplified method, the expansive energies of the specimens showed trivial increases with water curing after aging for 1 day (**Figs. 3.9(a) and 3.9(b)**). This indicates that supplying water to only the top surface is not sufficient for water curing of expansive concrete.

With the JIS method, the water-cured samples had significantly larger expansive energies than the sealed samples. In particular, there was a considerable deviation with 20 °C curing (**Fig.**

3.9(c)). This may be because the chemical reaction of the expansive agent continued after the aging for 1 day, and the free access of an outside water supply to all surfaces of the JIS specimens quickened the hydrate reaction of the expansive agent. In contrast, the divergence was smaller for steam curing with a high temperature history. This may be because the hydration of the expansive agent was mostly complete after 1 day of aging, so there was a negligible change in the expansion afterwards. The empirical relations for steam and 20 °C curing obtained from the current experimental results are approximated as follows:

$$U_{JIS\_water} = a \cdot U_{JIS\_seal} \tag{3.8}$$

where U_{JIS_water} is the calculated expansive energy per unit volume (N/mm^2) of the JIS samples cured in water after being aged for 1 day and a is the temperature-dependent coefficient based on the aging results for 7 days. This was found to be 1.14 and 3.77 for steam and 20 °C curing, respectively.

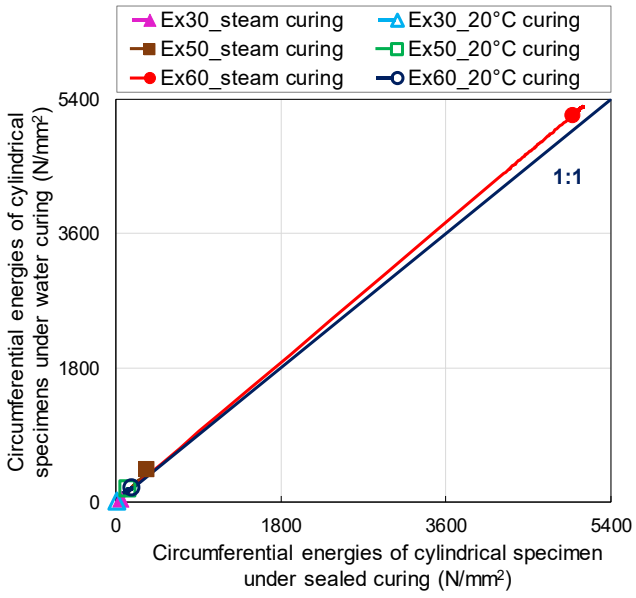

(a)

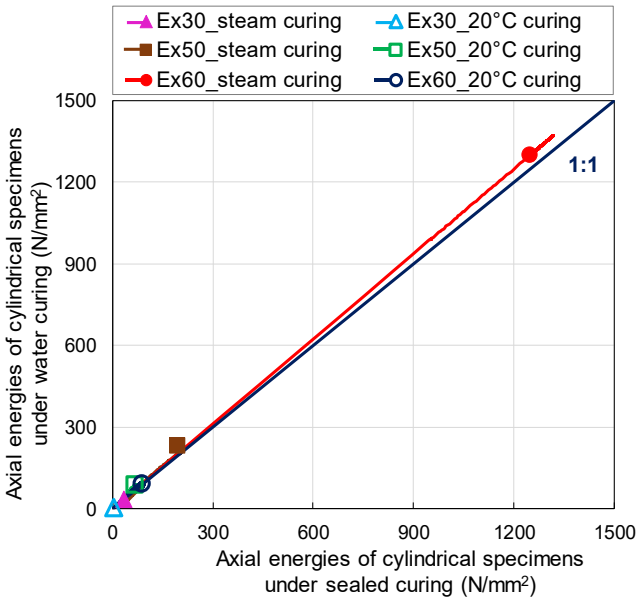

(b)

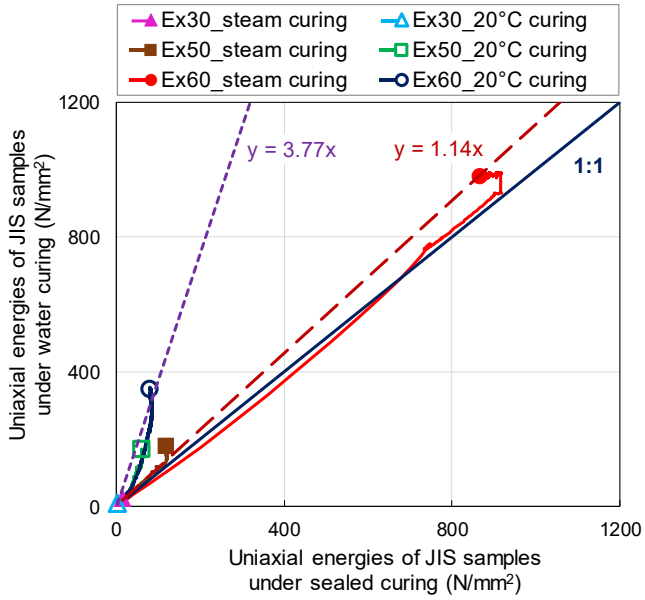

(c)

Fig. 3.9. Effects of the curing conditions on the expansion of the specimens with both testing methods: (a) circumferential expansive energies of the cylindrical specimens, (b) axial expansive energies of the cylindrical specimens, and (c) uniaxial energies of the JIS specimens.

3.3.3. Verification of the applicability of the simplified method with steam curing

To validate the applicability of the simplified method to steam curing, the relationships between the expansive strains of specimens obtained with both measurement methods were investigated. Specimens were cured in steam or at 20 °C from their first casting for 1 day. As noted in Subsection 3.3.2.3, the specimens for the simplified and JIS methods were then cured under sealed and water conditions, respectively, at 20 °C up to 7 days. Thus, the relations between the strains of the sealed cylindrical specimens and uniaxial strains of the water-cured JIS samples were examined for both cases of steam and 20 °C curing. The relations were derived from the expansive strains acquired at the age of 7 days.

The relations between the circumferential strains of the sealed cylindrical specimens and uniaxial strains of the water-cured JIS samples as inferred from Eqs. (3.6) and (3.8) can be broadly described as follows:

$$\varepsilon_\theta = \left(\frac{1}{a}\cdot\frac{r}{t}\cdot(1-\nu^2)\cdot\rho\cdot\left(1+\frac{-\nu+\sqrt{\nu^2+8}}{4}\cdot\nu\right)^{-1}\right)^{\frac{1}{2}}\cdot\varepsilon_{JIS\_water}$$

$$=\begin{cases}1.07\cdot\varepsilon_{JIS\_water}(\text{steam curing})\\ 0.59\cdot\varepsilon_{JIS\_water}(20°\text{C curing})\end{cases} \quad (3.9)$$

where ε_{JIS_water} is the measured uniaxial strain of the water-cured JIS samples after being aged for 1 day.

The relations between the axial strains of the sealed cylindrical specimens and uniaxial strains of water-cured JIS samples, as derived from Eqs. (3.7) and (3.8), can be roughly expressed as follows:

$$\varepsilon_z = \left(\frac{1}{a}\cdot\frac{1}{2}\cdot\frac{r}{t}\cdot\rho\cdot(1-\nu^2)\cdot\frac{-\nu+\sqrt{\nu^2+8}}{3\cdot\nu+\sqrt{\nu^2+8}}\right)^{\frac{1}{2}}\cdot\varepsilon_{JIS\_water}$$

$$=\begin{cases}0.69\cdot\varepsilon_{JIS\_water}(\text{steam curing})\\ 0.38\cdot\varepsilon_{JIS\_water}(20°\text{C curing})\end{cases} \quad (3.10)$$

Fig. 3.10(a) shows the relationship between the measured and predicted uniaxial strains of the water-cured JIS samples at the age of 7 days. The predicted values were calculated with Eq. (3.9) by using the circumferential strains of the sealed cylindrical specimens at the same age. The relation showed a great divergence from the 1:1 line for the steam-cured Ex60 specimens. This confirms the limited applicability of the simplified method with the circumferential strain. **Fig. 3.10(b)** illustrates the relationship between the measured uniaxial strains of the water-cured JIS samples and their predicted values calculated with Eq. (3.10) by using the axial strains of the sealed cylindrical specimens at the age of 7 days. The obtained experimental and

estimated values showed good agreement regardless of the curing conditions for the first day. This validates the applicability of the simplified method to steam curing.

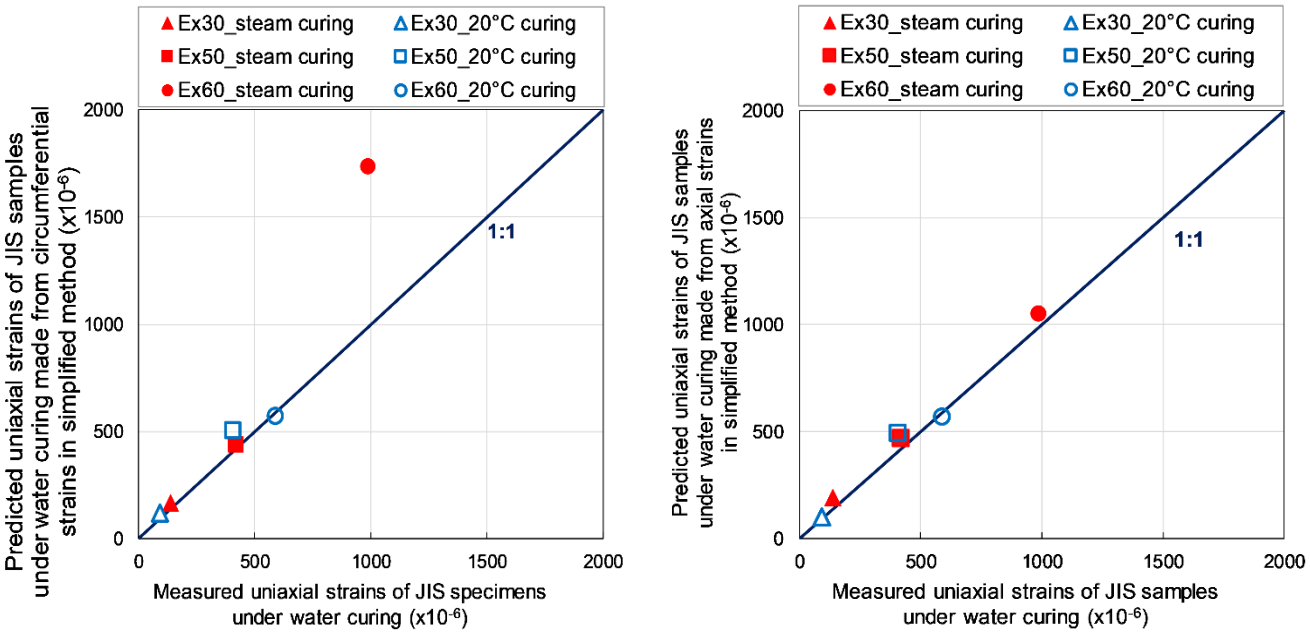

Fig. 3.10. Relationship between the measured and calculated uniaxial strains of the water-cured JIS samples at the age of 7 days: (a) calculation with the circumferential strains and (b) calculation with the axial strains.

3.4. Summary

Based on some previous studies and experimental results in this chapter, the following conclusion can be drawn.

- The simplified method using the circumferential strain is applicable to estimating the moderate expansion of concrete when the circumferential strain is 810×10^{-6} or less. Using the circumferential strain with larger expansions is overestimated because of yielding.

- The simplified method is applicable to concrete with large expansions of up to ~1000×10^{-6} according to the JIS method when the axial strain of cylindrical specimens is used. Measuring

the axial strain with the simplified method can cover ordinal expansive concrete with various magnitudes of expansion.

- The correlation between the simplified and JIS methods showed good agreement regardless of the curing conditions on the first day of aging. This implies that the simplified method can be used to evaluate the expansion behavior of steam-cured concrete.

References of chapter 3

[1] Japan Society of Civil Engineers, Standard Specifications for Concrete Structures – Materials and Constructions, JSCE, Tokyo, Japan, 2007, pp. 261–271.

[2] JIS A 6202:2017, Expansive additive for concrete, Japanese Industrial Standards Committee, Tokyo, 2017.

[3] R. Sahamitmongkol, T. Kishi, Tensile behavior of restrained expansive mortar and concrete, Cement Concr. Compos. 33 (1) (2011) 131–141.

[4] M. Ozawa, K. Suhara, H. Morimoto, Expansion energy and hydration products of expansive mortar at different temperatures, Third International Conference on Sustainable Construction Materials and Technologies, JCI, Tokyo, Japan, 2012, pp.1–10.

[5] N. Nakajima, K. Hirabe, S. Hashimoto, S. Date, Effects of curing conditions and addition of fine blast furnace slag powder on the initial performance of concrete using expanding material, IOP Conf. Ser. Mater. Sci. Eng. 264 (2017) 1–7.

[6] Micro-Measurements, Tech Note TN-504-1, Strain Gage Thermal Output and Gage Factor Variation with Temperature, (1989).

[7] H. Hashida, Proposal of Simplified Method Using a Thin Cylindrical Steel Mold, Technical Committee Report on Performance Evaluation of High Performance Expansive Concrete and System for Crack Control, Japan Concrete Institute (JCI), Tokyo, Japan, 2011, pp. 120–127 (in Japanese).

[8] M. Tsujino, H. Hashida, T. Kikuchi, H. Tanaka, Low Shrinkage Concrete with both Expansive Additive and Limestone Aggregates (Part2 Quality Control Method of Expansive Concrete), Summaries of Technical Papers of Annual Meeting AIJ A-1 (2010), pp. 925–926 (in Japanese).

[9] M. Tsujino, H. Hashida, R. Yuasa, T. Kikuchi, Quality control of expansive concrete using a thin cylindrical steel mold, Proc. JCI 34 (1) (2012) 520–525 (in Japanese).

[10] K. Nakarai, Y. Kurihara, H. Hashida, M. Tsujino, Analysis of applicability of simplified estimation method of expansive cement concrete using cylindrical lightweight steel mold based on mechanical work, Cem. Sci. Concr. Technol. 65 (1) (2011) 209–216 (in Japanese).

[11] ASTM C143 / C143M, Standard Test Method for Slump of Hydraulic-Cement Concrete, ASTM International, West Conshohocken, 2015.

[12] ASTM C231 / C231M, Standard Test Method for Air Content of Freshly Mixed Concrete by the Pressure Method, ASTM International, West Conshohocken, 2017.

[13] ASTM C192 / C192M, Standard Practice for Making and Curing Concrete Test Specimens in the Laboratory, ASTM International, West Conshohocken, 2016.

[14] H. Yazıcı, S. Aydın, H. Yiğiter, B. Baradan, Effect of steam curing on class C high-volume fly ash concrete mixtures, Cem. Concr. Res. 35 (6) (2005) 1122–1127.

[15] H. Zhimin, L. Junzhe, Z. Kangwu, Influence of mineral admixtures on the short and long-term performance of steam-cured concrete, Energy Procedia 16 (2012) 836–841.

[16] D.W. S. Ho, C.W. Chua, C. T. Tam, Steam-cured concrete incorporating mineral admixtures, Cem. Concr. Res. 33 (4) (2003) 595–601.

[17] A.A. Ramezanianpour, M.H. Khazali, P. Vosoughi, Effect of steam curing cycles on strength and durability of SCC: a case study in precast concrete, Constr. Build. Mater. 49 (2013) 807 – 813.

[18] M. Ba, C. Qian, X. Guo, X. Han, Effects of steam curing on strength and porous structure of concrete with low water/binder ratio, Constr. Build. Mater. 25 (2011) 123 – 128.

[19] A. G. Corominas, M. Etxeberria, C. S. Poon, Influence of steam curing on the pore structures and mechanical properties offly-ash high performance concrete prepared with recycled aggregates, Cem. Concr. Compos. 71 (2016) 77 – 84.

[20] B. Lothenbach, F. Winnefeld, C. Alder, et al., Effect of temperature on the pore solution, microstructure and hydration products of Portland cement pastes, Cem. Concr. Res. 37 (4) (2007) 483–491.

[21] J. Feng, M. Miao, P. Yan, The effect of curing temperature on the properties of shrinkage-compensated binder, Sci. China Technol. Sci. 54 (7) (2011) 1715–1721.

[22] Y. Nagao, K. Suzuki, Basic properties and utilization of steam-cured concrete using Ground Granulated Blast-Furnace Slag, Nippon Steel Sumitomo Met. Tech. Rep. 2015.

[23] B. A. Zulu, S. Miyazawa, N. Nito, Properties of blast-furnace slag cement concrete subjected to accelerated curing, Infrastructures, 4 (4) (2019), 69.

[24] S. Nagataki, H. Gomi, Expansive agents (mainly ettringite), Cem. Concr. Compos. 20 (2–3) (1998) 163–170.

[25] J. Han, D. Jia, P. Yan, Understanding the shrinkage compensating ability of type K expansive agent in concrete, Construct. Build. Mater. 116 (2016) 36–44.

[26] T.R. Gentry, Thermal compatibility of plastic composite reinforcement and concrete, in: M.M. El-Badry (Ed.), Advanced Composite Materials in Bridges and Structures, Canadian Society for Civil Engineering, Montreal, Quebec, 1996, pp. 149–156.

[27] N. Galati, A. Nanni, L.R. Dharani, F. Focacci, M.A. Aiello, Thermal effects on bond between FRP rebars and concrete, Composer Part A 37 (2006) 1223–1230.

[28] D.P. Bentz, O.M. Jensen, Mitigation strategies for autogenous shrinkage cracking, Cem. Concr. Compos. 26 (2004) 677–685.

[29] O.M. Jensen, P.F. Hansen, Influence of temperature on autogenous deformation and relative humidity change in hardening cement paste, Cem. Concr. Res. 29 (1999) 567–575.

[30] E. Tazawa, S. Miyazawa, Influence of cement and admixtures on autogenous shrinkage of cement paste, Cem. Concr. Res. 25 (2) (1995) 281–287.

[31] C.T.F. Ross, Mechanics of Solids, Horwood, Chichester, UK, 1999.

[32] ASTM D638 - 02a, Standard Test Method for Tensile Properties of Plastics, ASTM International, West Conshohocken, 2002.

[33] M. Ozawa, K. Suhara, H. Morimoto, Expansion energy and hydration products of expansive mortar at different temperatures, Third International Conference on Sustainable Construction Materials and Technologies, JCI, Tokyo, Japan, 2012, pp.1–10.

[34] Y. Tsuji, Estimation of expansive energy in concrete engineering, Concr. J. 26 (10) (1988) 5–13 (in Japanese).

[35] Y. Tsuji, Methods of estimating chemical prestress and expansion distribution in expansive concrete subjected to uniaxial restraint, Concr. Libr. JSCE 3 (1984) 131–143.

[36] H. Okamura, Y. Tsuji, K. Maruyama, Application of expansive concrete in structural elements, J. Fac. Eng. Univ. Tokyo (B), 34 (3) (1978) 481–507.

[37] A. Hosoda, M. Morioka, M. Tanimura, T. Kanda, E. Sakai, T. Kishi, Technical Committee on Performance Evaluation of High Performance Expansive Concrete and System for Crack Control, Technical Committee Reports 2011, Japan Concrete Institute (JCI), Tokyo, Japan, 2011, pp. 65–92.

[38] C. Maltese, C. Pistolesi, A. Lolli, A. Bravo, T. Cerulli, D. Salvioni, Combined effect of expansive and shrinkage reducing admixtures to obtain stable and durable mortars, Cem. Concr. Res. 35 (12) (2005) 2244–2251.

Chapter 4. Effects of slag type and curing method on the performance of expansive concrete

4.1. Introduction

Blast furnace slag is extensively used as a supplementary cementitious material to improve the performance of concrete. However, shrinkage and early cracking are common in such slag concretes, whereas expansive concrete has been applied as a countermeasure. This chapter therefore conducted and analyzed the results of the mechanical, physical, and durability properties of expansive concrete specimens containing blast furnace slag with and without gypsum initially cured under different conditions. The properties of the specimens were measured up to 91 days of age to determine the effects of the different slag materials and curing conditions on the engineering properties of the specimens. The two different slag compositions evaluated were combined with ordinary Portland cement at 50% replacement by mass. A sulfoaluminate-type expansive agent was used in a constant amount of 50 kg/m^3 in all specimens. Cylindrical specimens were cast and initially cured by one-day steam or seven-day sealed 20 ºC curing, and were then exposed to the ambient environment with 60% relative humidity at 20 ºC for the second stage of curing. The compressive strength tests of the ϕ100 × 200 mm cylindrical specimens were performed to examine strength development. The simplified method for measuring the restrained expansion of concrete was applied with a cylindrical tinplate mold (ϕ100 × 200 mm, 0.28-mm thick) to estimate the volumetric change. The air permeability and water absorption tests were employed to assess the durability of concrete. A chemical analysis of hydration components was conducted using the XRD/Rietveld method to discuss on the mechanisms of interaction between concrete mix materials during the curing process, particularly in terms of the formation of ettringite.

4.2. Experimental program

4.2.1. Materials and mixture proportions

Table 4.1 presents the properties of the materials used in this study. Both the fine and coarse aggregates were used under saturated, surface-dry conditions. Two types of slag, pure slag and slag with gypsum, were employed. The chemical and mineralogical compositions of the cement, expansive agent, and slags are given in **Table 4.2**.

Table 4.3 shows the mix proportions for the investigated concretes based on the mix design usually used in precast concrete factories [1]. Concrete specimens of normal concrete without any slag (NC), concrete incorporating pure slag without gypsum (SpC), and concrete incorporating slag with gypsum (SgC) were fabricated. A water-to-binder ratio of 45%, and water content of 168 kg/m^3 were maintained in all mixtures. A 50% (by mass) cement-replacement ratio was used as the optimum level regarding fresh concrete properties and greatest later strength development of hardened concrete [2, 3]. An expansive agent content of 50 kg/m^3 was applied as a required dosage for chemically prestressed concrete [1, 4]. In practical design, the chemical agents were adjusted so that the slumps of all concrete mixtures were 8.0 ±2.0 cm and the air contents were 4.5 ±1.5%.

Table 4.1. Material properties.

Material	Type	Properties	Notation
Cement	Ordinary Portland cement conforming to JIS R 5210 (equivalent to CEM I cement type in BS EN 197-1)	Density: 3.16 g/cm^3 Specific surface area: 3370 cm^2/g (Strength class: similar to 42.5 N strength class in BS EN 197-1)	C
Pure slag without gypsum	Pure slag conforming to JIS A 6206	Density: 2.89 g/cm^3 Specific surface area: 4170 cm^2/g Activity index 7 d: 61% 28 d: 94% 91 d: 122%	SG1
Slag with gypsum	Slag with additional gypsum, conforming to JIS A 6206	Density: 2.91 g/cm^3 Specific surface area: 4540 cm^2/g Activity index 7 d: 75% 28 d: 98% 91 d: 108% Gypsum content: 4.54% (calculated from SO_3 content in Table 4.2)	SG2
Expansive agent	Ettringite type (based on calcium sulphoaluminate)	Density: 2.95 g/cm^3 Specific surface area: 2900 cm^2/g	Ex
Fine aggregate	Crushed sandstone	Fineness modulus: 2.97 Surface-dry density: 2.59 g/cm^3 Water absorption: 1.23 %	S
Coarse aggregate	Crushed rhyolite	Grain size: 5–20 mm full grade Surface-dry density: 2.62 g/cm^3 Water absorption: 0.67 %	G
Chemical agents	Air entraining agent and superplasticizer	Denatured rosin acid-based and Polycarboxylic acid compound	Ad

Table 4.2. Chemical and mineralogical compositions of binders

Oxides (wt.%)	C	Ex	SG1	SG2	Phase (wt.%)	C	Ex
SiO_2	20.06	1.50	34.45	32.56	Alite, C_3S	58.9	
Al_2O_3	5.12	9.00	14.06	13.79	Belite, C_2S	22.5	
Fe_2O_3	3.05	0.60	0.27	0.46	Aluminate, C_3A	8.5	
CaO	64.85	51.8	43.78	42.57	Ferrite, C_4AF	6.1	
MgO	1.29	1.40	5.84	6.11	Gypsum, $C\overline{S}H_2$	5.3	
K_2O	0.38	0.29	0.23	0.28	Anhydrite, $C\overline{S}$		40.3
Na_2O	0.29	0.15	0.24	0.16	Ye'elimite, $C_4A_3\overline{S}$		24.8
SO_3	1.92	29.00	-	2.11	Free lime, CaO		13.4
LOI	2.27	2.55	0.05	0.35			

Note: LOI is loss on ignition.

Table 4.3. Mix proportions of fabricated concretes.

Specimen	W/B	Unit mass (kg/m^3)					
	(%)	W	C	SG	Ex	S	G
NC	45	168	323	0	50	744	998
SpC	45	168	162	162	50	738	990
SgC	45	168	162	162	50	739	990

Note: W/B is the water-to-binder (C + Ex + SG) ratio by mass.

4.2.2. Mixing and casting procedures

All concretes were mixed in a 0.5 m^3 laboratory pan mixer using the following steps. First, the fine materials including the cement, expansive agent, slag, and sand were mixed together for

30 s to provide initial homogeneity. Next, a blend of water and the necessary chemical agents were steadily added to the dry mixture over 60 s of mixing. The resulting wet mixture was then mixed for an additional 30 s to ensure thorough homogeneity. Finally, the coarse aggregates were introduced to the mixer followed by an additional 2 min of mixing. The fresh state of the fabricated concrete mixes was then assessed by measuring the slump flow and air content according to ASTM C 143/C 143M [5] and ASTM C 231 [6], respectively. Immediately after mixing, the concrete mixes were poured into ϕ100 × 200 mm cylindrical specimens using the procedure dictated by ASTM C 192/C 192M [7].

4.2.3. Curing conditions

Immediately after casting, specimens were either steam cured for one day or cured at 20 °C for seven days as the first curing stage. The applied steam curing cycle plan is depicted by the dashed line in **Fig. 4.1**. During steam curing, steam from a pipeline was applied for 24 h to maintain an ambient relative humidity (RH) of 90% ± 10%. Examples of the measured temperatures in the steam curing chamber (Room) and at the center of the ϕ100 × 200 mm cylindrical specimens (NC, SpC, and SgC samples) are also plotted in **Fig. 4.1**. The specimens cured at 20 °C were sealed and cured in a room in which the temperature was controlled at 20 °C.

All specimens were then exposed to an ambient environment in which a temperature of 20 ºC and RH of 60% were maintained. All specimens were cured without demolding to provide a consistent confinement condition. Although only the top surface was open to the environment as the exposure surface for measurements, longitudinal free expansion from the top was prevented by friction between the concrete and the internal surface of the mold [1].

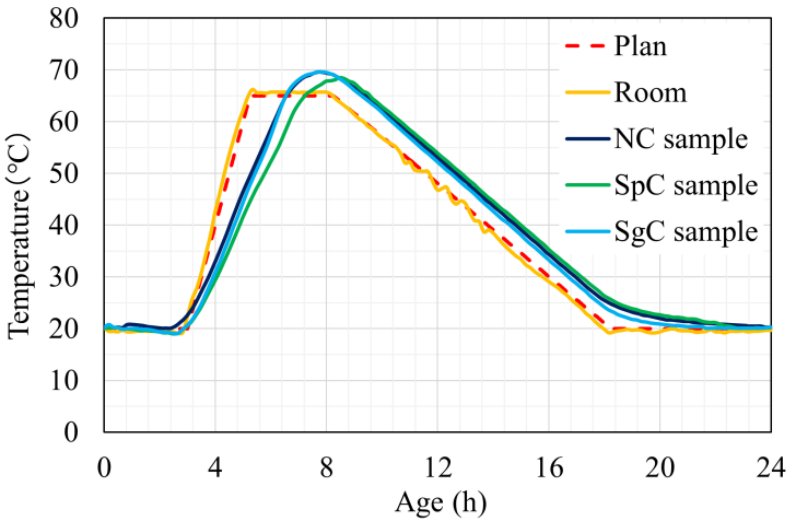

Fig. 4.1. Example of temperature treatment.

4.2.4. Test methods

4.2.4.1. Compressive strength test

Compressive strength tests of the ϕ100 × 200 mm cylindrical specimens were performed in accordance with JIS A 1108:2006 [8] after 1, 7, 28, 56, and 91 d of age. The load was continuously applied at a constant rate of 0.2 MPa/s using a hydraulic press machine with the parameters stipulated in the standard and the maximum value at failure was recorded to calculate the compressive strength. The average value of three duplicate specimens is reported as the compressive strength for each specimen age.

4.2.4.2. Expansion measurement

In this paper, the simplified method [1, 9] for measuring the restrained expansion of concrete in a cylindrical tinplate mold (ϕ100 × 200 mm, 0.28-mm thick) was employed. It typically includes a strain gauge horizontally affixed at the mid-height of the outside surface of each mold to automatically record the circumferential expansive strain in the concrete specimens. The concrete temperature variation was obtained continuously at the center of each specimen

using an embedded thermocouple. The expansion of the specimens was measured constantly from initial casting to 91 d of age. The average measured expansion of three specimens is reported as the expansion for each specimen. The thermal outputs [10] of the restraint device were canceled by subtracting them from the measured strain in the specimens.

4.2.4.3. Air permeability test

The air permeability coefficients were determined using a test method developed by Torrent [11] and contained in Swiss standard SN 505 262/1:2013 [12]. The tests were conducted in the ambient environment at 28, 56, and 91 d of age by using a vacuum pump to apply a negative relative pressure through a test chamber positioned over the top surface of the cylindrical specimens. The air permeability coefficient, kT, was then calculated and recorded automatically by the device as per the standard requirements.

4.2.4.4. Capillary absorption test

The sorptivity tests were conducted using the 91-day-old cast cylindrical specimens. The test procedure was determined with reference to ASTM C1585 [13] with some modifications: namely, the top surface of each cylindrical specimen was used without being cut to measure absorption in this experiment because the water absorption of the finished surface of concrete was thought to be more realistic, as it better reflects the conditions of a structural member in practice [14]. This adjustment also served to reduce possible errors due to cutting-induced cracking. In order to avoid evaporation and achieve uniaxial water flow, after demolding, the sides and bottom of the samples were sealed with adhesive aluminum foil, and the finished top surface was kept open. Sample conditioning with the accelerated drying process was not applied because the test was conducted after sufficient drying under 60% RH.

The initial weights of the specimens were measured to the nearest 0.01 g. The specimens were then placed upside down (top surface down) on several layers of blotting paper with a total thickness of 1 mm in a tray filled with water up to 2 mm above the base of the specimens (see **Fig. 4.2**). The masses of the specimens were then regularly measured to determine the absorption at several time intervals from 5 min to the first 6 h of immersion. The excess water on the immersed surface was always removed with a wet cloth before weighing. The specimens were placed back in the tray immediately after the mass was obtained in each measurement. During the test, the tray was refilled with water as necessary to maintain a depth of 2 mm above the base of the specimens.

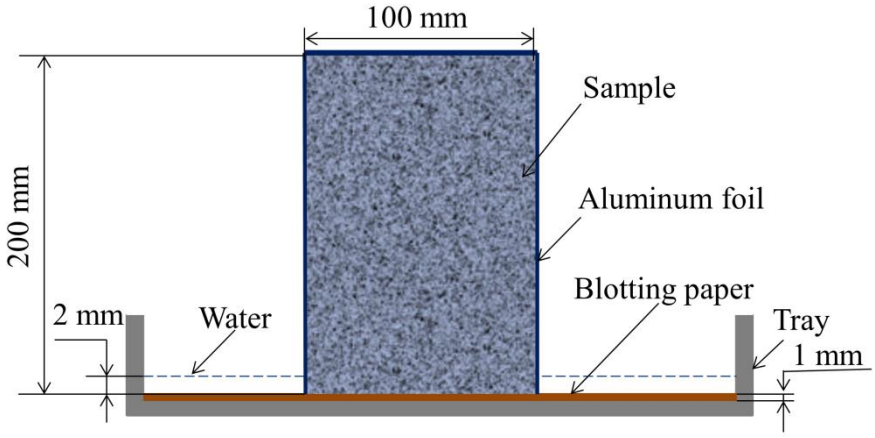

Fig. 4.2. Experimental set-up for capillary water absorption test

4.2.4.5. Hydration reaction analysis

A chemical analysis of hydration components was conducted using the XRD/Rietveld method to quantify the presence of AFt [15, 16]. The blended cementitious pastes used for this test were prepared with the mix compositions shown in **Table 4.4**, labeled NP, SpP, and SgP, to model the cement pastes in the NC, SpC, and SgC concretes, respectively, evaluated in this study. Mixing was conducted in accordance with JIS R 5201 [17] at 20 ºC. The paste specimens were then cast in a 4 × 5.5 cm plastic bag with a thickness of 3 mm. Curing temperature regimes

similar to those used for the concrete specimens were then applied under sealed conditions. The specimens were removed from the bags after 1, 3, 7, and 28 d of curing, then immersed in sufficient isopropanol to stop hydration, dried at 40 ºC for 24 h, and finally subjected to analysis using XRD.

Table 4.4. Mix proportions of the blended pastes

Specimen	W/B (%)	Binder composition (%)		
		C	SG	Ex
NP	45	86.6	0.0	13.4
SpP	45	43.3	43.3	13.4
SgP	45	43.3	43.3	13.4

Note: W/B is water-to-binder (C + Ex + SG) ratio in mass.

4.3. Results and discussion

4.3.1. Compressive strength development

The evolutions of the compressive strengths of the fabricated concrete specimens are depicted in **Fig. 4.3**, in which it can be clearly seen that compressive strength increase in all specimens with time under both curing conditions. At all ages, the compressive strengths are the smallest for specimen SpC. The observed lower strength at an early age is due to the lower proportion of cement content and the low hydraulic activity of the pure slag without a gypsum activator [18, 19]. The lower strength in later age is likely due to several factors. One, at normal temperature, the early hydration of slag is dominated by alkali hydroxide, but the consequent reaction largely contains CH [20]. Accordingly, at higher degrees of cement replacement, the amount of cement available for the hydration and liberation of CH decreases, leading to greater mobility of unhydrated slag particles. Two, because pure slag has a lower hydration rate than

ordinary Portland cement, the concrete containing it requires prolonged curing [21]. As a result, the concrete specimen containing pure slag suffered greatly from the short curing time.

However, the strengths of specimen SgC can be observed to be comparable to those of specimen NC, except for the first-day strength of the 20 ºC cured specimens. This might be due to the presence of additional gypsum serving as an activator to considerably promote the hydration of the slag in specimen SgC [22, 23]. Interestingly, the first-day strength of specimen SgC was nearly the same as that for specimen SpC, likely because in specimen SgC, the chemical reaction of the gypsum to form the AFt did not initially take place [24], resulting in no early contribution to strength development. The dissolved aluminum, calcium, and silicon ions from the slag were likely consumed dynamically, forming AFt and calcium silicate hydrate (C–S–H) phases [25], which are responsible for the enhancement of concrete strength. AFt formation will be discussed in the later section with XRD results. In addition, the slag with gypsum used in this study has a slightly greater fineness (~9%) than that of the pure one, which has a somewhat higher slag reactivity and filling effect, thereby contributing positively to the compressive strength of the concrete during early aging [26-28].

It can be observed in **Fig. 4.3** that the strengths of the concrete specimens are considerably dependent on curing conditions, especially the slag concretes. The first-day strengths of the steam-cured NC, SpC, and SgC specimens are 56%, 223%, and 263% higher, respectively, than those of the respective 20 ºC cured specimens. After the first day of curing, the inverse trend can be observed: for example, at 7 d of age, the steam-cured NC, SpC, and SgC specimens exhibit strengths about 19%, 7%, and 11%, respectively, lower than those of the respective 20 ºC cured specimens. This trend could be explained by the fact that the specimens subjected to steam curing under a high-temperature history for one day initially experienced accelerated binder hydration and C–S–H formation resulting in rapid strength growth [29]. Once these specimens were exposed to an ambient environment that contained insufficient water to

maintain such a high rate of hydration, the growth in strength slowed. Additionally, the application of the steam curing cycle with a high maximum temperature could have had a negative effect on the strength at the later ages due to the rapid formation of C–S–H and CH crystalline structures, resulting in a heterogeneous and coarser pore structure [30]. Furthermore, the rapid hydration of the expansive agent under high-temperature history of steam curing facilitated significant expansion during initial aging; this was likely to deteriorate the immature structure of the concrete—a negative impact of residual expansive stress [31].

Table 4.5. Compressive strength results of fabricated concretes

Specimen	Curing condition	Compressive strength				
		1 d	7 d	28 d	56 d	91 d
NC	Steam	24.35	28.74	34.91	41.17	40.91
	20 ºC	15.57	35.65	44.57	48.78	51.02
SpC	Steam	16.97	25.01	28.76	30.78	32.68
	20 ºC	5.26	26.81	37.01	38.26	44.22
SgC	Steam	24.04	29.26	33.96	38.13	40.47
	20 ºC	6.63	33.01	43.81	47.93	49.8

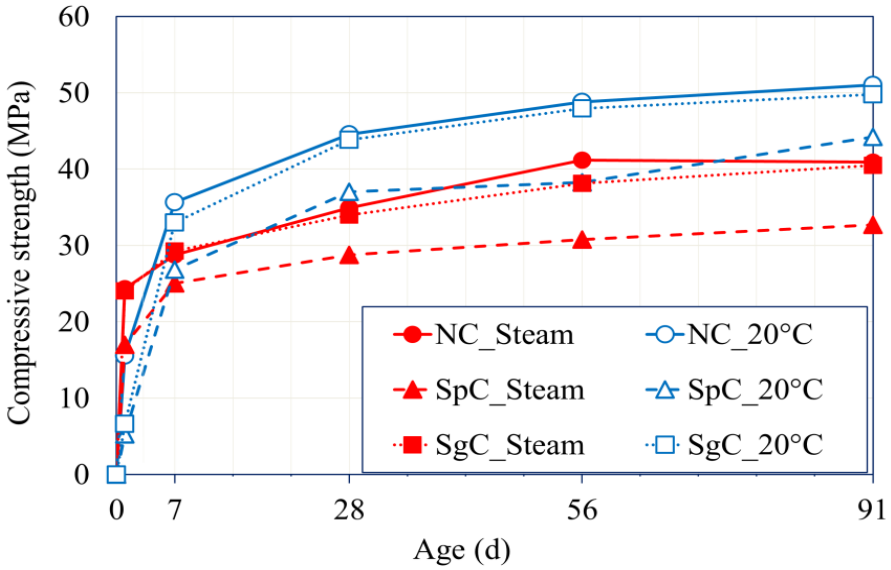

Fig. 4.3. Strength variations of concrete specimens with curing time.

4.3.2. Expansion/shrinkage behaviors

Figures 4.4 – 4.6 illustrate the variation in expansion for all mixtures over time under different curing conditions; all concrete specimens basically exhibit the same increasing expansion tendency in their early ages and the same decreasing expansion tendency afterwards. Indeed, as can be seen in **Figs. 4.4(b), 4.5(b)**, and **4.6(b)**, in the case of steam curing, the specimens expand rapidly and almost reach their maximum values within the first day because of the rapid rate of binder hydration under elevated temperatures [1]. For the specimens cured at 20 ºC, the slag concretes reach their highest expansion values several days later than the steam-cured specimens due to their lower hydration rate. Furthermore, a more rapid decline in expansion can be observed for the slag specimens compared to the NC, particularly in the case of the pure-slag specimen SpC. This increase in shrinkage might be due to: (i) the higher moisture consumption of slag concrete resulting in strong autogenous shrinkage at an early age [32]. (ii) the use of slag makes a cement paste have a finer pore structure that contribute to a lower relative humidity, which increases the degree of self-desiccation within concrete [33], and (iii) the greater volume of paste in the slag concrete specimens resulting from the replacement of the cement by slag on an equal weight basis [34].

In this investigation, the lowest expansion values were observed for the SpC specimen similar to the previous studies [35 - 37]. The obtained trends can be explained mainly by the specimen with pure slag had decreased cement content that could contain less Ca^{2+} and SO_4^{2-}, which are necessary for the formation and growth of AFt crystals. The observed higher expansion of the SgC specimen was likely a result of the additional gypsum in the slag, leading to the generation and growth of AFt and the subsequent increase in the volume of crystals and thus the expansive effect.

To further quantitatively investigate the expansion behaviors of the concrete specimens, the AFt quantity was determined by XRD analysis with the results shown in **Fig. 4.7**. All steam-cured specimens can be observed to exhibit considerable AFt content at 1 d of curing that concurred with the observed expansion behavior. Additionally, the smallest amount of AFt was present in specimen SpC and the largest amount was present in specimen SgC. As the result, although both specimens showed a similar expansion tendency in **Fig. 4.6**, specimen SgC exhibited greater overall expansion. Evidently, the supplemental Ca^{2+} and SO_4^{2-} provided by the addition of gypsum in the slag was beneficial to the development of AFt, thus increasing expansion.

However, it can also be observed that the expansion in all specimens declines in later ages while the AFt content does not in some cases. This contributed the claim that the expansion characteristics cannot be explained solely based on the change in the amount of Aft as reported in former studies [38-40]. Obviously, **Figs. 4.8(a), 4.8(b) and 4.8(c)** exhibit the low correlation between expansion and AFt contents. Except the magnitude of ettringite, the location where ettringite is formed is critical for expansion to take place [41, 42]. Han et al. [43] reported that, once using the sulfoaluminate-type expansive agent, the small sized ettringite formed on the surface of origin particle due to high nucleation rate during its initial forming stage and the repulsive force between particles caused by the growth of the small sized ettringite is responsible for the generation of expansion.

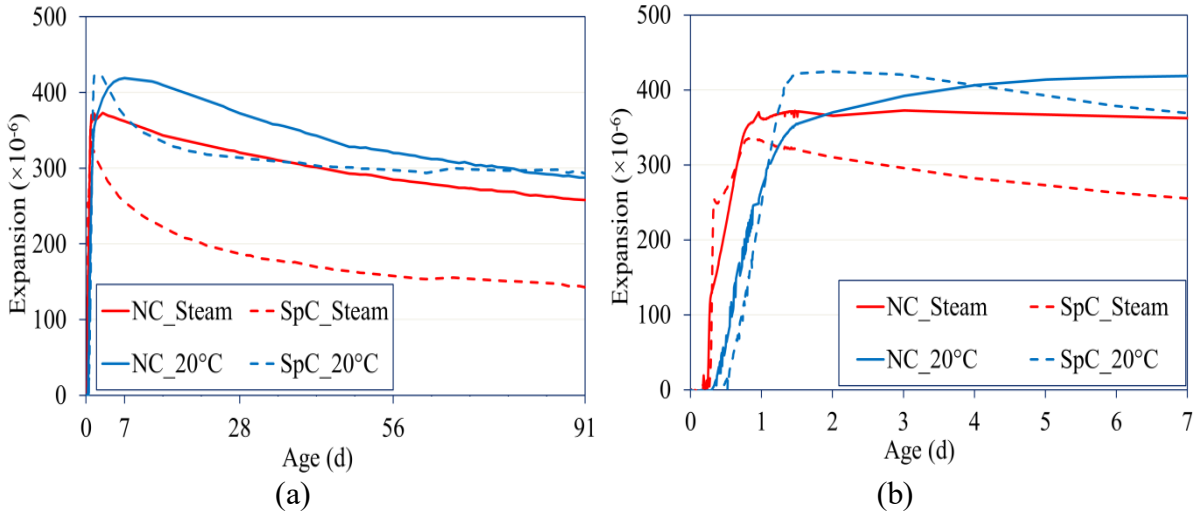

Fig. 4.4. Expansion behaviors of specimens NC and SpC with age: (a) overview from 0 to 91 d, and (b) close-up view from 0 to 7 d.

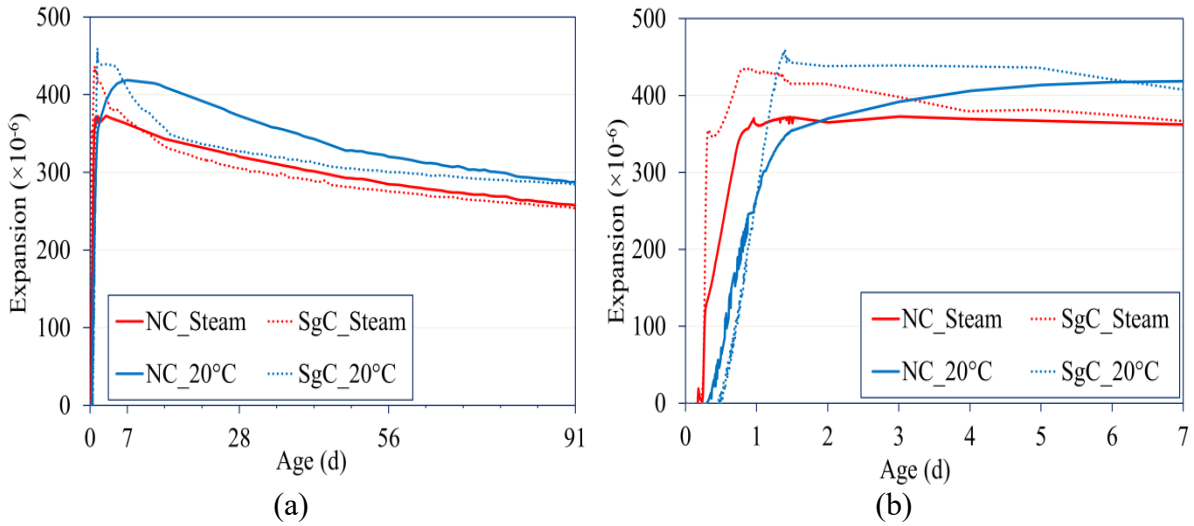

Fig. 4.5. Expansion behaviors of specimens NC and SgC with age: (a) overview from 0 to 91 d, and (b) close-up view from 0 to 7 d.

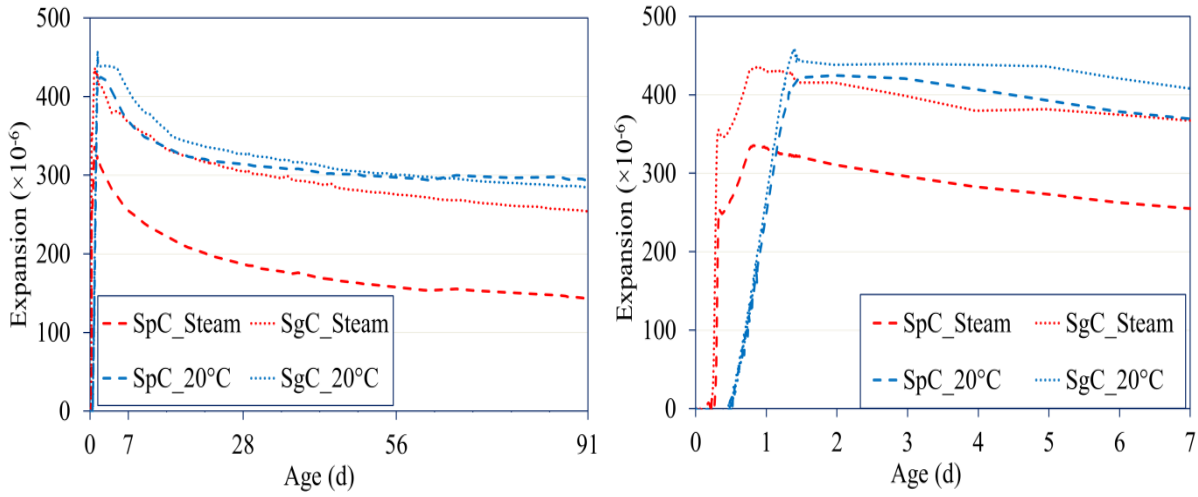

Fig. 4.6. Expansion behaviors of specimens SpC and SgC with age: (a) overview from 0 to 91 d, and (b) close-up view from 0 to 7 d.

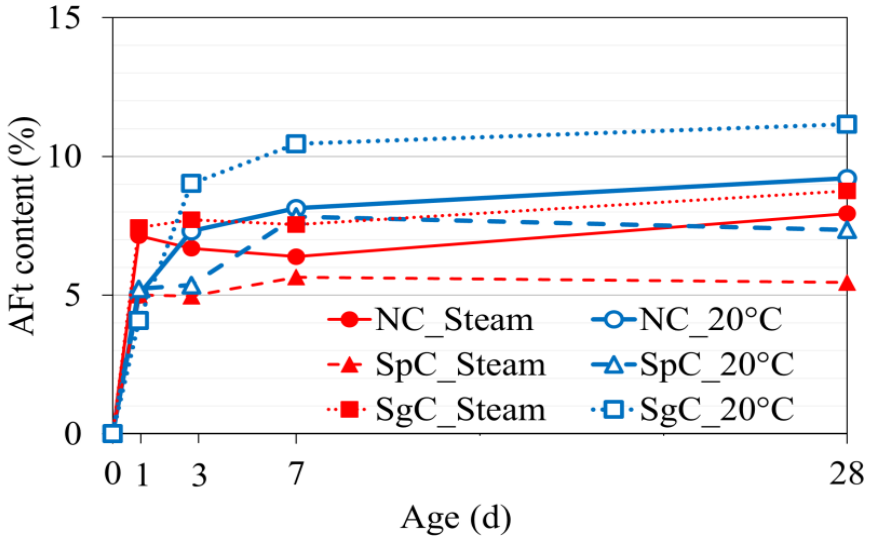

Fig. 4.7. Formation of AFt with curing age

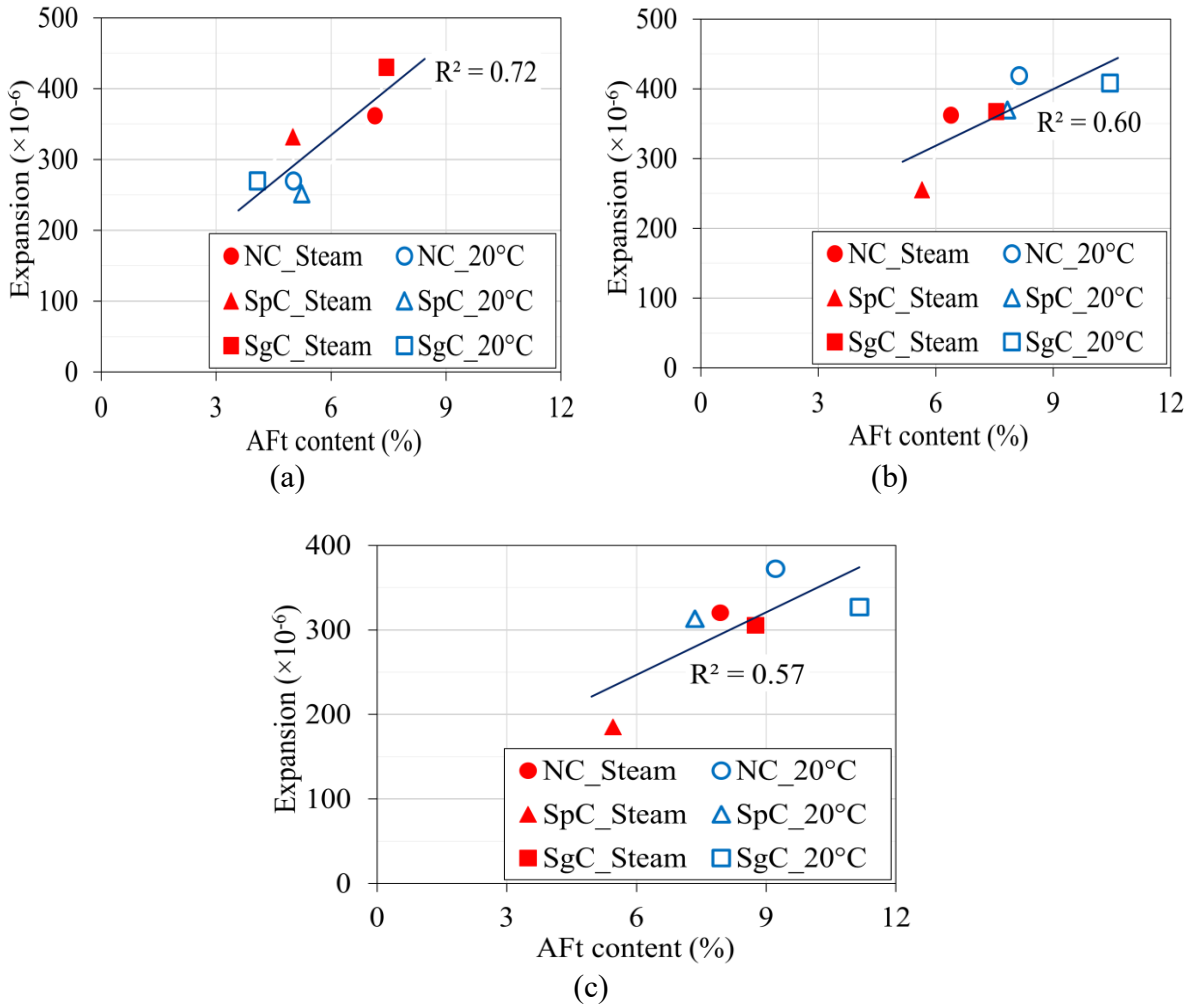

Fig. 4.8. Expansion versus AFt content: (a) at 1 d, (b) at 7 d, and (c) at 28 d curing

4.3.3. Air permeability

The air permeability coefficients (kT) of the different evaluated specimens are given in **Fig. 4.9**, in which it can be clearly seen that specimen SpC exhibits a greater kT than specimen NC, while specimen SgC exhibits a kT comparable to or slightly less than that of specimen NC under either curing condition. These results are consistent with the observed strength behaviors, indicating that lower permeability referred to higher strength when using gypsum-containing slag, as demonstrated by the correlation in **Fig. 4.10**.

Accounting for curing conditions, Liu et al. [44] reported that the permeability of concrete with a high volume of mineral admixtures is highly responsive to curing condition. Similarly, test

results obtained by Idowu et al. [45] showed that improper curing is detrimental to the performance of concrete, and increases its permeability. Dinku et al. [46] proved that the gas permeability coefficients are sensitive to changes in curing duration, test age, and concrete composition: an increase in curing duration from 1 to 7 d resulted in a reduction in gas permeability.

In the present study, it is clear that the kT of the steam-cured specimens are much higher than those of the 20 ºC cured specimens. This result is likely due to the following factors: (i) the specimens subjected to one-day steam curing were next directly exposed to the ambient environment, so the water loss rates from their surfaces were faster, resulting in more open pores on the surface and a decreased degree of cement hydration, leading to a more porous concrete whose effects prevailed over the benefits of accelerated steam curing; (ii) although rapidly hydrated due to the initially high temperatures, a resulting increase in the porosity and capillary cracks of the specimens was observed due to these early high temperatures, especially in terms of more pores on the concrete surface [44, 47]; and (iii) the seven-day, 20 ºC cured samples were sealed during curing, enabling further hydration and the improvement of a well-developed microstructure, resulting in better concrete qualities.

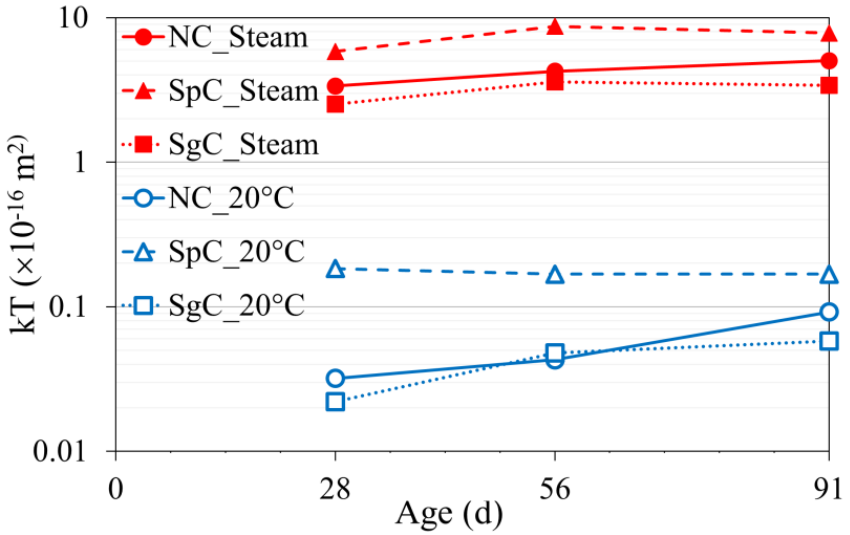

Fig. 4.9. Air permeability coefficients of specimens with age

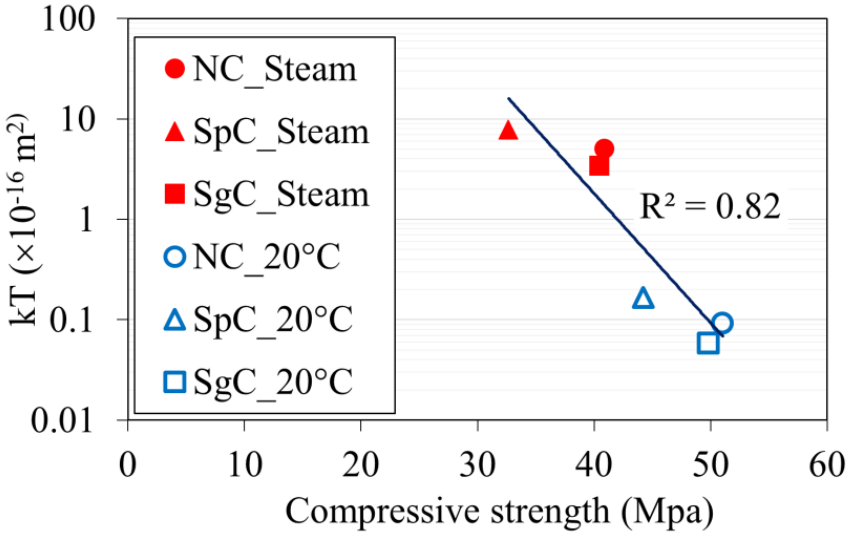

Fig. 4.10. Strength versus air permeability of specimens at 91 d of age

4.3.4. Capillary water absorption

4.3.4.1. Method of consideration

Water sorptivity is broadly used to characterize the ingress of water into the pores of unsaturated concrete due to capillary suction. It is computed as the slope of the best-fit line describing the amount of absorbed water per unit area as a function of the elapsed time during which the concrete is in contact with water.

From the increase in the mass of the specimen due to water absorption, the amount of absorbed water per unit area of inflow surface can be calculated by [13]:

$$i = \frac{m_t}{a \cdot \rho} \tag{4.1}$$

where i is the cumulative absorbed water per unit area of inflow surface (mm), m_t is the specimen mass change at time t (g), a is the area of the inflow surface (mm^2), and ρ is the density of water (g/mm^3).

The cumulative absorbed water i typically increases with time following the square root funct ion of the water contact time. However, in some cases, the literature has reported a more nonli near relationship between the absorbed water and $t^{0.5}$ [48 - 51]. This nonlinearity is also in the case of the present study that the correlation coefficient of less than 0.98 stipulated in ASTM C 1585 [13] (see **Fig. 2** (Appendix A)). Indeed, some studies have attributed the anomalous absorption to the hygroscopicity of calcium silicate hydrates (CSH) and the effect of its swelling during the absorption process [52, 53]. Since the swelling of C-S-H affects the pore size distribution of pre-dried cementitious materials when they get in contact with water, it causes a reduction in hydraulic diffusivity due to internal restrictions to the deformation of the material. Furthermore, the expansion also takes place by the presence of remaining expansive particles in concrete with the additional water supply as the case of my study. Besides, Wu et al. [54] revealed that the presence of microcracks induced by drying shrinkage causes cumulative water absorption to scale non-linearly with the square root of time ($t^{0.5}$). The microcracks were observed to occur even under the gentle drying at 21°C with low RH of 55%, and to be more extensive at elevated temperature. Thus, in my experiment, the samples subjected to the drying at 20°C with low RH of 60% are likely to suffer from microcracks, particularly for steam cured samples.

To address this observation, a new approach that defines the sorptivity as the rate of water absorption following the fourth root of time (t0.25) has been proposed as follows [52, 55]:

$$i = S \cdot t^{0.25} \tag{4.2}$$

where S is the sorptivity coefficient (mm/s$^{0.25}$) and t is the elapsed time during which the concrete is in contact with water (s).

The theoretical basis of the new $t^{0.25}$ approach considers the effect of swelling with time and applied for the case of capillary absorption of cracked cementitious materials, but also applicable to uncracked materials. This approach is empirically based on improved fitting in comparison with the $t^{0.5}$ relation. As a result, the capillary absorption rate can be determined as the slope of the relation between the water uptake and the $t^{0.25}$ with the excellent fit in the analysis of results from the capillary absorption test. Thus, in this study, the $t^{0.25}$ approach was used for the analysis of results from the capillary absorption test.

4.3.4.2. Water sorptivity of fabricated concretes

The cumulative absorbed water during the initial 6 h of testing for samples cured under different conditions is shown in **Fig. 4.11**, in which it can be observed that the progression of water uptake exhibits the utmost linearity with the $t^{0.25}$ trend, as the best-fit lines of all specimens possess coefficients of determination (R^2) greater than 0.98. It can be observed that the cumulative volume of water absorbed in the concrete specimens increases with increasing $t^{0.25}$. The plotting of kT against water sorptivity in **Fig. 4.12** indicates nearly identical water sorptivity and air permeability coefficient behaviors for all cases, with a best-fit line R^2 value of 0.99. Specimen SpC consistently exhibits the largest kT and water sorptivity values, whereas specimen SgC consistently exhibits poorer sorptivity under either curing condition. This difference is believed to be related to the more porous SpC concrete resulting from the lower hydration reaction of the pure slag, and conversely to the denser structure of the SgC concrete formed by the accelerated hydration of the slag due to the presence of gypsum, as well as the space-filling effect of its finer particle size. With respect to the effect of curing conditions, all mixtures exhibited greater water sorptivity after one day of steam curing compared to seven

days of 20 ºC curing with a sealed specimen. This finding agrees with the results of a previous study [44], which determined that early high-temperature curing caused an increase in pores and microcracks, as well as a coarser concrete microstructure, resulting in an increase in water sorptivity.

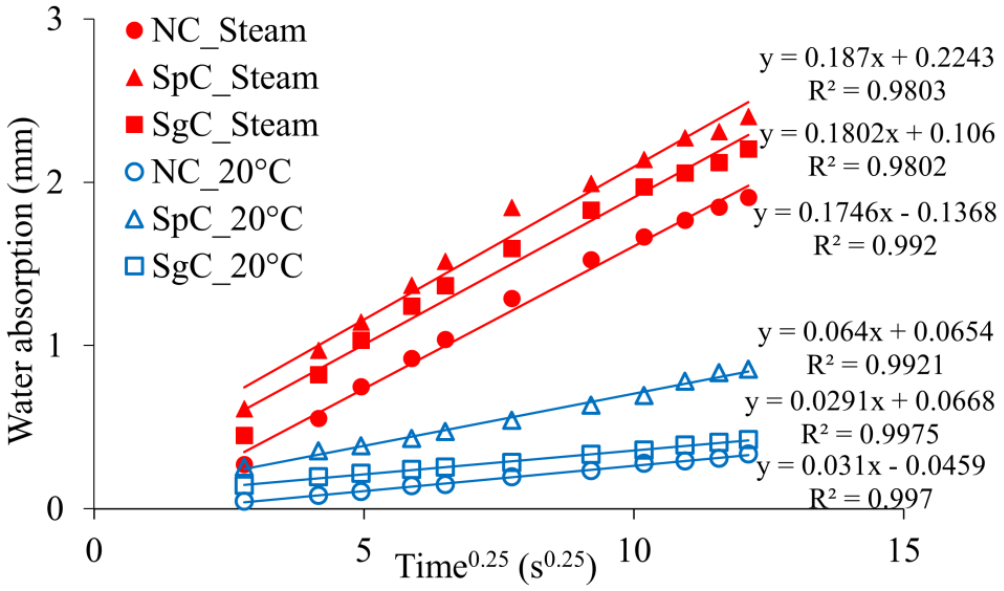

Fig. 4.11. Cumulative absorbed water with the fourth root of time for the different concrete specimens.

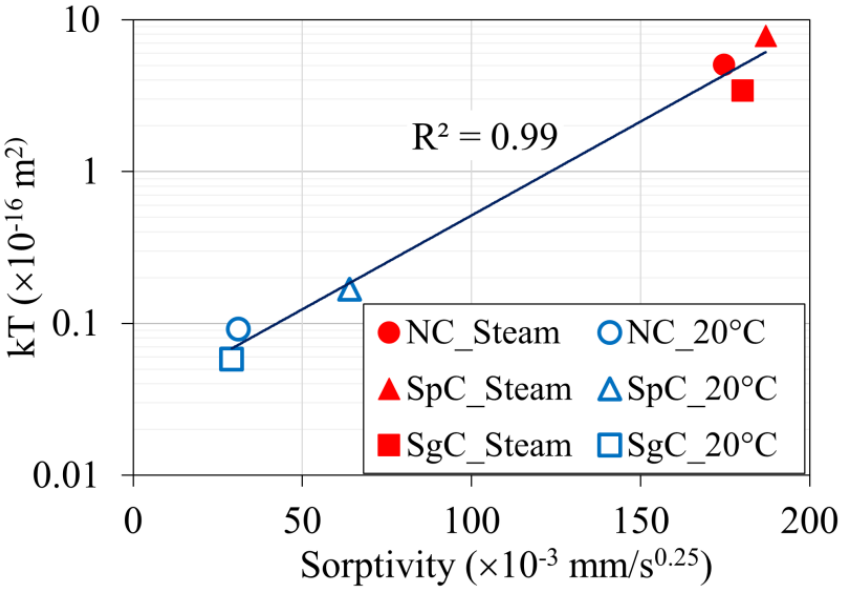

Fig. 4.12. Air permeability versus sorptivity of fabricated concrete specimens.

4.4. Summary

Based on experimental results in this chapter, the following conclusion can be drawn.

- The strength, expansion, and transport properties of expansive concrete were weakened by the incorporation of pure slag at 50% cement replacement by mass.
- The use of slag with gypsum was found to enhance the mechanical, physical, and durability properties of concrete by promoting the hydration of the slag.
- Slag concrete requires prolonged curing to optimize its potential. Steam curing at a high temperature therefore improved only the early strength of the concrete, but impaired the later development of concrete properties, particularly the transport characteristics.
- For normal and slag blended concretes, a high correlation observed in relationships between the studied properties showed a decrease in air permeability with increasing compressive strength and with decreasing sorptivity. Further, the permeability coefficient exhibited a better correlation with water absorption ($R= 0.99$) than with compressive strength ($R= 0.82$).

References in chapter 4

[1] H.V. Nguyen, K. Nakarai, A. Okazaki, H. Karasawa, Y. Tadokoro, M. Tsujino, Applicability of a simplified estimation method to steam-cured expansive concrete, Cem. Concr. Compos. 95 (2019) 217–227.

[2] N. De Belie, M. Soutsos, E. Gruyaert, Properties of fresh and hardened concrete containing supplementary cementitious materials: state-of-the-Art Report of the RILEM Technical Committee 238-SCM, Working Group 4, vol. 25, Springer International Publishing, Cham, 2018.

[3] ACI R233, Ground Granulated Blast-Furnace Slag as a Cementitious Constituent in Concrete, 2000.

[4] Japan Society of Civil Engineers, Standard Specifications for Concrete Structures – Materials and Constructions, JSCE, Tokyo, Japan, 2007, pp. 261–271.

[5] ASTM C143 / C143M, Standard Test Method for Slump of Hydraulic-Cement Concrete, ASTM International, West Conshohocken, 2015.

[6] ASTM C231 / C231M, Standard Test Method for Air Content of Freshly Mixed Concrete by the Pressure Method, ASTM International, West Conshohocken, 2017.

[7] ASTM C192 / C192M, Standard Practice for Making and Curing Concrete Test Specimens in the Laboratory, ASTM International, West Conshohocken, 2016.

[8] JIS A 1108:2006, Method of Test for Compressive Strength of Concrete, Japanese Industrial Standards Committee, Tokyo, 2006.

[9] M. Tsujino, H. Hashida, T. Kikuchi, H. Tanaka, Low Shrinkage Concrete with both Expansive Additive and Limestone Aggregates (Part 2: Quality Control Method of Expansive Concrete), Summaries of Technical Papers of Annual Meeting AIJ A-1 (2010), pp. 925–926 (in Japanese).

[10] Tech Note TN-504-1: Strain Gage Thermal Output and Gage Factor Variation with Temperature, VPG Micro-Measurements, Raleigh, 1989.

[11] R.J. Torrent, A two-chamber vacuum cell for measuring the coefficient of permeability to air of the concrete cover on site. Mater. Struct. 25 (1992) 358–365.

[12] SN 505 262/1. Construction en béton – Spécifications complémentaires, Annexe E: perméabilité à l'air dans les structures. SSIA, Switzerland, 2013.

[13] ASTM C1585, Standard Test Method for Measurement of Rate of Absorption of Water by Hydraulic-Cement Concretes, ASTM International, West Conshohocken, 2004.

[14] M.K. Gopalan, Sorptivity of fly ash concretes, Cem. Concr. Res. 26 (1996) 1189–l197.

[15] S. Hoshino, K. Yamada, H. Hirao, XRD/Rietveld analysis of the hydration and strength development of slag and limestone blended cement, J. Adv. Concr. Technol. 4 (3) (2006) 357–367.

[16] K.L. Scrivener, T. Fu¨llmann, E. Gallucci, G. Walenta, E. Bermejo, Quantitative study of Portland cement hydration by X-ray diffraction/Rietveld analysis and independent methods, Cem. Concr. Res. 34 (2004) 1541–1547.

[17] JIS R 5201, Physical Testing Methods for Cement, Japanese Industrial Standards Committee, Tokyo, 2015.

[18] M. Shariq, J. Prasad, A. Masood, Effect of GGBFS on time dependent compressive strength of concrete, Constr. Build. Mater. 24 (2010) 1469–1478.

[19] S.J. Barnett, M.N. Soutsos, S.G. Millard, J.H. Bungey, Strength development of mortars containing ground granulated blast-furnace slag: Effect of curing temperature and determination of apparent activation energies, Cem. Concr. Res. 36 (2006) 434–440.

[20] ACI 233 R03, Slag Cement in Concrete and Mortar, American Concrete Institute, Detroit, 2003.

[21] A. A. Ramezanianpour, Effect of curing on the compressive strength, resistance to chloride-ion penetration and porosity of concretes incorporating slag, fly ash or silica fume, Cem. Concr. Compos. 17 (1995) 125-133.

[22] M. Singh, M. Garg, Activation of gypsum anhydrite-slag mixtures, Cem. Concr. Res. 25 (1995) 332–338.

[23] N.C. Collier, X. Li, Y. Bai, N.B. Milestone, The effect of sulfate activation on the early age hydration of BFS:PC composite cement, J. Nucl. Mater. 464 (2015) 128–134.

[24] T.K. Aly, J.G. Sanjayan, Effect of gypsum on free and restrained shrinkage behaviour of slag-concretes subjected to various curing conditions, Mater. Struct. 41 (2008) 1393–1403.

[25] C.A. da Luz, R.D. Hooton, Influence of curing temperature on the process of hydration of supersulfated cements at early age, Cem. Concr. Res. 77 (2015) 69–75.

[26] J. Dai, Q. Wang, C. Xie, Y. Xue, Y. Duan, X. Cui, The Effect of fineness on the hydration activity index of ground granulated blast furnace slag, Materials 12 (2019) 2984.

[27] S. Teng, T.Y.D. Lim, B.S. Divsholi, Durability and mechanical properties of high strength concrete incorporating ultra fine Ground Granulated Blast-furnace Slag, Constr. Build. Mater. 40 (2013) 875–881.

[28] S.C. Pal, A. Mukherjee, S.R. Pathak, Investigation of hydraulic activity of ground granulated blast furnace slag in concrete, Cem. Concr. Res. 33 (2003) 1481–1486.

[29] L. Baoju, X. Youjun, Z. Shiqiong, L. Jian, Some factors effecting early compressive strength of steam-curing concrete with ultrafine fly ash, Cem. Concr. Res. 31 (2001) 1455–1458.

[30] A.A. Ramezanianpour, M.H. Khazali, P. Vosoughi, Effect of steam curing cycles on strength and durability of SCC: A case study in precast concrete, Constr. Build. Mater. 49 (2013) 807–813.

[31] Q. Xia, H. Li, A. Lu, Q. Tian, J. Liu, Damage analysis of concrete members containing expansive agent by mechanical and acoustic methods, Engineering Failure Analysis 74 (2017) 95–106.

[32] T. Aly, J.G. Sanjayan, Factors contributing to early age shrinkage cracking of slag concrete subjected to 7-days moist curing, Mater. Struct. 41 (2008) 633–642.

[33] K.M. Lee, H.K. Lee, S.H. Lee, G.Y. Kim, Autogenous shrinkage of concrete containing granulated blast-furnace slag, Cem. Concr. Res. 36 (2006) 1279–1285.

[34] J.C. Chern, Y.W. Chan, Deformations of concretes made with blast-furnace slag cement and ordinary Portland cement, ACI Mater. J. 86 (1989) 372–382.

[35] A. Hadjsadok, S. Kenai, L. Courard, F. Michel, J. Khatib, Durability of mortar and concretes containing slag with low hydraulic activity, Cem. Concr. Compos. 34 (2012) 671–677.

[36] D. D. Higgins, Increased sulfate resistance of GGBS concrete in the presence of Carbonate, Cem. Concr. Compos. 25 (2003) 913–919.

[37] R. Siddique, Waste materials and by-products in concrete, Berlin: Springer, Verlag; 2008.

[38] K. Sato, T. Saito, M. Kikuchi, T. Saeki, Relationship Between Expansion Characteristics of Heat-Cured Mortars During Water Curing and Origins of Ettringite Formation, J. Adv. Concr. Technol. 17 (5) (2019) 260 – 268.

[39] W. Kunther, B. Lothenbach, K.L. Scrivener, On the relevance of volume increase for the length changes of mortar bars in sulfate solutions, Cem. Concr. Res. 46 (2013) 23-29.

[40] C. Famy, K. Scrivener, A. Atkinson, A. Brough, Influence of the storage conditions on the dimensional changes of heat-cured mortars, Cem. Concr. Res. 31 (2001) 795-803.

[41] D. Min, T. Mingshu, Formation and expansion of ettringite crystals, Cem. Concr. Res. 24 (1) (1994) 119–126.

[42] I. Odler, Y. Chen, Effect of cement composition on the expansion of heat-cured cement pastes, Cem. Concr. Res. 25, (4) (1995) 853-862.

[43] J. Han, D. Jia, P. Yan, Understanding the shrinkage compensating ability of type K expansive agent in concrete, Constr. Build. Mater. 116 (2016) 36–44.

[44] B. Liu, G. Luo, Y. Xie, Effect of curing conditions on the permeability of concrete with high volume mineral admixtures, Constr. Build. Mater. 167 (2018) 359–371.

[45] O. Idowu, L. Black, The effect of improper curing on properties that may affect concrete durability, Mag. Concr. Res. 70 (2018) 633–647.

[46] A. Dinku, H.W. Reinhardt, Gas permeability coefficient of cover concrete as a performance control, Mater. Struct. 30 (1997) 387–393.

[47] G. Camarini, Curing effects on air permeability of concrete, Adv. Mater. Res. 214 (2011) 602–606.

[48] W.P.S. Dias, Influence of drying on concrete sorptivity, Mag. Concr. Res. 56 (2004) 537–543.

[49] N.S. Martys, C.F. Ferraris, Capillary transport in mortars and concrete, Cem. Concr. Res. 27 (1997) 747–760.

[50] J. Kaufmann, W. Studer, One-dimensional water transport in covercrete—application of non-destructive methods, Mater. Struct. 28 (1995) 115–124.

[51] L.J. Parrott, Water absorption in cover concrete, Mater. Struct. 25 (1992) 284–292.

[52] Y.A.V. Zaccardi, N.M. Alderete, N. De Belie, Improved model for capillary absorption in cementitious materials: Progress over the fourth root of time, Cem. Concr. Res. 100 (2017) 153–165.

[53] C. Hall, W.D. Hoff, S.C. Taylor, M.A. Wilson, B.-G. Yoon, H.-W. Reinhardt, et al.,Water anomaly in capillary liquid absorption by cement-based materials, J. Mater. Sience Lett. 14 (1995) 1178–1181.

[54] Z. Wu, H.S. Wong, C. Chen, N.R. Buenfeld, Anomalous water absorption in cement-based materials caused by drying shrinkage induced microcracks, Cem. Concr. Res. 115 (2019) 90-104.

[55] C. Wagner, V. Slowik, G.P.A.G. Van Zijl, W.P. Boshoff, S.C. Paul, V. Mechtcherine, et al., Transfer of fluids, gases and ions in and through cracked and uncracked composites crack patterns capillary absorption, A Framework for Durability Design with Strain-Hardening Cement-Based Composites (SHCC), 2017, pp. 27–59.

Chapter 5. Conclusions and recommendations

5.1. Conclusions

The following conclusions can be drawn from the results presented in this study:

(1) Verification of applicability of the simplified estimation method to steam-cured expansive concrete by comparing its results to that of the conventional JIS method.

(a) The simplified method using the circumferential strain is applicable to estimating the moderate expansion of concrete when the circumferential strain is 810×10^{-6} or less. Using the circumferential strain with larger expansions is overestimated because of yielding.

(b) The simplified method is applicable to concrete with large expansions of up to ~1000×10^{-6} according to the JIS method when the axial strain of cylindrical specimens is used. Measuring the axial strain with the simplified method can cover ordinal expansive concrete with various magnitudes of expansion.

(c) The correlation between the simplified and JIS methods showed good agreement regardless of the curing conditions on the first day of aging. This implies that the simplified method can be used to evaluate the expansion behavior of steam-cured concrete.

(d) The findings in this study indicate that the simplified estimation method can cover a wide range of expansion. The simplified method allows the test to be carried out straightforwardly and conveniently anywhere by anyone. The method is therefore likely to find more widespread use, both in research and in production control.

(2) Effects of slag type and curing method on the performance of expansive concrete.

(a) The strength, expansion, and transport properties of expansive concrete were weakened by the incorporation of pure slag at 50% cement replacement by mass because of the low hydration rate of the slag.

(b) The use of slag with gypsum was found to enhance the mechanical, physical, and durability properties of concrete by increasing the AFt content and promoting the hydration of the slag.

(c) Slag concrete requires prolonged curing to optimize its potential. Steam curing at a high temperature therefore improved only the early strength of the concrete, but impaired the later development of concrete properties, particularly the water transport characteristics.

(d) For normal and slag blended concretes, a high correlation observed in relationships between the studied properties showed a decrease in air permeability with increasing compressive strength and with decreasing sorptivity. Further, the permeability coefficient exhibited a better correlation with water absorption than with compressive strength.

5.2. Recommendations for further study

The present study investigated several properties of expansive concrete incorporating two slag types under different curing methods. Some recommendations for future work can be made in details as follows.

- Investigation of the performance of concrete was only employed for 91 days. Thus, it should be stretched for longer time (such six months or one year) to achieve further understanding of long-term effect of slag on concrete properties.

- The specimen used in this study was subjected to air and steam curing, it should be extended to other conditions such as the water curing.

- In this investigation, though a chemical analysis of hydration components using the XRD/Rietveld method was performed, the discussion was solely relating to Aft content. Hence it needs to optimize the analysis and discussion on the reaction rates and amounts of hydration products of binders to comprehensively explain the mechanisms of the blended cementitious system.

Appendix A: Verification of applicability of the simplified estimation method to steam-cured expansive concrete

A.1. Strain behaviors of the dummy restraining device with temperature

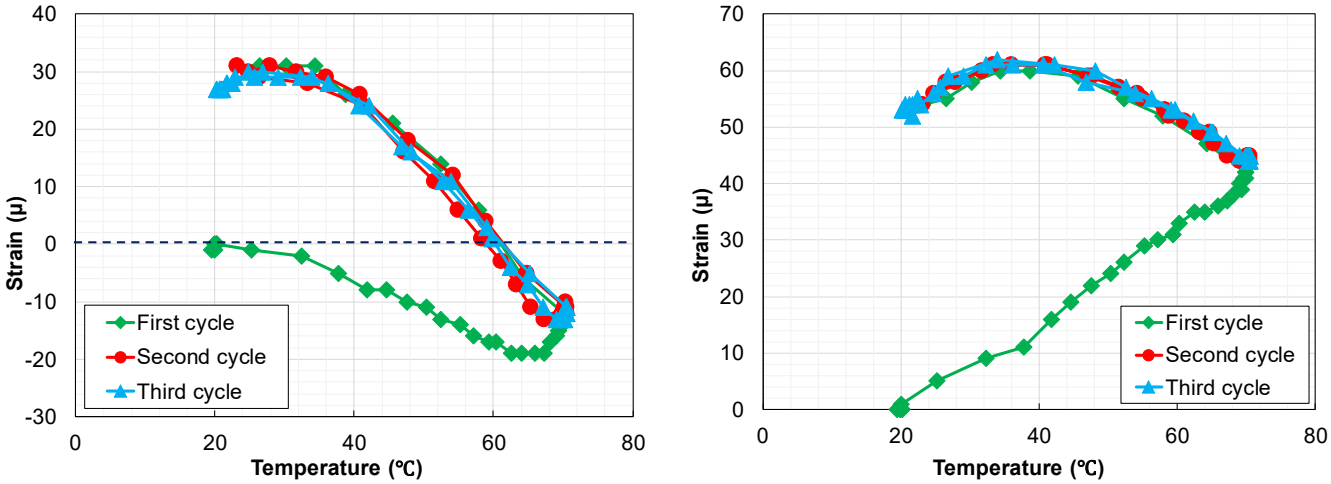

(a) JIS method (b) Simplified method

Fig.1. Examples of the strain of the dummy restraining device and temperature

A.2. The relation between the absorbed water and the square root of time for fabricated concrete

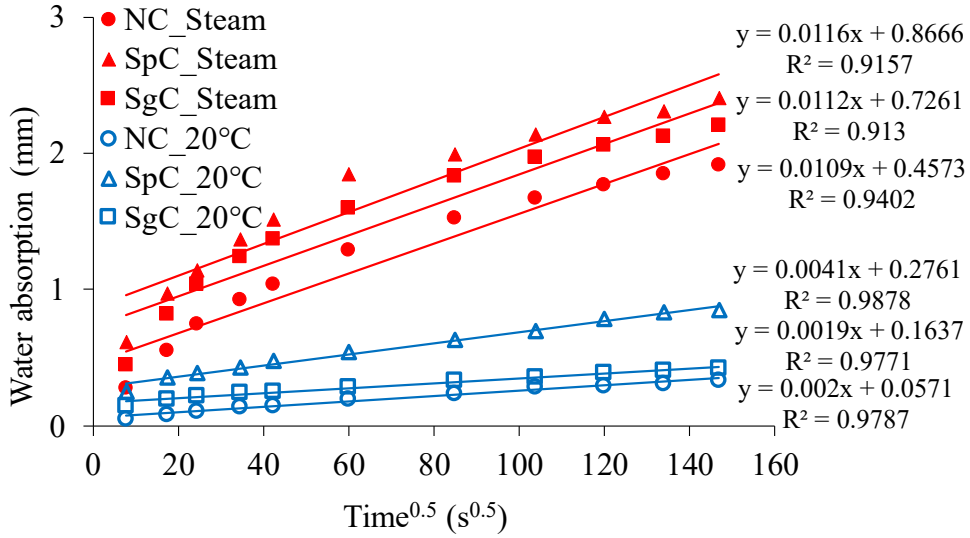

Fig. 2. Cumulative absorbed water with the square root of time for fabricated concretes

Appendix B: Publications arising from this research

List of papers were published or are in the process of publishing from this research:

1.1. Academic Journals

1) Hoang Viet Nguyen, Kenichiro Nakarai, Akeru Okazaki, Hideaki Karasawa, Yuji Tadokoro, Masato Tsujino, Applicability of a simplified estimation method to steam-cured expansive concrete, *Cement and Concrete Composites*, 95 (2019) 217–227. (Published)

2) Hoang Viet Nguyen, Kenichiro Nakarai, Kien Hoang Pham, Saeko Kajita, Takahiro Sagawa, Effects of slag type and curing method on the performance of expansive concrete, *Construction and Building Materials*, 262 (2020) 120422. (Published)

1.2. Presentations at International Conferences

1) Hoang Viet Nguyen, Kenichiro Nakarai, Saeko Kajita, Akeru Okazaki, An experimental study on steam cured expansive concrete incorporating slag, Proceeding of the second International Conference on Sustainability in Civil Engineering (ICSCE-2018), Hanoi Vietnam, 24-25th November 2018, ISBN 978-604-89-8380-2, pp. 293-296.

2) Saeko Kajita, Akeru Okazaki, Hoang Viet Nguyen, Kenichiro Nakarai, Hideaki Karasawa, Yuji Tadokoro, Performance evaluation of expansive concrete members affected by drying, International Conference on Civil and Environmental Engineering (ICCEE-2018), Dalian, China, 14-17th October 2018.